# Supplementary Information for

Genomic Consequences of Long-term Population Decline in Brown Eared Pheasant

Pengcheng Wang, [1,2,3] John T. Burley,[4] Yang Liu,[5] Jiang Chang,[6] De Chen,[1] Qi Lu,[1] Shou-hsien Li,[7] Xuming Zhou,[2] Scott Edwards, [*,3] Zhengwang Zhang[*,1]

[1.] Ministry of Education Key Laboratory for Biodiversity and Ecological Engineering, College of Life Sciences, Beijing Normal University, Beijing 100875, China

[2.] Key Laboratory of Animal Ecology and Conservation Biology, Institute of Zoology, Chinese Academy of Sciences, Beijing 100101, China

[3.] Department of Organismic and Evolutionary Biology / Museum of Comparative Zoology, Harvard University, Cambridge, MA 02138, USA

[4.] Department of Ecology and Evolutionary Biology / Institute at Brown for Environment and Society, Brown University, Providence, RI 02912, USA

[5.] State Key Laboratory of Biocontrol, School of Ecology, Sun Yat-sen University, Guangzhou, 510275, China

[6.] State Key Laboratory of Environmental Criteria and Risk Assessment, Chinese Research Academy of Environmental Sciences, Beijing 100012, China

[7.] School of Life Science, National Taiwan Normal University, Taipei 11677, Taiwan, China

[*] **Co-corresponding authors:** E-mails: zzw@bnu.edu.cn; sedwards@fas.harvard.edu

**This PDF file includes:**

Supplementary Information Text

Figures S1 to S20

Datasets S1 to S12

**Supplementary Information Text**

## DNA sample collection

Tissue for *de novo* whole genome sequencing was obtained from a female Brown eared pheasant (*Crossoptilon mantchuricum*) from the central population in the Pangquangou National Natural Reserve, Jiaocheng, Shanxi Province, China. For genome re-sequencing, tissue samples were obtained from 11, 18, and 11 individuals from Shanxi (Central population, Brown-C), Shaanxi (Western population, Brown-W), Hebei, and Beijing (Eastern population, Brown-E), respectively. The blue eared pheasant (*C. auritum*) was used as the control group in this study, of which 11 individuals were sampled for re-sequencing (the geographic distribution of the studied populations can be seen in Fig. 1a and S12. Sampling information can be seen in Dataset S9). All samples were stored at -80 °C at Beijing Normal University. For genome annotation, we also sequenced the transcriptome of the *C. mantchuricum* individual used for the *de novo* genome assembly using blood samples, developing tail feathers, and primaries. The tissues used to isolate the RNA were mixed with an RNA preservation solution (RNA-In-Safe; Sangon Biotech, Beijing, China). All tissues used for transcriptome sequencing were stored in liquid nitrogen. Sample collection was performed by an accredited veterinarian, and all sampling procedures were approved by the Forestry Department of China and the Ethics and Animal Welfare Committee at the College of Life Science, Beijing Normal University, China (Approval Number CLS-EAW-2015-012).

## DNA, RNA isolation, sequencing, and data filtering

DNA and RNA isolation and library construction were performed at the Novogene Sequence Center (Beijing, China). DNA and RNA quality and quantity were evaluated using a Nanodrop spectrophotometer, a Qubit Fluorometer, an Agilent 2100, and gel electrophoresis. Fragment libraries (insert length 250 bp) and jumping libraries (insert lengths 2000 bp and 5000 bp) were constructed for *de novo* genome sequencing. For *de*

*novo* genome sequencing, the targeted total amount of sequences from the fragment libraries and jumping libraries was ~150 Gb (~150×) and ~100 Gb (~100×), respectively. A total of 51 fragment libraries (insert length 350 bp) were constructed for genome re-sequencing, targeting more than 15× coverage per individual. The targeted total amount of transcriptome sequences was ~190 Gb from the RNA libraries (insert length 250 bp). All libraries were sequenced on the Illumina HiSeq platform at the paired-end 150 bp. Adapter content was trimmed and five base pairs were removed from both the 5' and 3' ends of each read in Trim Galore v0.4.2, with other default parameters (http://www.bioinformatics.babraham.ac.uk/projects/trim_galore/). FastQC v0.11.5 (http://www.bioinformatics.babraham.ac.uk/projects/fastqc/) was used to assess the quality of the raw sequencing data and clean data.

**Genome assembly and evaluation**

After removing the low-quality data, 220.6 Gb of DNA data (1.37 billion reads, 195.6-fold sequence coverage) were used for the *de novo* genome assembly of *C. mantchuricum* in ALLPATHS-LG v52488 (Butler, et al. 2008). Basic metrics (e.g., scaffold and contig N50) were calculated from the genome assembly with a minimum contig length of 100 bp. We used BUSCO v3 (Simão, et al. 2015) to evaluate the completeness of the draft genome by searching for 4915 Benchmarking Universal Single-Copy Orthologs from 40 avian lineages (aves_odb9 dataset) in the *C. mantchuricum* assembly.

**Genome annotation**

The *de novo* repetitive elements annotation was performed in RepeatModeler-open v4.0.6 (http://www.repeatmasker.org/) with repeat masker libraries v20160829 (Bao, et al. 2015) and repeat finding programs (RECON v1.08 (http://selab.janelia.org/recon.html) and RepeatScout v1.0.5 (http://repeatscout.bioprojects.org/)). Repetitive elements were identified with RepeatMasker-open v4.0.6, in which repetitive elements were searched against *de novo*

repetitive elements and homologous sequences (Dfam 2.0 database (Hubley, et al. 2015) and RepBase database v20160829 (Bao, et al. 2015) ). Tandem repeats were identified across the genome using Tandem Repeats Finder v404 (Benson 1999). The repetitive elements were masked in the whole genome for annotation purposes.

We employed an integrative approach to identify a protein-coding gene set of the repeated-masked genome in MAKER v2.31.8 (http://www.yandell-lab.org/software/maker.html), which used homologous genes, *ab initio* predictions, expressed sequence tags (ESTs), and RNA sequence evidence. The homologous gene sets were from human, zebra finch, chicken, and turkey protein sequences downloaded from Ensembl genome browser 87 (http://useast.ensembl.org/info/data/ftp/index.html). The *ab initio* prediction was performed in both SNAP (Korf 2004) and AUGUSTUS v3.0.3 (Stanke and Waack 2003). The 80.0-Gb clean RNA sequences were used to produce splice junction information of the repeat-masked draft genome in TopHat v2.0.13 (http://ccb.jhu.edu/software/tophat/index.shtml) and to *de novo* assemble mRNA-sequences in Trinity v2.3.2 (Grabherr, et al. 2011). To improve the accuracy of the annotation procedure, we ran MAKER twice. For the initial MAKER run, both the AUGUSTUS chicken models and SNAP chicken models that we trained were used to predict the coding genes. The assembled chromosomes and annotation file of *Gallus_gallus*-5.0 (Consortium 2004) were used to train the SNAP chicken models. After the initial MAKER run, we used the gene models produced during the initial MAKER run to retrain AUGUSTUS and SNAP. For the final MAKER run, we used the retrained gene predictors to obtain a consensus set of protein-coding genes. In both MAKER runs, the minimum length required for single exon ESTs was set to 250 bp. The gene set preserved genes that encoded 20 or more amino acids (Eilbeck, et al. 2009). To identify protein function, Interproscan-5.27-66.0 (Zdobnov and Apweiler 2001) was employed to analyze proteins from MAKER with known functional domains and GO terms from the Pfam database. Then, the genes were filtered to remove those without domain content support or those with a quality metric (Annotation Edit Distance, AED)

greater than or equal to 1 (Eilbeck, et al. 2009).

To assess annotation quality, two summary statistics were considered: the percentage of the genes with an AED value less than 0.5, and the percentage of the genes with recognizable domain content. The gene set from annotation was also assessed using BUSCO v3 (Simão, et al. 2015), which was performed on the protein sets from MAKER with 4915 Benchmarking Universal Single-Copy Orthologs from 40 avian lineages (aves_odb9 dataset).

**Read mapping**

Cleaned reads in all the fragment libraries for each individual were mapped to the *C. mantchuricum* reference genome produced in this project and a complete mitochondrial genome that was downloaded from the GenBank database (accession number: KP259807) with a Burrows–Wheeler alignment-maximal exact matches (BWA-MEM, v0.7.9a) algorithm (Li and Durbin 2009). Samtools v1.3.1 was used to calculate the per-base sequence depth, and was then used to calculate the mean coverage for each scaffold (Li, et al. 2009). Sorting and marking of duplicate sequences and generation of alignment metrics were performed with Picard Tools v2.8.0 (https://broadinstitute.github.io/picard/).

Local realignment around indels and recalibration of base quality scores was performed using the Genome Analysis Toolkit v3.7 (GATK) pipeline according to the GATK best practice recommendations (McKenna, et al. 2010). To obtain a database of known polymorphic sites for realignment and recalibration, the raw variants were called in three programs: FreeBayes v0.9.20 (Garrison and Marth 2012), which required at least five supporting observations to consider a variant, the GATK UnifiedGenotyper tool that set the minimum phred-scaled quality score threshold to 50, and samtools mpileup v1.3.1 with default parameters (Li, et al. 2009). The genotypes identified by all three approaches were extracted with bcftools v1.2 (Li, et al. 2009) and used as a database of

known genotypes for realignment and recalibration. To obtain convergence between the average reported quality scores and empirical quality scores, this process was repeated four times.

**Identification of sex chromosomes and mitochondrial genome-linked scaffolds**

We employed two criteria to identify scaffolds belonging to either the sex chromosomes or the mitochondrial genome. For one, we used the proportion of the chicken (*Gallus gallus*) sex chromosome and mitochondrial orthologous genes on each scaffold. We employed the tblastn and blastp functions with an e-value of 1 $e^{-5}$ in BLAST+ v2.2.28 (Camacho, et al. 2009) to search for the one-to-one orthologous genes of *G. gallus* and *C. mantchuricum*. The sex chromosomes and mitochondrial protein sequences of *G. gallus* were downloaded from Ensembl Release 87 (ftp://ftp.ensembl.org/pub/release-87/). We used in-house scripts to calculate the proportion of orthologous genes on each scaffold. For the second criterion, we used the ratio of scaffold coverage between males and females. We calculated the per-scaffold ratio of sequence coverage between males and females, which is expected to be equal to 1 on autosomes and 2 on Z-linked scaffolds. Considering the coverage bias, we assumed that scaffolds with a ratio between 1.6 and 2.4 belong to the Z chromosome. Based on this coverage ratio criteria, we assumed that the scaffolds that have equal to or more than 25% orthologous sex and mitochondrial genes are sex chromosomes and mitochondrial genome-linked scaffolds. Because we mapped the re-sequencing reads to a complete sequence of *Crossoptilon crossoptilon* mitochondrion DNA, we excluded all mitochondrial genome-linked scaffolds and SNPs in the downstream analyses.

For visualization and downstream analysis purposes, all autosome-linked scaffolds were ordered based on their alignment to autosomes in the *G. gallus* genome (ftp://ftp.ensembl.org/pub/release-87/fasta/gallus_gallus/dna/). All autosome-linked scaffolds were aligned to each *G. gallus* autosome using the PROmer function in the MUMmer V 3.23 package (Kurtz, et al. 2004). After alignment, we merged all Delta

files together and filtered the results with the following criteria: retain the longest consistent alignment, minimum alignment identity is 50, and minimum alignment length is 500. After filtering, we determined the location of each scaffold based on the position of the longest alignment.

**SNP calling**

After realignment and recalibration, sites with a phred-scaled confidence ≥ 30 were used to perform joint genotyping with the GATK HaplotypeCaller and GenotypeGVCFs tool. Raw variant sets on autosomes, the Z-chromosome, and the mitochondrial genome were generated separately based on our designation scaffolds. The quality metrics of each raw variant were extracted with vcftools v0.1.14 (Danecek, et al. 2011) and plotted on the density curve of each parameter in RStudio. The distribution of each parameter was used to set the filtering criteria based on the suggestion of the GATK best practices. Based on the distribution of each parameter, quality filtering of the raw variants on autosomes was performed with the following criteria to maintain high-quality SNPs: minor allele frequency > 0.05, strand odds ratio < 3, quality by depth > 2, Fisher Strand < 60, RMS mapping quality > 50, mapping quality rank sum > -4, read position rank sum > -2, minimum depth (summing all 51 samples) > 870, and maximum depth (summing all 51 samples) < 1304; explanation of these parameters can be found in the GATK user manual (McKenna, et al. 2010). These high-quality variants were used in the analyses performed in this study. Variants on the Z chromosome were filtered using the same quality thresholds as above, except that the minimum and maximum depths were 545 and 1207. Considering the huge amount of mitochondrial DNA in cells, we set the minimum depth to 966 for filtering the raw variants. The percentage of missing SNPs in each individual was calculated using vcftools v0.1.14 (Danecek, et al. 2011).

**Inference of kinship**

In population genetic analyses, it is often necessary to exclude closely related

individuals. The three populations of *C. mantchuricum* are all small isolated wild populations where individuals may have familial relationships. We estimated the relatedness of all samples in each population using KING v 2.1.3 (Manichaikul, et al. 2010) to estimate the kinship coefficient using our library of autosomal SNPs with no missing sites. Pairs with a kinship coefficient > 0.177 (twins and first-degree relationship) were not included in subsequent analyses. There were 14 samples with close (duplicate/twins, first degree) relationships to other individuals in the data. These samples were removed, leading to a total of 37 samples that were retained in downstream analyses (Fig. S13; Dataset S10).

**Phylogenetic inference and the mitochondrial haplotype network**

Phylogenetic relationships were inferred separately using a maximum-likelihood (ML) approach with autosomes, the Z chromosome, and mitochondrial SNP data. Aligned autosome sequences were generated from the SNP library using the SNPhylo pipeline with the filtering criteria of a linkage disequilibrium coefficient ($R^2 < 0.2$) and no missing sites (Lee, et al. 2014). After filtering with SNPhylo, 2,274,011 autosome SNPs were used to infer phylogenetic relationships. Sequences for the Z chromosome and mitochondria were generated with in-house scripts and aligned in the Mafft v 7.271 program (Yamada, et al. 2016). The phylogenetic trees were constructed in PhyML v 3.0 (Guindon, et al. 2010) with 1000 bootstrap replicates for autosomes, the Z chromosome, and mitochondrial sequences. Nucleotide frequencies, the transition/transversion ratio, and the value of the gamma shape parameter were estimated by ML. Tree topology, branch length, and substitution rate parameters were optimized in this program. The median joining haplotype network of mitochondria was constructed using Popart (Leigh and Bryant 2015).

**Population structure and principal component analysis**

Principal component analysis (PCA) of the genotypes from 37 individuals was performed using a stringently filtered set of 49,701 autosomal SNPs (no missing sites,

Hardy-Weinberg equilibrium exact test *p*-value > 0.00001, linkage disequilibrium coefficient, $r^2 < 0.2$) in the Genome-wide Complex Trait Analysis (GCTA) v 1.91.3 (Yang, et al. 2011). Using the same SNP set, population structure was inferred using ADMIXTURE v 1.3.0 (Alexander, et al. 2009) with cross-validation (CV) (Alexander and Lange 2011) and 100 bootstraps. This approach estimates the ancestry proportion of each sample based on SNP data, given the *a priori* specification of K ancestral populations. To test the stability of the results, we performed the analysis using all 37 samples, and subsets of individuals belonging to the putative populations *C. mantchuricum*: Blue, Brown-W, Brown-C, Brown-E. We predefined the K value from 1 to 10 for all individuals (including *C. auritum* and *C. mantchuricum*), and from 1 to 6 within *C. mantchuricum*. For the isolated populations (Blue, Brown-W, Brown-C, and Brown-E), we predefined the K value from 1 to 3. For each K value, the analysis was performed ten times with different random seeds, which aimed to obtain the most stable results.

**Estimation of genetic diversity**

To assess the genetic diversity within and among *C. mantchuricum* populations, we calculated the heterozygosity of each sample, defined as the proportion of heterozygous sites in all callable sites across the autosomes. For each population or species, we defined the genetic diversity as the mean heterozygosity per individual within each population or species. We compared the diversity estimates of the two species to 21 other avian species for which comparable estimates were available, some of which are also highly inbred, such as White tailed eagle (*Haliaeetus albicilla*), Bald eagle (*Haliaeetus leucocephalus*), Crested ibis (*Nipponia nippon*), and Dalmatian pelican (*Pelecanus crispus*).

We also computed population genetic statistics including pairwise nucleotide diversity ($\theta_\pi$) and Watterson's expected nucleotide diversity ($\theta_W$) on both synonymous (four-fold degenerate sites) and non-synonymous sites (zero-fold degenerate sites). These

summary statistics were calculated based on the site frequency spectrum (SFS) with in-house scripts. In both the synonymous and non-synonymous sites, low-quality and missing genotypes were inferred separately for each population using the program BEAGLE v 4.1 (Browning and Browning 2016). To test whether *C. mantchuricum* has accumulated more missense mutations than *C. auritum*, we computed $\Theta_\pi$ (zero-fold degenerate sites) / $\Theta_\pi$ (four-fold degenerate sites) for each population. If the populations of *C. mantchuricum* have accumulated more missense mutations, then this value is expected to be higher in *C. mantchuricum* than that in *C. auritum*. To compare these summary statistics between populations, these statistics were calculated using 1,000 bootstrap replicates (resampling with replacement). Because the variance of any summary statistics between two randomly selected populations was not homoscedastic, non-paired Welch two-sample t-tests were used to test whether the summary statistics of the two populations were significantly different from each other.

**Estimating inbreeding patterns**

Estimation of inbreeding using whole genome resequencing data has been shown to outperform estimates using extensive pedigree data (Kardos, et al. 2018). To understand the genomic extent of inbreeding in *C. mantchuricum*, we identified genome-wide patterns of runs of homozygosity (ROH), estimated linkage disequilibrium (LD), and the inbreeding coefficient ($F_{is}$) in each of the three populations of *C. mantchuricum*. For comparison, we also performed the same analysis in the sampled population of *C. auritum*.

ROH arises through the process of inbreeding that gives offspring the opportunity to inherit identical haplotypes from each parent (Ceballos, et al. 2018). The location and number of ROHs were identified in each sample using plink v1.90 with default parameters (Howrigan, et al. 2011). Because meiosis can break down the segments that are identical-by-descent, we assume that longer ROH (≥ 0.5 Mb) arose from recent inbreeding, and shorter ROH (< 0.5 Mb) arose from more ancient inbreeding (Kirin, et

al. 2010). To compare the relative extents of recent and ancient inbreeding, the average fraction of the longer and shorter ROH on the autosomes was summarized for each population.

To avoid biases caused by the different sample sizes of the sampled populations in the LD analysis, we randomly selected six unrelated samples from each population and repeated this analysis 10 times. We employed Haploview (Barrett, et al. 2004) to calculate the correlation coefficient ($R^2$) between any pair of SNPs in each population. The parameters were set as follows: -maxdistance 500 -dprime -minGeno 0.75 -minMAF 0.05 -hwcutoff 0.001. To plot the LD decay curves, we merged the SNPs that had a similar physical distance (1 kb) into one group and calculated the mean $R^2$ for each group. We estimated the inbreeding coefficient per individual in plink v1.90 (Howrigan, et al. 2011) and then calculated the average inbreeding coefficient for each population.

**Evaluating the genetic load**

Genetic load is a factor that can drive the extinction of small populations. Evaluating the genetic load of endangered species is an important component of conservation genetics. Thus, we sought to gauge the genetic load of *C. mantchuricum* using population genomic data. We estimated the relative excess of derived loss-of-function (LOF) and missense variants in three populations of *C. mantchuricum* compared to those of *C. auritum* to test whether these isolated populations experience inbreeding depression.

To measure the genetic load, we employed methods previously used for gorillas (Xue, et al. 2015). We used SnpEff to identify LOF, missense, and synonymous variations in the coding region (Cingolani, et al. 2012). We inferred the ancestral and derived allele at each location based on comparison to the genome of their close relatives, the White eared pheasant (*C. crossoptilon*) (Wang, et al. 2018). In order to estimate the relative

number of derived LOF and missense alleles found in each population of *C. mantchuricum* compared to those in *C. auritum*, we used the following formula to calculate the number of derived LOF or missense alleles found in population *A* rather than in population *B*:

$$L_{A,B}(C) = \frac{\sum_{i \in C} f^{A}i(1 - f^{B}i)}{\sum_{j \in I} f^{A}j(1 - f^{B}j)}$$

We used $f^{A}i = d^{A}i / n^{A}i$ to calculate the observed derived allele frequency in population A, where $d^{A}i$ is the number of derived alleles in population *A*, and $n^{A}i$ is the total number of alleles in population *A*. In population *B,* $f^{B}i$ was similarly defined. We defined *C* as a set of protein-coding sites, and I as a set of intergenic sites. For each comparison, the relative number of derived LOF or missense variations was measured by $R_{A/B}(C) = L_{A,B}(C)/L_{B,}A(C)$. If the $R_{A/B}(C)$ is larger than one, it means that the A population has more LOF or missense mutations than the B population; otherwise, the B population has excess corresponding mutations. To estimate the variance of $R_{A/B}(C)$, we performed a 100-block jackknife at the sites of the C set.

To evaluate inbreeding depression, we used three strategies to analyze the outcome of inbreeding. We first calculated whether the ROH regions accumulated much more homozygosity missense mutations than those outside the ROH regions. If the homozygous lethal variations did not come from inbreeding, we expected the ratio of the number of homozygous missense genotypes to the number of homozygous synonymous genotypes to be equal to one; otherwise, the ratio should be less than one. Next, we tested whether there were more heterozygous missense mutations compared to the number of homozygous mutations. If one population accumulates homozygous lethal mutations, the ratio of the number of missense alleles to the number of synonymous alleles in the homozygous sites would be significantly less than the ratio in the heterozygous sites. To test whether there was a significant difference between the homozygous and heterozygous sites, we employed the Kolmogorov-Smirnov test to compare the distribution. For the third strategy, we compared the genetic diversity of

the functional region (MHC, conserved non-exonic elements, conserved intron, conserved intergenic region, and coding region) and non-functional region (putative non-functional region, non-conserved intron, and non-conserved intergenic region) between each population of *C. mantchuricum* and *C. auritum*. If *C. mantchuricum* experienced inbreeding depression, both the functional and non-functional regions would have a lower genetic diversity than that of *C. auritum*.

To identify the conserved non-exonic elements (CNEE), putative non-function region, conserved and non-conserved introns, and conserved and non-conserved intergenic regions, we followed the method described in a comparative genomics project on paleognaths (Sackton, et al. 2019) to identify the *G. gallus* (galGal5) CNEE coordinates. After getting the information regarding the *G. gallus* CNEE coordinates, we aligned the scaffolds of *C. mantchuricum* to the *G. gallus* genome in LAST software (Kiełbasa, et al. 2011). To obtain the CNEE coordinates of *C. mantchuricum*, we lifted the *G. gallus* CNEE coordinates to *C. mantchuricum*. We defined the putative non-functional region as the region far away from the genes, with CNEE regions at least 50 kb and at least 1 kb in length. The conserved intron and conserved intergenic region are defined as the regions with overlap between CNEE and the intron and intergenic regions, respectively. Otherwise, the regions that do not have any overlap are considered non-conserved introns and non-conserved intergenic regions.

As an additional assessment of the fitness of *C. mantchuricum*, we calculated the genetic diversity in the MHC region. We identified the MHC region with the most effective reciprocal hit BLAST method. By comparing the protein sequences of *C. mantchuricum* and *G. gallus*, the ortholog genes were identified. Using the annotation information of *G. gallus*, the ortholog MHC region was identified. With the in-house scripts, we calculated the genetic diversity of the MHC.

In order to more intuitively understand whether purifying selection could remove

deleterious mutations in *C. mantchuricum*, we investigated whether or not derived missense mutations in potential adaptative genes are deleterious. Because the genomic islands identified by the statistic $F_{ST}$ may occur due to reduced diversity (Cruickshank and Hahn 2014), and *C. mantchuricum* typically has low genome-wide diversity, we employed $d_{XY}$, a statistic that is independent of the genetic diversity within the populations, to identify the candidate adaptive genes (Cruickshank and Hahn 2014). We also used pi, a measure of genetic variation, to infer the candidate adaptive genes. We first employed "popgenWindows.py" written by Simon Martin at The University of Edinburgh, UK, to calculate the $d_{XY}$ between *C. auritum* and each population of *C. mantchuricum*. The measure of genetic variation, pi, was also calculated using this script. We set the window size to 100 kb, and the minimum number of sites within a window was 10. The size of the step for the sliding window was set to 25 kb. The window size was determined by the results of the linkage disequilibrium test. Then, we Z-transformed the $d_{XY}$ and pi to $Zd_{XY}$ and Zpi. Because there was almost no genetic diversity in *C. mantchuricum*, we only employed the Zpi of *C. auritum* and $Zd_{XY}$ to infer the candidate adaptive genes. The windows with high (top 5%) $Zd_{XY}$ and extremum (both top 5% and bottom 5%) of Zpi were determined as the candidate regions containing the genes under selection. Genes with more than 50% of their length contained within the candidate regions were selected as the genes putatively under positive selection. PROVEAN v 1.1.5 (Choi, et al. 2012) was used to predict whether the derived missense mutations in the genes putatively under positive selection were deleterious mutations. The derived missense mutations with PROVEAN scores lower than -2.5 were identified as deleterious mutations. The genetic diversity of each potential adaptive gene and the frequency of the derived missense mutations were also calculated. KOBAS v 3.0 (Wu, et al. 2006) was used to perform KEGG and GO enrichment analyses for these genes putatively under positive selection.

**Demographic History Reconstruction**

To explore the potential historical factors that are linked to low present-day genetic

diversity, we used the Multiple Sequential Markovian Coalescence (MSMC2) model (Schiffels and Durbin 2014) to reconstruct demographic histories for each of our study populations. Because MSMC2 uses phased haplotypes as input data, we used SHAPEIT v2.904.3.10.0 (Delaneau, et al. 2012) to phase 33 scaffolds separately, with a minimum length of 132 kb. Based on the results from MUMmer, we selected at least one scaffold from each chromosome. The total length of these 33 scaffolds covered 18.48% of the draft genome. To prepare the input file, we followed the procedure of Heng Li's SNPable program (http://lh3lh3.users.sourceforge.net/snpable.shtml) to generate Mappability mask files for each scaffold. Under the general guidelines of MSMC2 (https://github.com/stschiff/msmc/blob/master/guide.md), we ran MSMC2 and calculated the effective population size ($N_e$) of *C. mantchuricum*. To test the convergence of the result, we performed both analyses with 100 bootstrap replicates. Based on the comparison of the four-fold degenerate sites among the lineages of Galliformes, we set the mutation rate of *C. mantchuricum* as $4.02 \times 10^{-9}$ per site per generation (Zhang, et al. 2014), and the generation time as 2 years per generation (Zheng 2015).

We used Migrate-n v 3.6.11 (Beerli and Felsenstein 2001) to investigate whether gene flow occurs between adjacent populations of *C. mantchuricum*. We evaluated four possible gene flow patterns among the three populations of *C. mantchuricum*: migration between adjacent populations, migration between Brown-C and Brown-W, migration between Brown-C and Brown-E, or no gene flow between adjacent populations. The best-fit model was inferred by the maximum likelihood in the Migrate-n. To prepare the input data for Migrate-n, we first selected the putative non-functional regions whose lengths were longer than 1 kb and then randomly selected 1 kb from each of these putative non-functional regions. Among the selected 1 kb putative non-functional regions, we randomly selected 30 regions to create the bed file. In the vcftools software, we extracted the phased vcf file for each bed and then employed the bcftools software to produce sequences for each region of each sample. Using the 60 sequences of each

sample, we performed Migrate-n to estimate the gene flow patterns.

In order to distinguish whether the populations experienced continuous population decline or consistent small population size in *C. mantchuricum*, we employed fastsimcoal26 (Excoffier, et al. 2013), a simulation-based framework, to infer the demographic history of the three populations of *C. mantchuricum*. Fastsimcoal26 uses SFS information to infer the most suitable evolutionary model given a range of scenarios. Using this method, we also tested whether *C. mantchuricum* experienced inbreeding and whether there was gene flow among the adjacent populations of *C. mantchuricum*. The three-dimensional SFS of the three populations of *C. mantchuricum* was estimated using the -doSaf and -realSFS methods in ANGSD (Korneliussen, et al. 2014). To minimize misidentification of the derived allele in *C. mantchuricum*, we only selected the sites whose alleles were fixed in the population of *C. auritum*, and excluded the sites that were not located in the putative non-functional region and were not present in all individuals within each population. We first estimated the unfolded one-dimensional SFS for each of the *C. mantchuricum* populations. We then estimated the three-dimensional SFS among the three populations. The three-dimensional SFS was used to estimate the composite likelihoods of the different evolutionary models. Because we wanted to test 1) whether *C. mantchuricum* experienced long-term population decline (D) or consistent small population size (S), 2) whether there was gene flow between the adjacent populations of *C. mantchuricum* (no gene flow between adjacent populations: I; gene flow occurred between adjacent populations: WCE; gene flow occurred between the Western and Central populations: CW; gene flow occurred between the Central and Eastern populations: CE), and 3) whether there had been inbreeding (IN) in the populations of *C. mantchuricum*, we devised 16 historical models for the three populations. The 16 models were as follows: a) S+I; b) S+WCE; c) S+CW; d) S+CE; e) D+I; f) D+WCE; g) D+CW; h) D+CE; i) S+I+IN; j) S+WCE+IN; k) S+CW+IN; l) S+CE+IN; m) D+I+IN; n) D+WCE+IN; o) D+CW+IN; and p) D+CE+IN (these models are illustrated in Fig. S11). For each model, we performed 1,000,000

simulations to estimate the expected derived SFS, and 100 expectation conditional maximization cycles were performed. We also required the minimum console output and set the minimum observed SFS entry count as 20 accounting for parameter estimation. The multiSFS and infinite site options were also used for estimating the model parameters. To obtain the global maximum likelihood for each model, the above procedure was replicated 100 times. To infer the best-fit model, the replicate with the highest estimated likelihood was used to calculate the AIC values and Akaike weights (w).

## Results

### Mapping and SNP quality

The sequencing coverage of the re-sequence individuals varied from 13.4 to 43.2 (the average coverage was 19.0), and the mapping rate varied from 83.6% to 98.9% (the average mapping rate was 97.3%) (Dataset S9).

The average proportion of high-quality bases (the call quality of the bases was Q20 or higher) in the BAM files was 93.30% (varied from 90.20% to 95.00%), 93.28% (varied from 89.07% to 95.27%), and 95.46% (varied from 95.24% to 95.75%) of the autosomes, Z chromosome, and mitochondria, respectively (Fig. S14a, Fig. S15a, Fig. S16a, Dataset S11). This proportion was defined as the number of high-quality bases divided by the number of aligned bases in the BAM file. In the BAM files of the autosomes, Z chromosome, and mitochondrial genome, the average percentage of sites covered by at least five reads was 97.58% (varied from 83.37% to 98.56%), 88.83% (varied from 45.00% to 98.44%) and 100% (no variation), respectively (Fig. S14b, Fig. S15b, Fig. S16b, Dataset S11).

After variant calling, we obtained 7,556,341 and 65 single-nucleotide variants for the genome (including autosomes and sex chromosomes) and mitochondria, respectively. After hard-filtering, the final SNP library contained 2,327,376 and 134,081 variable

492 sites on the autosome and Z chromosome, respectively. In the mtDNA dataset, we
493 retained 24 substitution sites. In the autosome, Z chromosome, and mitochondrial SNP
494 library, the mean proportion of missing SNPs was 0.047% (varied from 0.006% to
495 0.372%), 0.392% (varied from 0.003% to 4.144%), and 0 (no variation), respectively
496 (Fig. S14c, Fig. S15c, Fig. S16c, Dataset S11).
497
498 The average number of heterozygous sites of the autosomes and Z chromosome was
499 230,681 (varied from 38,525 to 902,604) and 10,764 (varied from 808 to 28,595),
500 respectively (Fig. S17, Fig. S18). In the autosome SNP library, *C. auritum* had the
501 highest heterozygosity (average= 0.083%, SD = 0.0055%). Among the three
502 populations of *C. mantchuricum*, Brown-C had the highest heterozygosity (average=
503 0.014%, SD= 0.001%), while both Brown-W and Brown-E had similar heterozygosity
504 (Fig. S14d). On the Z chromosomes, *C. auritum* had the highest genetic diversity
505 (average= 0.029%, SD= 0.007%), but the three populations of *C. mantchuricum* had
506 similar genetic diversity (Fig. S15d). For the mitochondria, the Brown-C and Brown-E
507 populations had a low average number of nucleotide differences (the value was 0) (Fig.
508 S16d).
509
510 **Scaffolds linked to the Z chromosome and mitogenome**
511 We identified 49 Z chromosome-linked scaffolds (Dataset S12), which had 71.05 Mb
512 bases with a scaffold N50 of 2432.56 kb. The length of the Z chromosome of *C.*
513 *mantchuricum* was similar to that of *G. gallus* (82.53 Mb) (Consortium 2004). The
514 distribution of single-base sequencing depths across all individuals showed two peaks
515 for all scaffolds, but there was one single peak for the scaffolds designated as autosome-
516 linked, indicating that the Z-linked scaffolds had effectively been removed from this
517 set (Fig. S19). Female individuals had lower sequencing coverage on the Z
518 chromosome compared to that of the male individuals, while the female and male
519 individuals had similar sequencing coverage of the autosomes (Fig. S20). All the
520 evidence indicated that the process of identifying and removing Z-linked scaffolds was

effective.

Interestingly, the W-chromosome did not appear in this assembly, even though the individual used to generate the *de novo* assembly was a female. This may be due to the typical characteristics of the avian W chromosomes, such as they tend to be highly heterochromatic and degenerated (Zhou, et al. 2014; Peichel 2017). We identified 3 scaffolds that are on the mitochondrial genome (Dataset S12), which have 5,875 bp.

## References

Alexander DH, Lange K. 2011. Enhancements to the ADMIXTURE algorithm for individual ancestry estimation. BMC Bioinformatics 12:246.

Alexander DH, Novembre J, Lange K. 2009. Fast model-based estimation of ancestry in unrelated individuals. Genome Research 19:1655-1664.

Bao W, Kojima KK, Kohany O. 2015. Repbase update, a database of repetitive elements in eukaryotic genomes. Mobile DNA 6:11.

Barrett JC, Fry B, Maller J, Daly MJ. 2004. Haploview: analysis and visualization of LD and haplotype maps. Bioinformatics 21:263-265.

Beerli P, Felsenstein J. 2001. Maximum likelihood estimation of a migration matrix and effective population sizes in n subpopulations by using a coalescent approach. Proceedings of the National Academy of Sciences 98:4563-4568.

Benson G. 1999. Tandem repeats finder: a program to analyze DNA sequences. Nucleic Acids Research 27:573-580.

Browning Brian L, Browning Sharon R. 2016. Genotype imputation with millions of reference samples. The American Journal of Human Genetics 98:116-126.

Butler J, MacCallum I, Kleber M, Shlyakhter IA, Belmonte MK, Lander ES, Nusbaum C, Jaffe DB. 2008. ALLPATHS: De novo assembly of whole-genome shotgun microreads. Genome Research 18:810-820.

Camacho C, Coulouris G, Avagyan V, Ma N, Papadopoulos J, Bealer K, Madden TL. 2009. BLAST plus: architecture and applications. BMC Bioinformatics 10:421.

Ceballos FC, Joshi PK, Clark DW, Ramsay M, Wilson JF. 2018. Runs of homozygosity: windows into population history and trait architecture. Nature Reviews Genetics 19:220–234.

Choi Y, Sims GE, Murphy S, Miller JR, Chan AP. 2012. Predicting the functional effect of amino acid substitutions and indels. PLOS ONE 7:e46688.

Cingolani P, Platts A, Wang LL, Coon M, Nguyen T, Wang L, Land SJ, Lu X, Ruden DM. 2012. A program for annotating and predicting the effects of single nucleotide polymorphisms, SnpEff. Fly 6:80-92.

Consortium ICGS. 2004. Sequence and comparative analysis of the chicken genome provide unique perspectives on vertebrate evolution. Nature 432:695-716.

Cruickshank TE, Hahn MW. 2014. Reanalysis suggests that genomic islands of speciation are due to reduced diversity, not reduced gene flow. Molecular ecology 23:3133-3157.

561 Danecek P, Auton A, Abecasis G, Albers CA, Banks E, DePristo MA, Handsaker RE, Lunter G, Marth
562 GT, Sherry ST, et al. 2011. The variant call format and VCFtools. Bioinformatics 27:2156-2158.
563 Delaneau O, Marchini J, Zagury J-F. 2012. A linear complexity phasing method for thousands of
564 genomes. Nature Methods 9:179-181.
565 Eilbeck K, Moore B, Holt C, Yandell M. 2009. Quantitative measures for the management and
566 comparison of annotated genomes. BMC Bioinformatics 10:67.
567 Excoffier L, Dupanloup I, Huerta-Sánchez E, Sousa VC, Foll M. 2013. Robust demographic inference
568 from genomic and SNP data. PLOS Genetics 9:e1003905.
569 Garrison E, Marth G. 2012. Haplotype-based variant detection from short-read sequencing. arXiv
570 1207:3907.
571 Grabherr MG, Haas BJ, Yassour M, Levin JZ, Thompson DA, Amit I, Adiconis X, Fan L, Raychowdhury
572 R, Zeng Q, et al. 2011. Full-length transcriptome assembly from RNA-Seq data without a reference
573 genome. Nature Biotechnology 29:644–652.
574 Guindon S, Dufayard J-F, Lefort V, Anisimova M, Hordijk W, Gascuel O. 2010. New algorithms and
575 methods to estimate maximum-likelihood phylogenies: assessing the performance of PhyML 3.0.
576 Systematic Biology 59:307-321.
577 Howrigan DP, Simonson MA, Keller MC. 2011. Detecting autozygosity through runs of
578 homozygosity: A comparison of three autozygosity detection algorithms. BMC Genomics 12:460.
579 Hubley R, Finn RD, Clements J, Eddy SR, Jones TA, Bao W, Smit AFA, Wheeler TJ. 2015. The Dfam
580 database of repetitive DNA families. Nucleic Acids Research 44:D81-D89.
581 Kardos M, Åkesson M, Fountain T, Flagstad Ø, Liberg O, Olason P, Sand H, Wabakken P, Wikenros
582 C, Ellegren H. 2018. Genomic consequences of intensive inbreeding in an isolated wolf population.
583 Nature Ecology & Evolution 2:124-131.
584 Kiełbasa SM, Wan R, Sato K, Horton P, Frith MC. 2011. Adaptive seeds tame genomic sequence
585 comparison. Genome Research 21:487-493.
586 Kirin M, McQuillan R, Franklin CS, Campbell H, McKeigue PM, Wilson JF. 2010. Genomic runs of
587 homozygosity record population history and consanguinity. PLOS ONE 5:e13996.
588 Korf I. 2004. Gene finding in novel genomes. BMC Bioinformatics 5:59.
589 Korneliussen TS, Albrechtsen A, Nielsen R. 2014. ANGSD: Analysis of next generation sequencing
590 data. BMC Bioinformatics 15:356.
591 Kurtz S, Phillippy A, Delcher AL, Smoot M, Shumway M, Antonescu C, Salzberg SL. 2004. Versatile
592 and open software for comparing large genomes. Genome Biology 5:R12.
593 Lee T-H, Guo H, Wang X, Kim C, Paterson AH. 2014. SNPhylo: a pipeline to construct a
594 phylogenetic tree from huge SNP data. BMC Genomics 15:162.
595 Leigh JW, Bryant D. 2015. Popart: full-feature software for haplotype network construction.
596 Methods in Ecology and Evolution 6:1110-1116.
597 Li H, Durbin R. 2009. Fast and accurate short read alignment with Burrows–Wheeler transform.
598 Bioinformatics 25:1754-1760.
599 Li H, Handsaker B, Wysoker A, Fennell T, Ruan J, Homer N, Marth G, Abecasis G, Durbin R,
600 Subgroup GPDP. 2009. The sequence alignment/map format and SAMtools. Bioinformatics
601 25:2078-2079.
602 Manichaikul A, Mychaleckyj JC, Rich SS, Daly K, Sale M, Chen W-M. 2010. Robust relationship
603 inference in genome-wide association studies. Bioinformatics 26:2867-2873.
604 McKenna A, Hanna M, Banks E, Sivachenko A, Cibulskis K, Kernytsky A, Garimella K, Altshuler D,

Gabriel S, Daly M, et al. 2010. The Genome Analysis Toolkit: A MapReduce framework for analyzing next-generation DNA sequencing data. Genome Research 20:1297-1303.

Peichel CL. 2017. Convergence and divergence in sex-chromosome evolution. Nature Genetics 49:321-322.

Sackton TB, Grayson P, Cloutier A, Hu Z, Liu JS, Wheeler NE, Gardner PP, Clarke JA, Baker AJ, Clamp M, et al. 2019. Convergent regulatory evolution and loss of flight in paleognathous birds. Science 364:74-78.

Schiffels S, Durbin R. 2014. Inferring human population size and separation history from multiple genome sequences. Nature Genetics 46:919-925.

Simão FA, Waterhouse RM, Ioannidis P, Kriventseva EV, Zdobnov EM. 2015. BUSCO: assessing genome assembly and annotation completeness with single-copy orthologs. Bioinformatics 31:3210-3212.

Stanke M, Waack S. 2003. Gene prediction with a hidden Markov model and a new intron submodel. Bioinformatics 19:ii215-ii225.

Wang P, Yao H, Gilbert KJ, Lu Q, Hao Y, Zhang Z, Wang N. 2018. Glaciation-based isolation contributed to speciation in a Palearctic alpine biodiversity hotspot: evidence from endemic species. Molecular Phylogenetics and Evolution 129:315-324.

Wu J, Mao X, Cai T, Luo J, Wei L. 2006. KOBAS server: a web-based platform for automated annotation and pathway identification. Nucleic Acids Research 34:W720-W724.

Xue Y, Prado-Martinez J, Sudmant PH, Narasimhan V, Ayub Q, Szpak M, Frandsen P, Chen Y, Yngvadottir B, Cooper DN, et al. 2015. Mountain gorilla genomes reveal the impact of long-term population decline and inbreeding. Science 348:242-245.

Yamada KD, Tomii K, Katoh K. 2016. Application of the MAFFT sequence alignment program to large data—reexamination of the usefulness of chained guide trees. Bioinformatics 32:3246-3251.

Yang J, Lee SH, Goddard ME, Visscher PM. 2011. GCTA: A tool for genome-wide complex trait analysis. The American Journal of Human Genetics 88:76-82.

Zdobnov EM, Apweiler R. 2001. InterProScan – an integration platform for the signature-recognition methods in InterPro. Bioinformatics 17:847-848.

Zhang G, Li C, Li Q, Li B, Larkin DM, Lee C, Storz JF, Antunes A, Greenwold MJ, Meredith RW, et al. 2014. Comparative genomics reveals insights into avian genome evolution and adaptation. Science 346:1311-1320.

Zheng G-M. 2015. Pheasants in China. Beijing, China: Higher Education Press.

Zhou Q, Zhang J, Bachtrog D, An N, Huang Q, Jarvis ED, Gilbert MTP, Zhang G. 2014. Complex evolutionary trajectories of sex chromosomes across bird taxa. Science 346:1246338.

## Figures

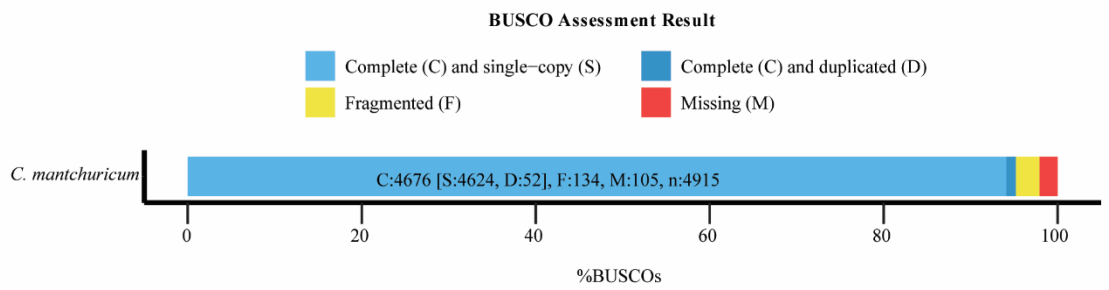


Fig. S1. Benchmarking Universal Single-Copy Orthologs (BUSCO) assessment Result. The numbers after the letters indicate the amount of BUSCO groups of the corresponding groups. n indicates the number of BUSCO groups in the avian dataset.

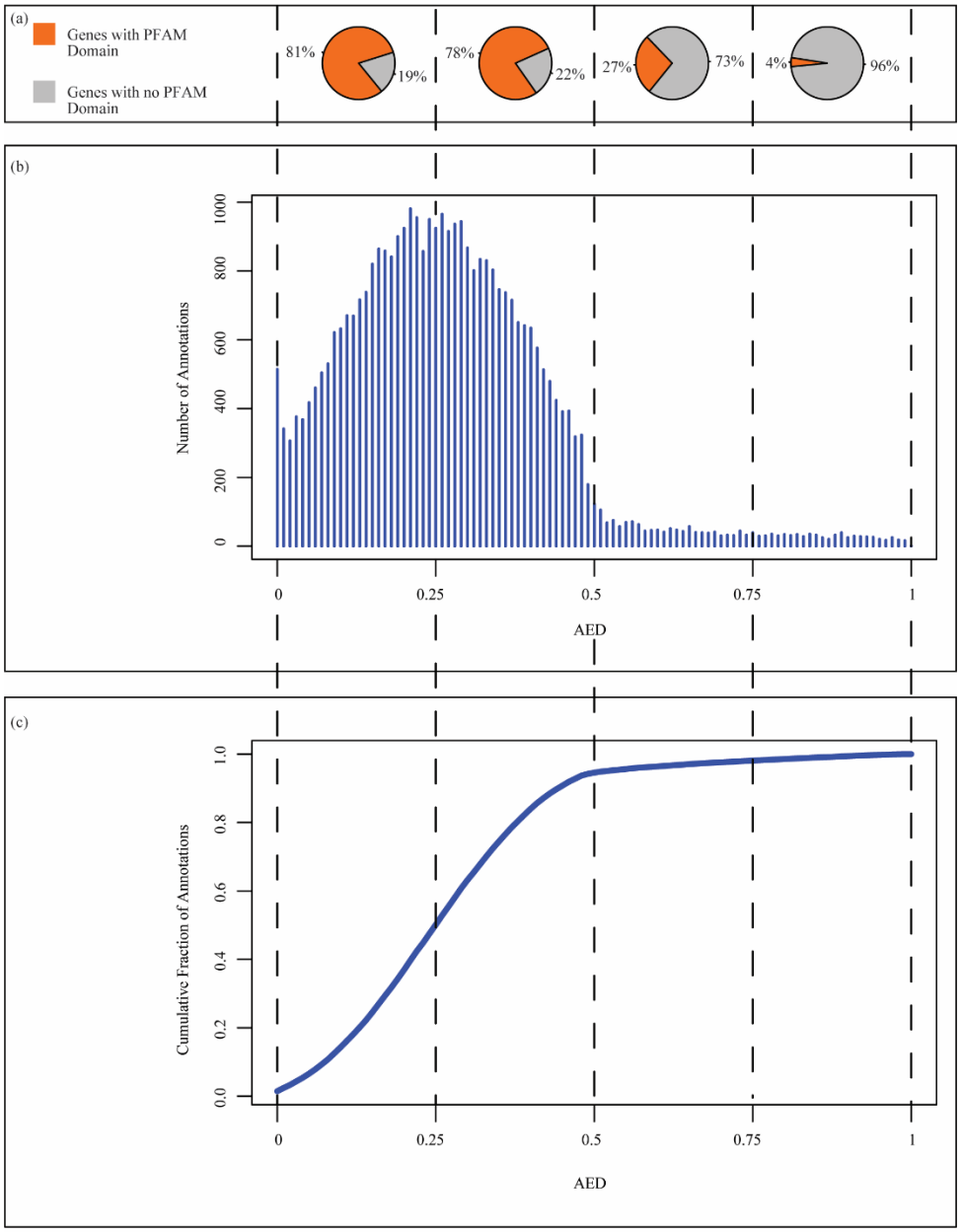


Fig. S2. Annotated gene set assessment result. AED means Annotation Edit Distance, which is used to measure the suitability between the annotated gene model and the supporting evidence of that model. AED is represented by a number between 0 and 1. An AED value of 0 indicates the annotated gene model is perfected supported by available evidence, and an AED of 1 denotes that the annotated gene model is completely lacks supportive evidence. (a) The pie charts represent the annotated gene models with different AED values (0~0.25, 0.25~0.5, 0.5~0.75, and 0.75~1). (b) The number of annotated gene models with different AED values from 0 to 1. (c) The curve of the cumulative fraction of the annotated gene models.

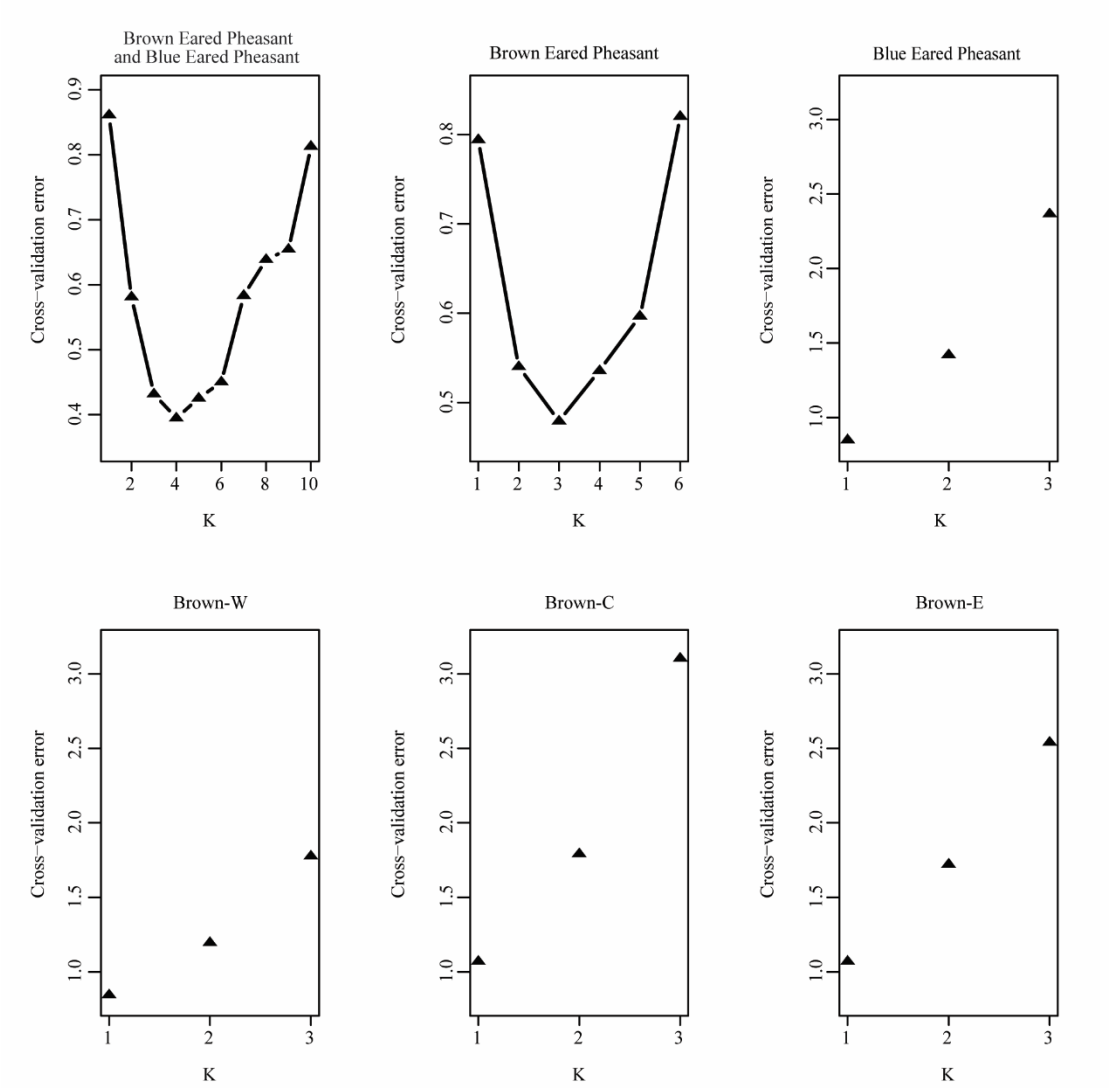


Fig. S3. Cross-validation (CV) values of different ancestral number (K) values. The CV values from the ADMIXTURE analyses performed on the different population scales with 10 independent runs with different random seeds.

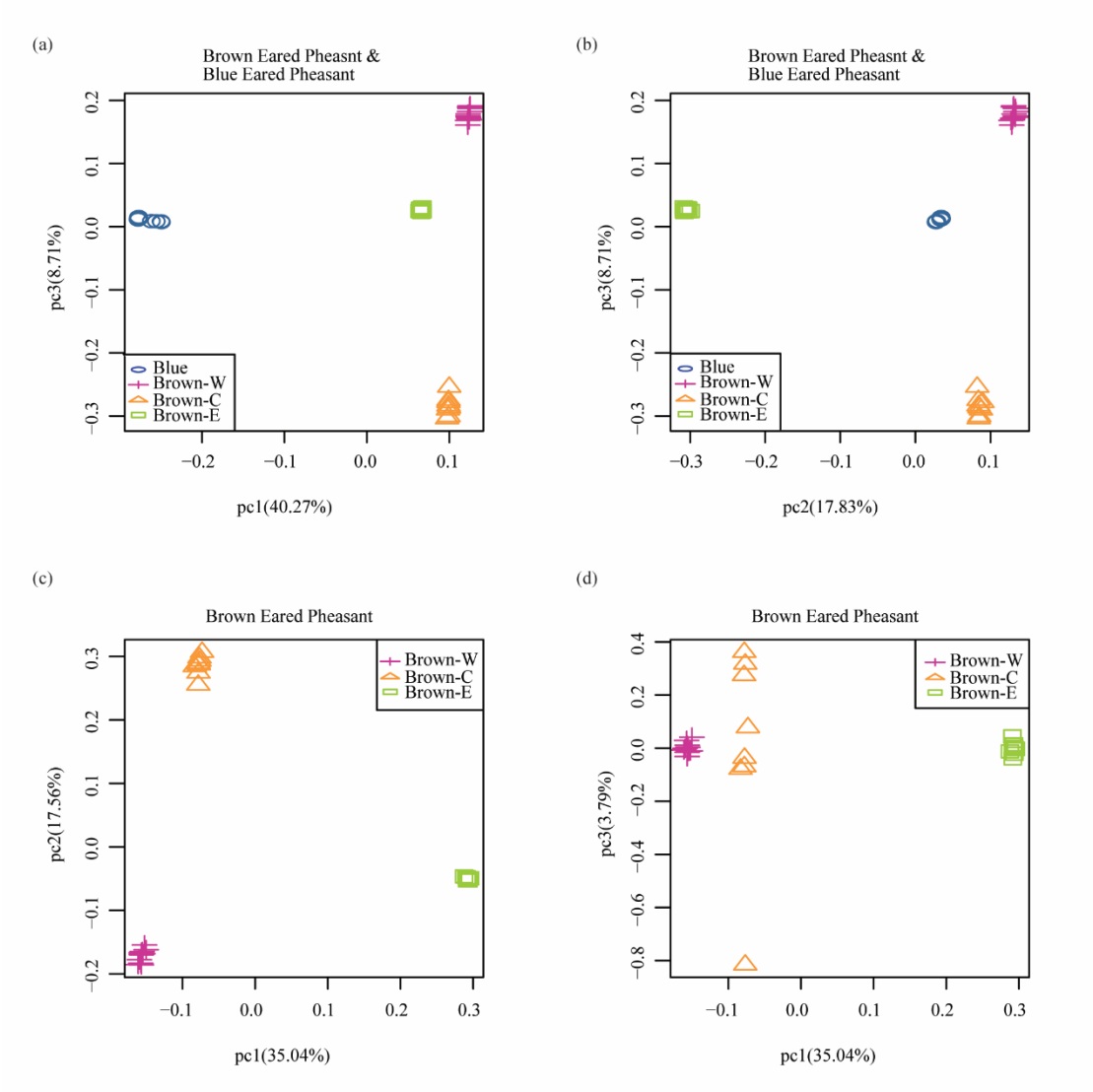


Fig. S4. Principal component analysis (PCA) of *Crossoptilon mantchuricum* and *Crossoptilon auritum*. The numbers in brackets are the contribution values of the corresponding eigenvectors.

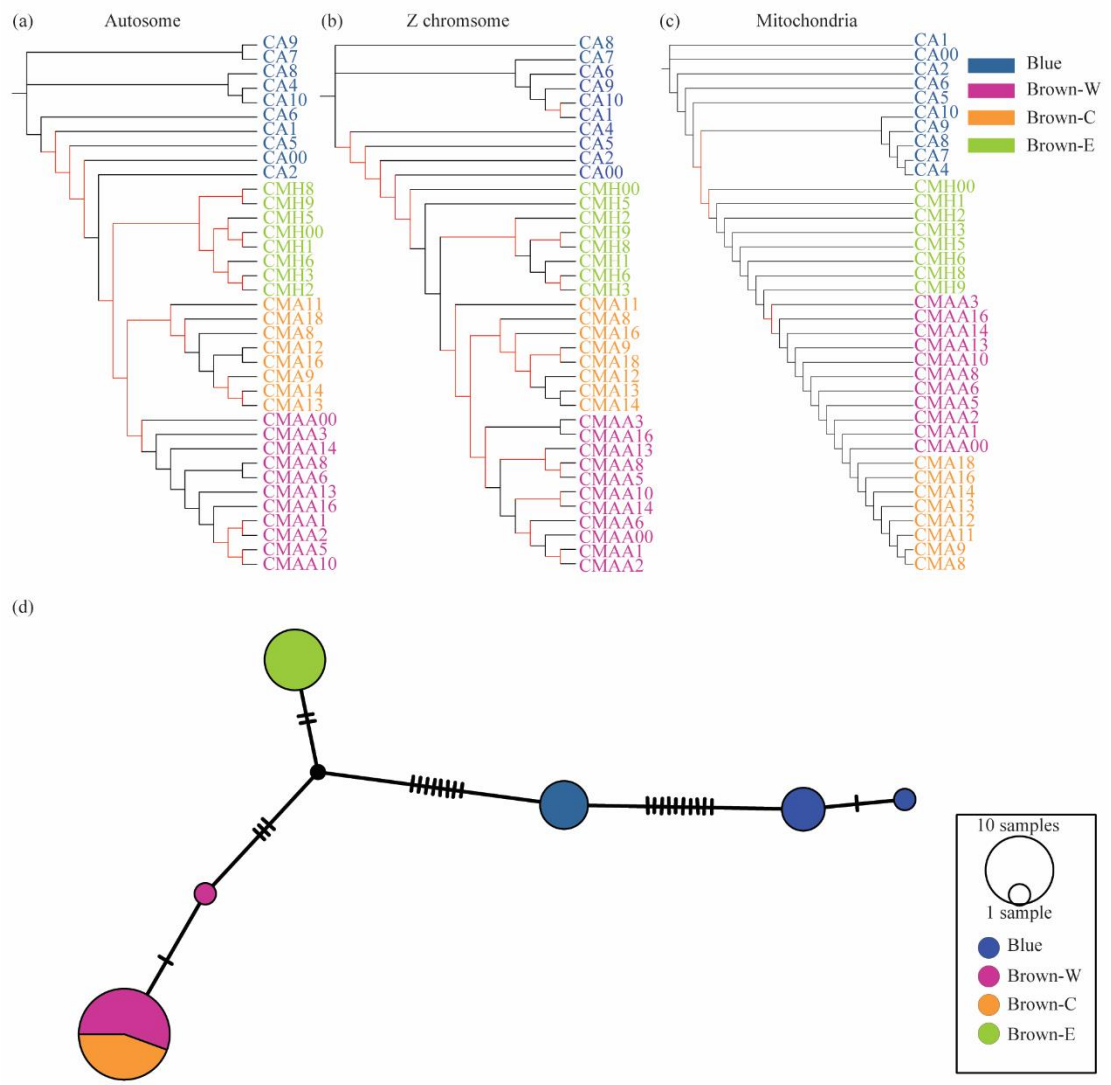


Fig. S5. Phylogenetic relationships and haplotype networks within *Crossoptilon mantchuricum*. The colors represent sampling populations; blue represents *Crossoptilon auritum* (Blue) as outgroups, while orange, green, and red represent the Western (Brown-W), Central (Brown-C), and Eastern (Brown-E) populations of *C. mantchuricum*, respectively. (a), (b), and (c) The unrooted maximum-likelihood (ML) trees reconstructed using autosomes, the Z chromosome, and mitochondria, respectively. The bootstrap values larger than 80% of the bootstrap number were associated with the corresponding branches. (d) Median joining mitochondrial haplotype network. Lines on the linking branches indicate single base variations, and circle size represents the number of samples that share a single haplotype.

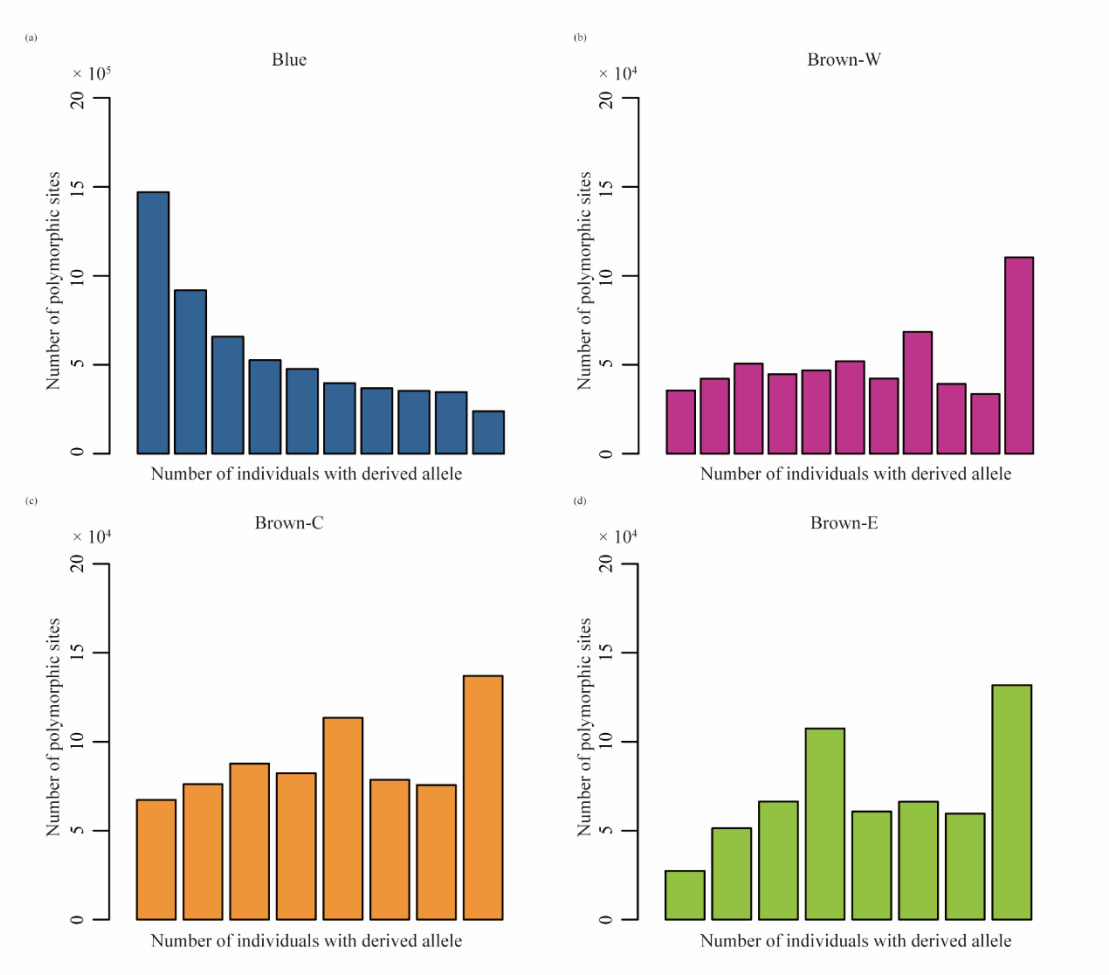


Fig. S6. Folded site frequency spectrum. (a) *C. auritum*. (b) Brown-W, the western population of *C. mantchuricum*. (c) Brown-C, the central population of *C. mantchuricum*. (d) Brown-E, the eastern population of *C. mantchuricum*.

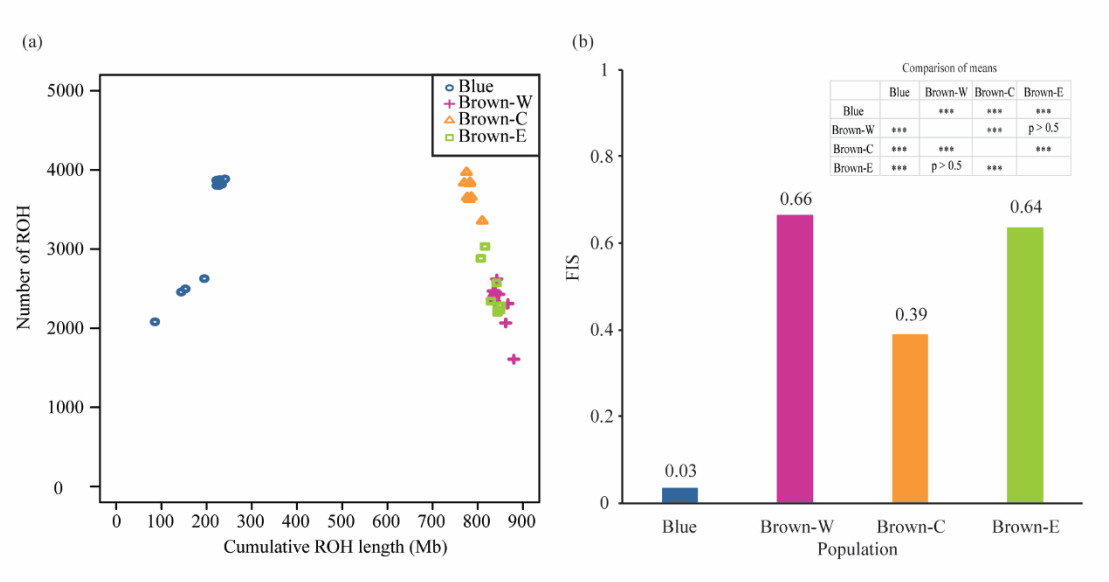


677

678 Fig. S7. Census of the Runs of Homozygosity (ROHs) and inbreeding coefficients ($F_{is}$).

679 (a) The cumulative ROH length against the total number of observed ROH segments

680 for each sample. (b) The mean inbreeding coefficient of each population. Three

681 asterisks indicate that the non-adjusted P values were less than $10^{-3}$.

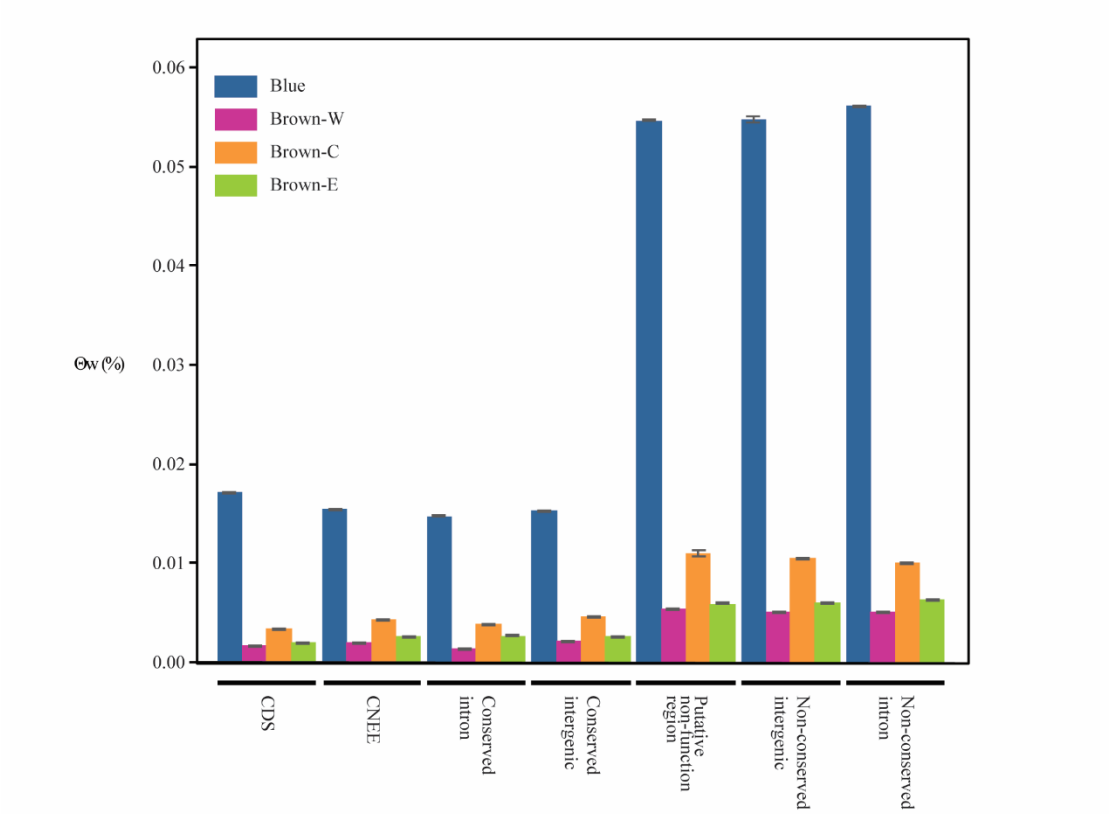


682

683 Fig. S8. Genetic diversity ($\Theta_w$) of each population in different regions (CDS: coding
684 region; CNEE: conserved non-exonic elements; conserved intron; conserved intergenic;
685 putative non-function region; non-conserved intergenic; and non-conserved intron).
686 Error bars represent 95% confidence intervals estimated from 1,000 bootstrap
687 resampling.

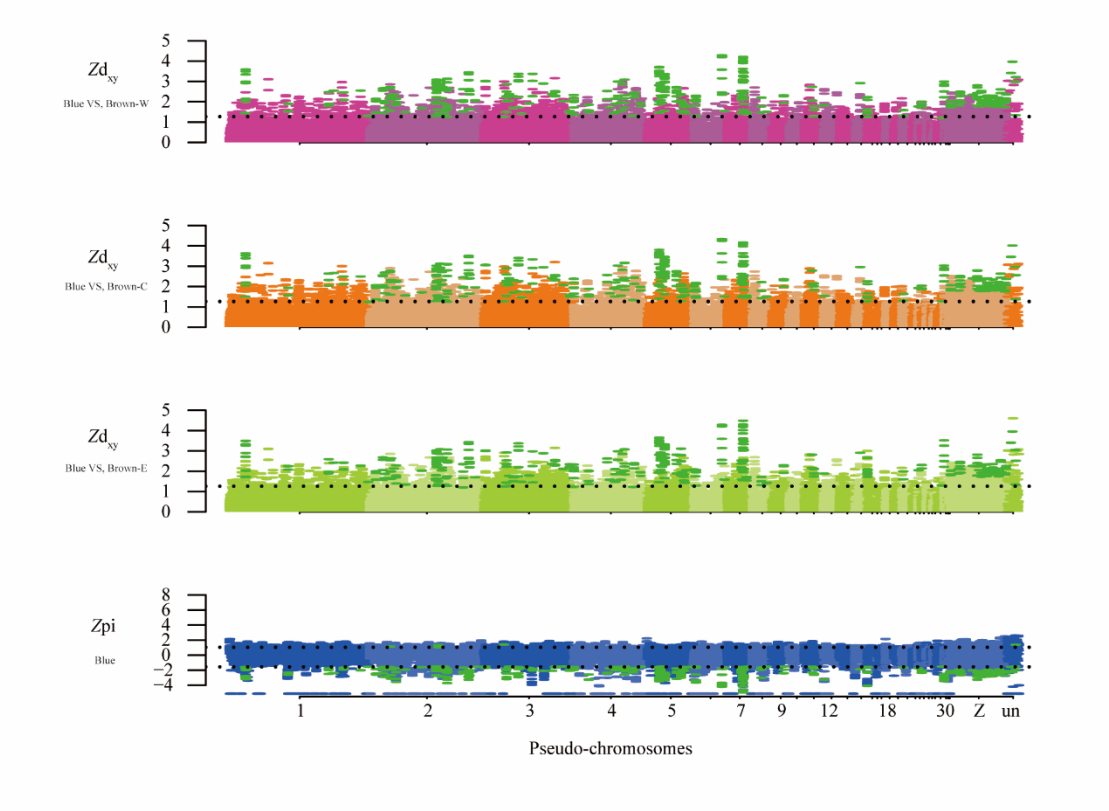


Fig. S9. Manhattan plots of the genome-wide $Zd_{xy}$ and *Z*pi. The points above the dotted line in the *Z*dxy Manhattan plots are the windows with the top 5% *Z*dxy. The points above the upper dotted line and the points under the lower dotted line in the *Z*pi Manhattan plot are the windows with top 5% and bottom 5% *Z*pi. The green points are the windows with the genes putatively under positive selection.

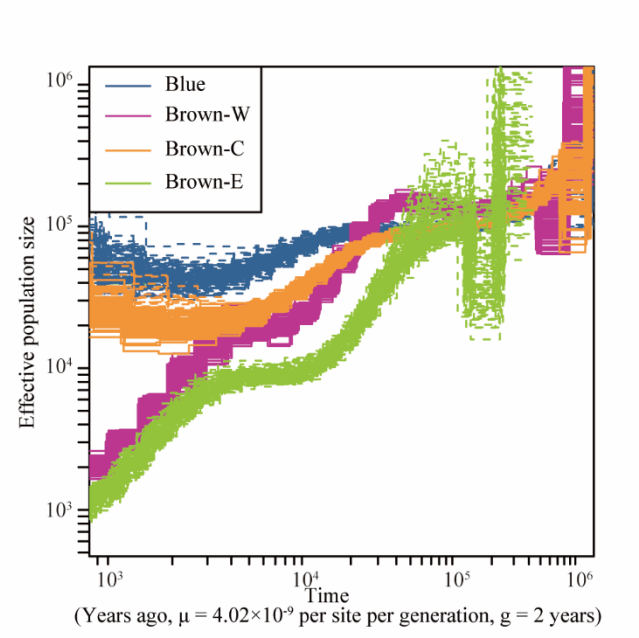


Fig. S10. Demographic history of *Crossoptilon mantchuricum* and *Crossoptilon auritum* estimated from the 100 times MSMC bootstrap. The MSMC results show the demographic history of the four populations. The blue line represents *C. auritum* (Blue); the purple, brown, and green lines represent the Western (Brown-W), Central (Brown-C), and Eastern (Brown-E) populations of *C. mantchuricum*, respectively.

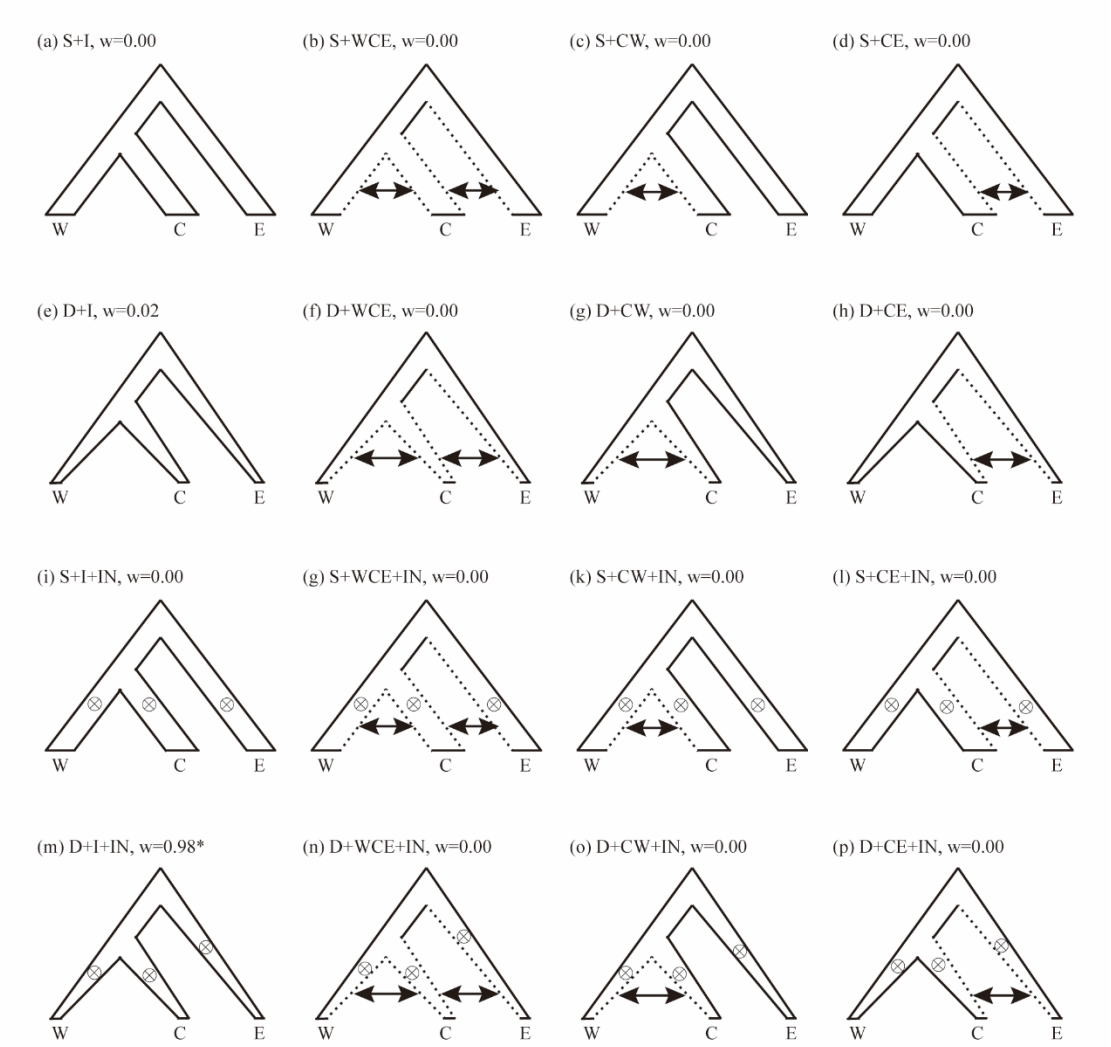


Fig. S11. The demographic models inferred by fastsimcoal26. S represents consistent small population size, D represents population decline, I indicates that there was no gene flow between adjacent populations, WCE indicates that there was gene flow between adjacent populations, CW indicates that the gene flow only existed between the Western and Central populations, CE indicates that the migration only occurred between the Central and Eastern populations, and IN indicates that inbreeding occurred. w represents the Akaike weights. The D+I+IN model obtained the ideal amount of support, which was marked by the asterisk.

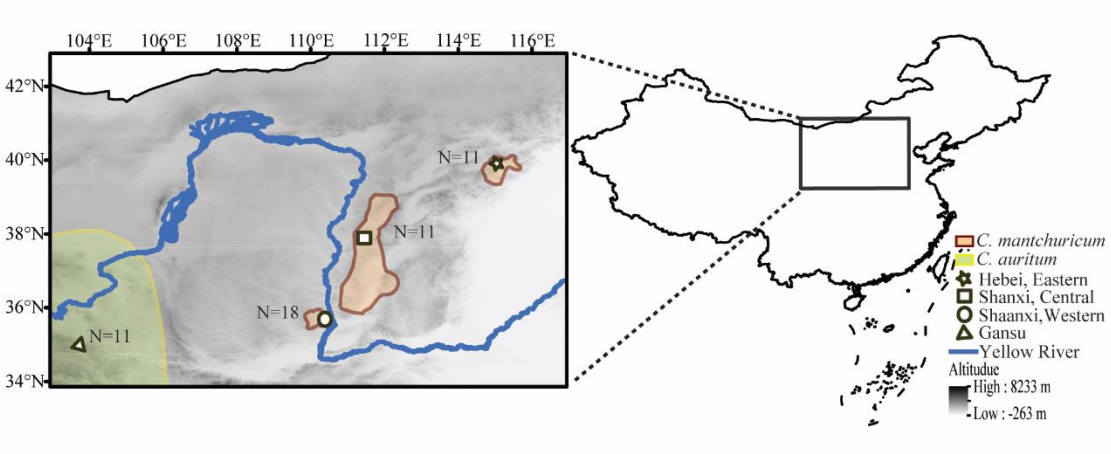


Fig. S12. Sample locations. N indicates the number of samples for each population. The brown regions indicate the distribution of *Crossoptilon mantchuricum*, while the light-yellow region indicates the distribution of *Crossoptilon auritum*. The star represents the Eastern population of *C. mantchuricum* (Brown-E), the square represents the Central population of *C. mantchuricum* (Brown-C), the circle represents the Western population of *C. mantchuricum* (Brown-W), and the triangle represents *C. auritum* (Blue).

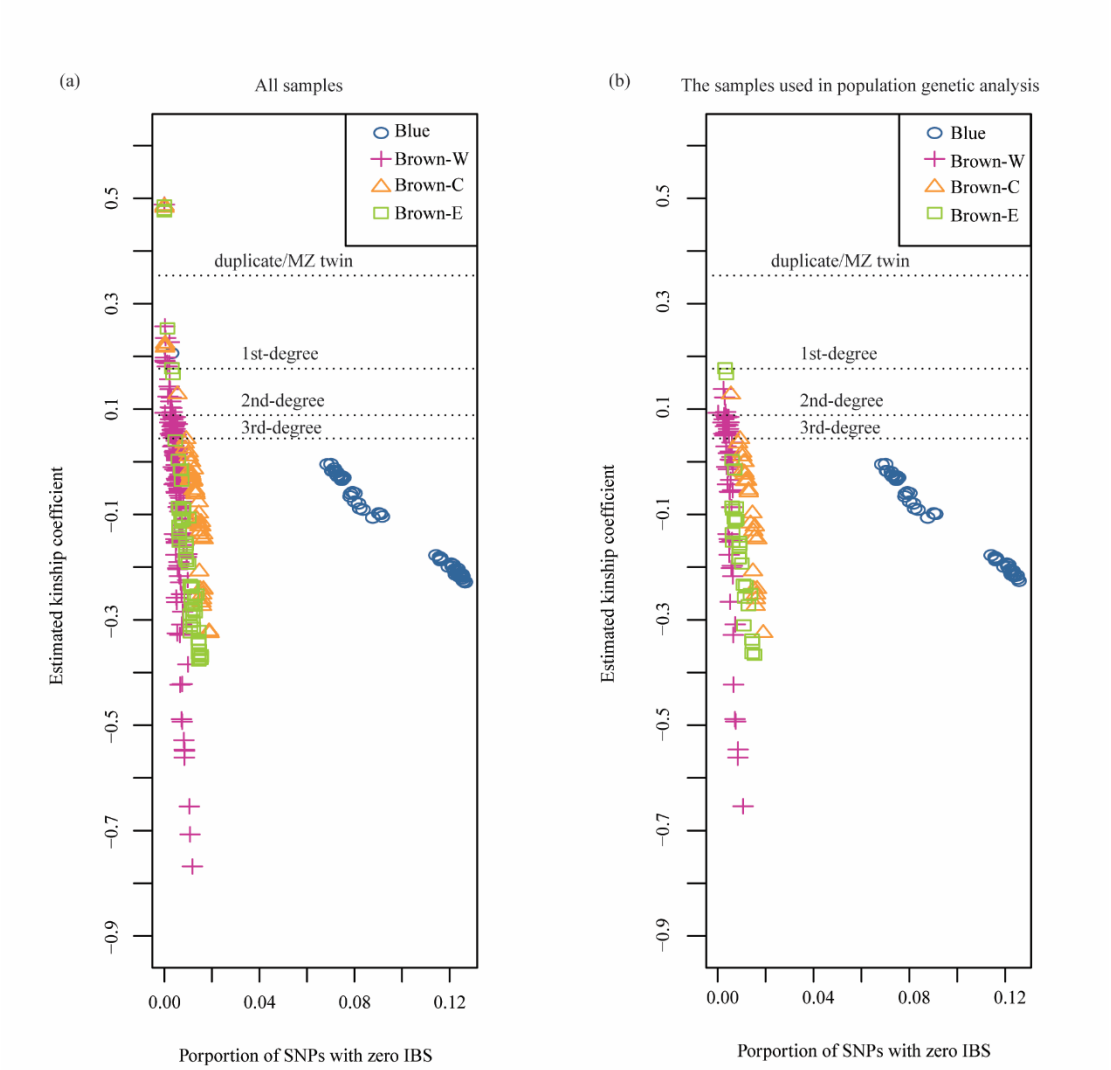


Fig. S13. Individuals' kinship within populations. Zero IBS indicates non-Identical-By-State. The dashed lines show the kinship thresholds (duplicate/MZ twin, 1st-degree, 2nd-degree, 3rd-degree). (a) and (b) show the relatedness of all samples within populations and the individuals used in the population genetic analysis in each population, respectively.

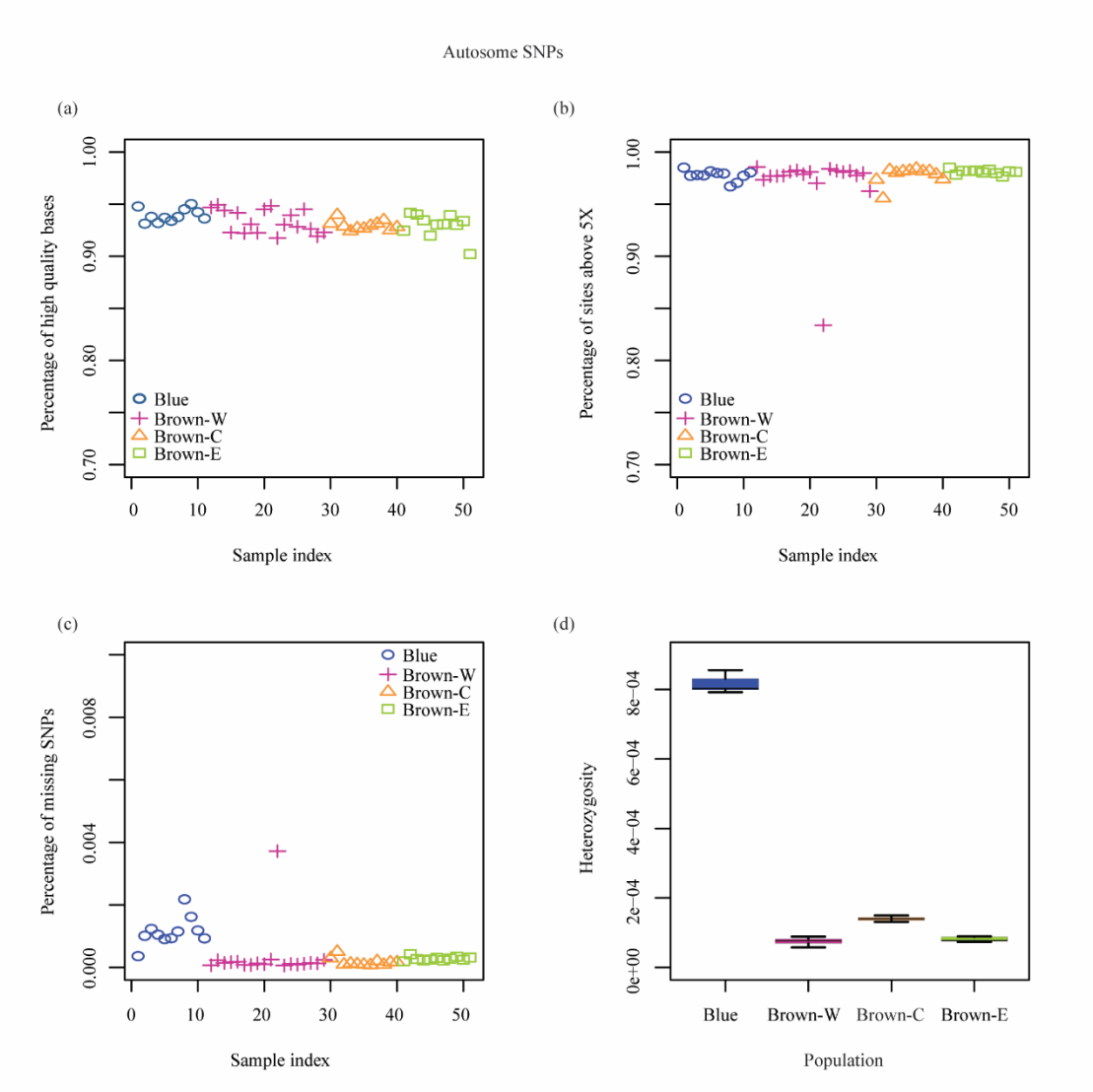


Fig. S14. Variant quality metrics of autosomes. The corresponding sample of each sample index can be seen in Supplementary Dataset S11. (a) Individual percentage of high-quality sites in the BAM file (the call quality of the bases was Q20 or higher). (b) Individual percentage of sites in the BAM file with coverage greater than 5 X. (c) Individual percentage of missing SNPs. (d) Heterozygosity of each sample in the four populations. In the box plots, the bold black line represents the median, and the boxes limit the 25$^{th}$ and 75$^{th}$ percentiles of the distributions.

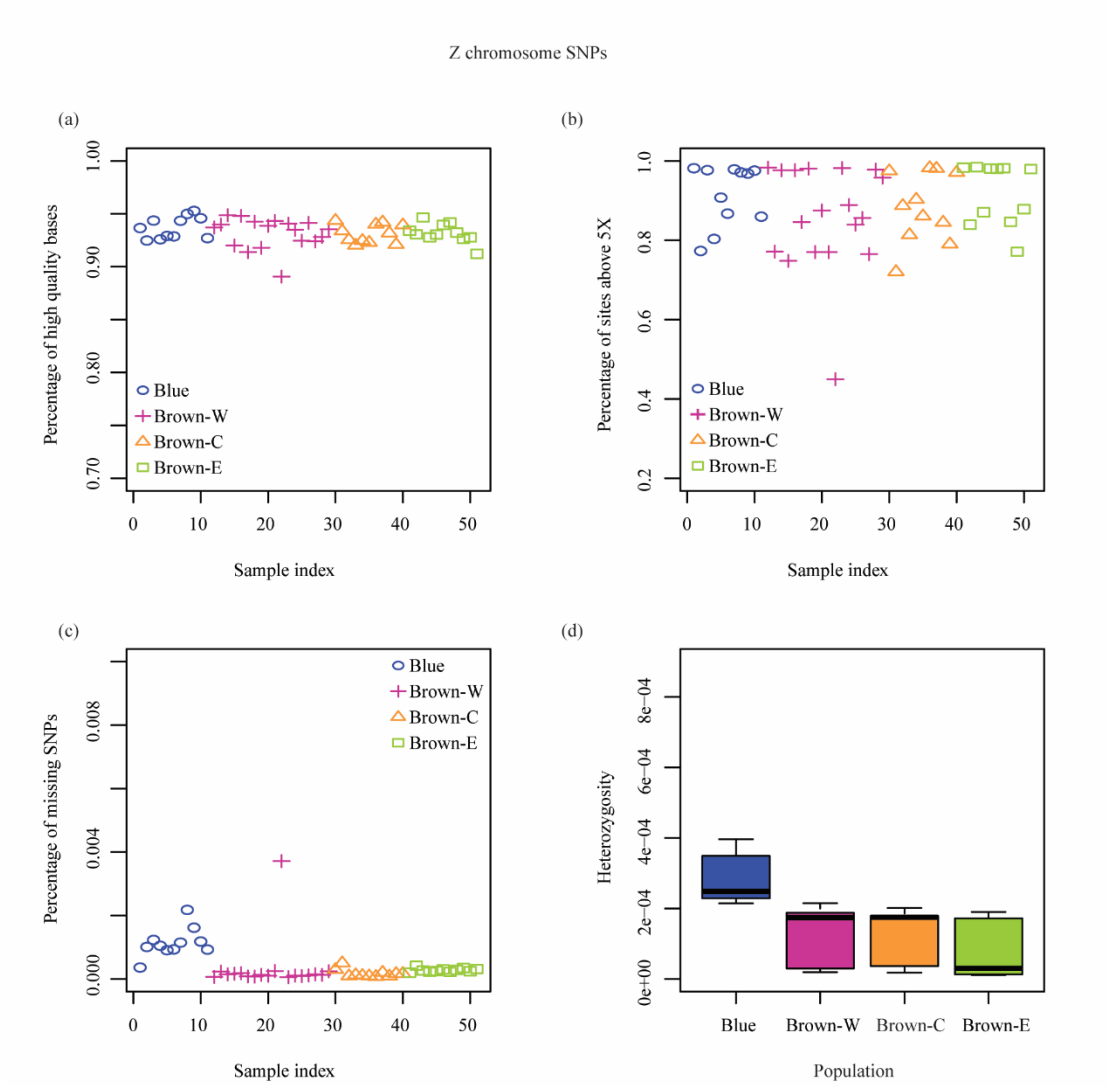


Fig. S15. Variant quality metrics of the Z chromosome. The corresponding sample of each sample index can be seen in Supplementary Dataset S11. (a) Individual percentage of high-quality sites in the BAM file (the call quality of the bases was Q20 or higher). (b) Individual percentage of sites in the BAM file with coverage greater than 5 X. (c) Individual percentage of missing SNPs. (d) Heterozygosity of each sample in the four populations. In the box plots, the bold black line represents the median, and the boxes limit the 25$^{th}$ and 75$^{th}$ percentiles of the distributions.

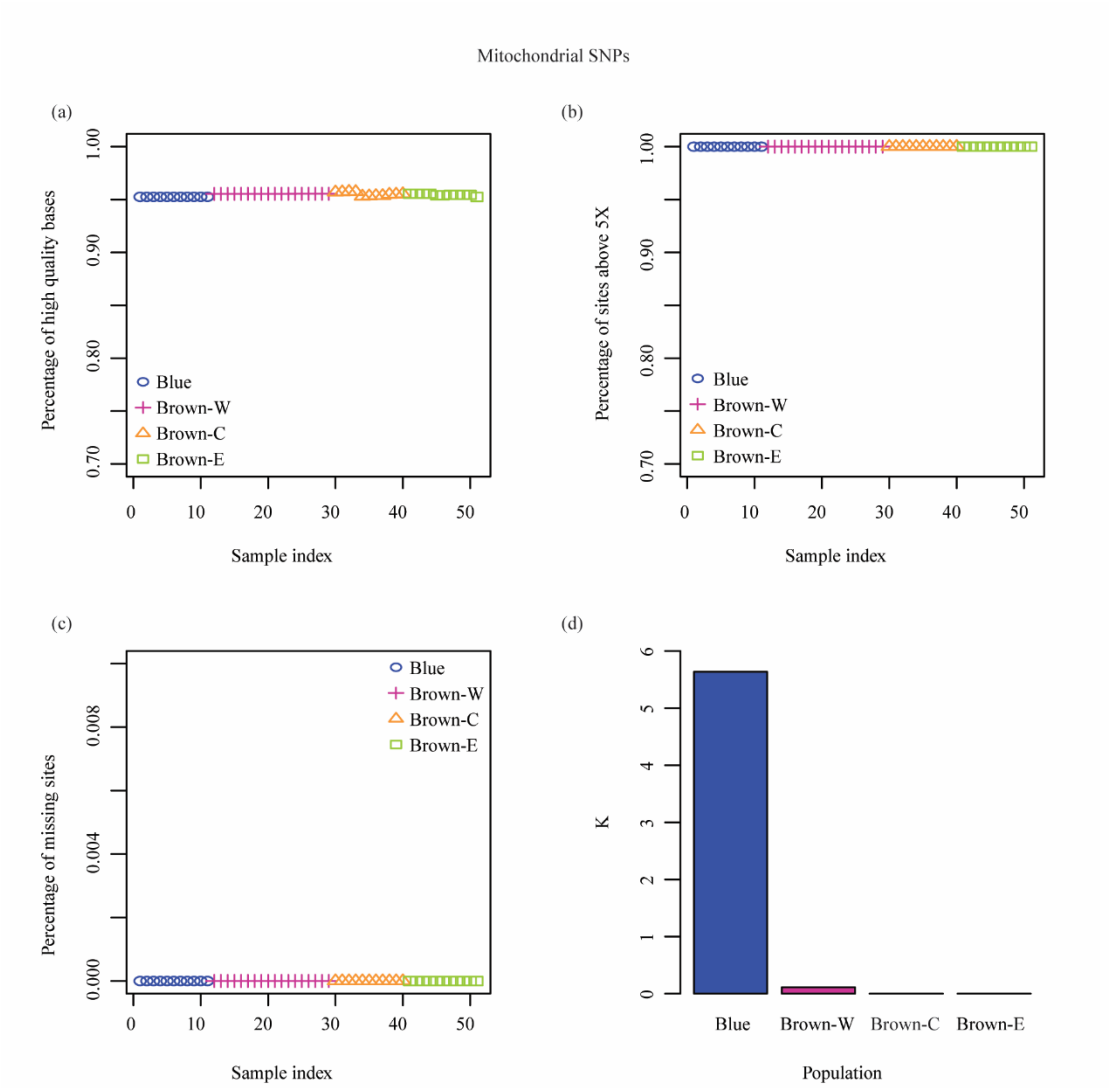


Fig. S16. Variant quality metrics of the mitogenome. The corresponding sample of each sample index can be seen in Supplementary Dataset S11. (a) Individual percentage of high-quality sites in the BAM file (the call quality of the bases was Q20 or higher). (b) Individual percentage of sites in the BAM file with coverage greater than 5 X. (c) Individual percentage of missing sites. (d) Average number of nucleotide differences for each population (K).

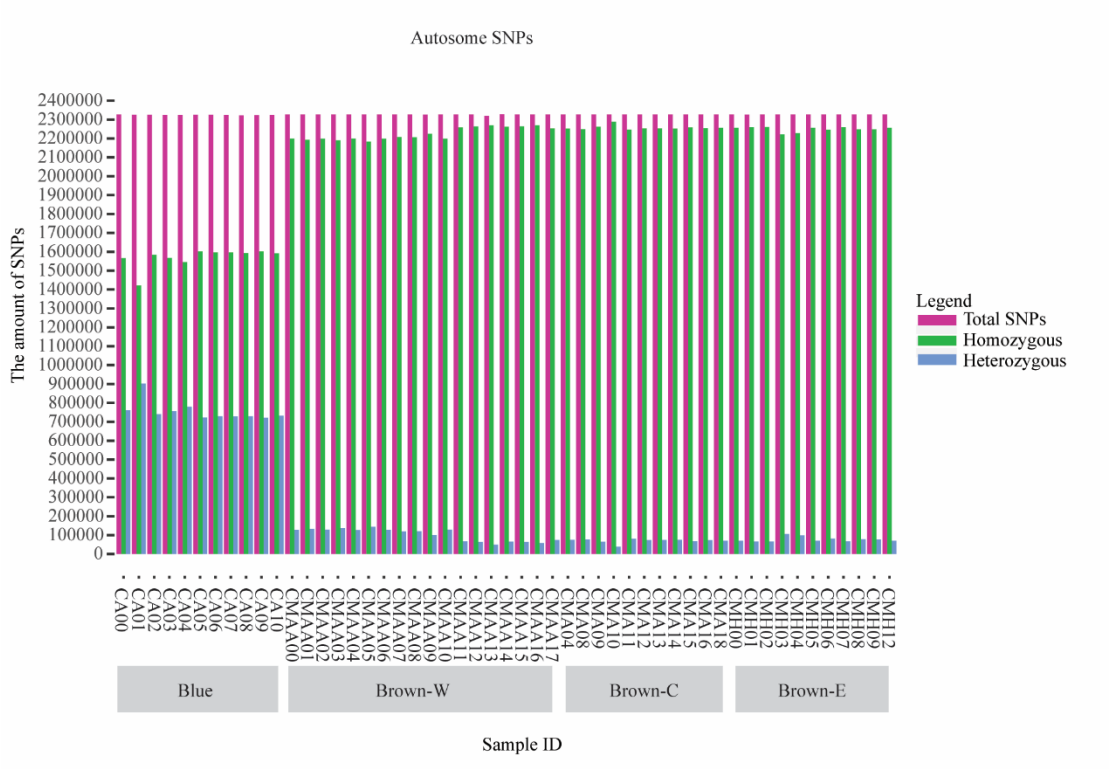


Fig. S17. Variant number of autosomes for the 51 individuals on a population-scale. Sample IDs with the abbreviations Blue, Brown-W, Brown-C, and Brown-E denoted individuals from *Crossoptilon auritum* and the Western, Central, and Eastern populations of *Crossoptilon mantchuricum*, respectively.

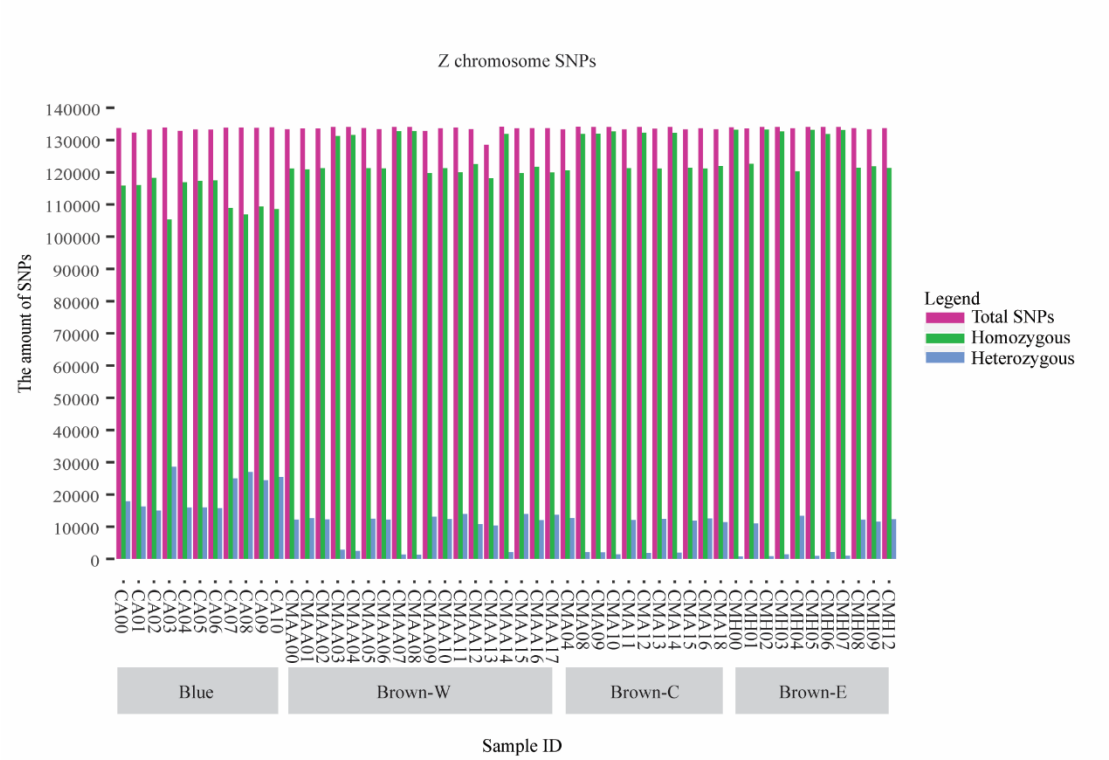


Fig. S18. Variant number of the Z chromosome for the 51 individuals on a population-scale. Sample IDs with the abbreviations Blue, Brown-W, Brown-C, and Brown-E indicate individuals from *Crossoptilon auritum* and the Western, Central, and Eastern populations of *Crossoptilon mantchuricum*, respectively.

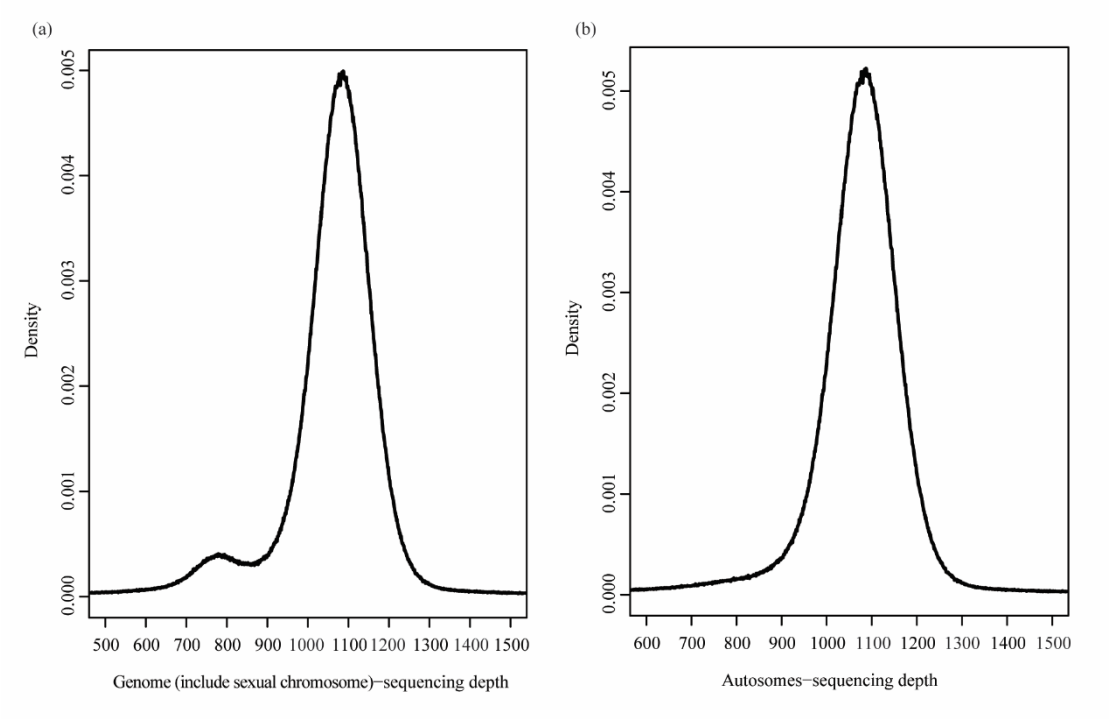


Fig. S19. Distribution of sequencing depth across 51 individuals for (a) the whole genome (including sex chromosomes) and (b) the autosomes.

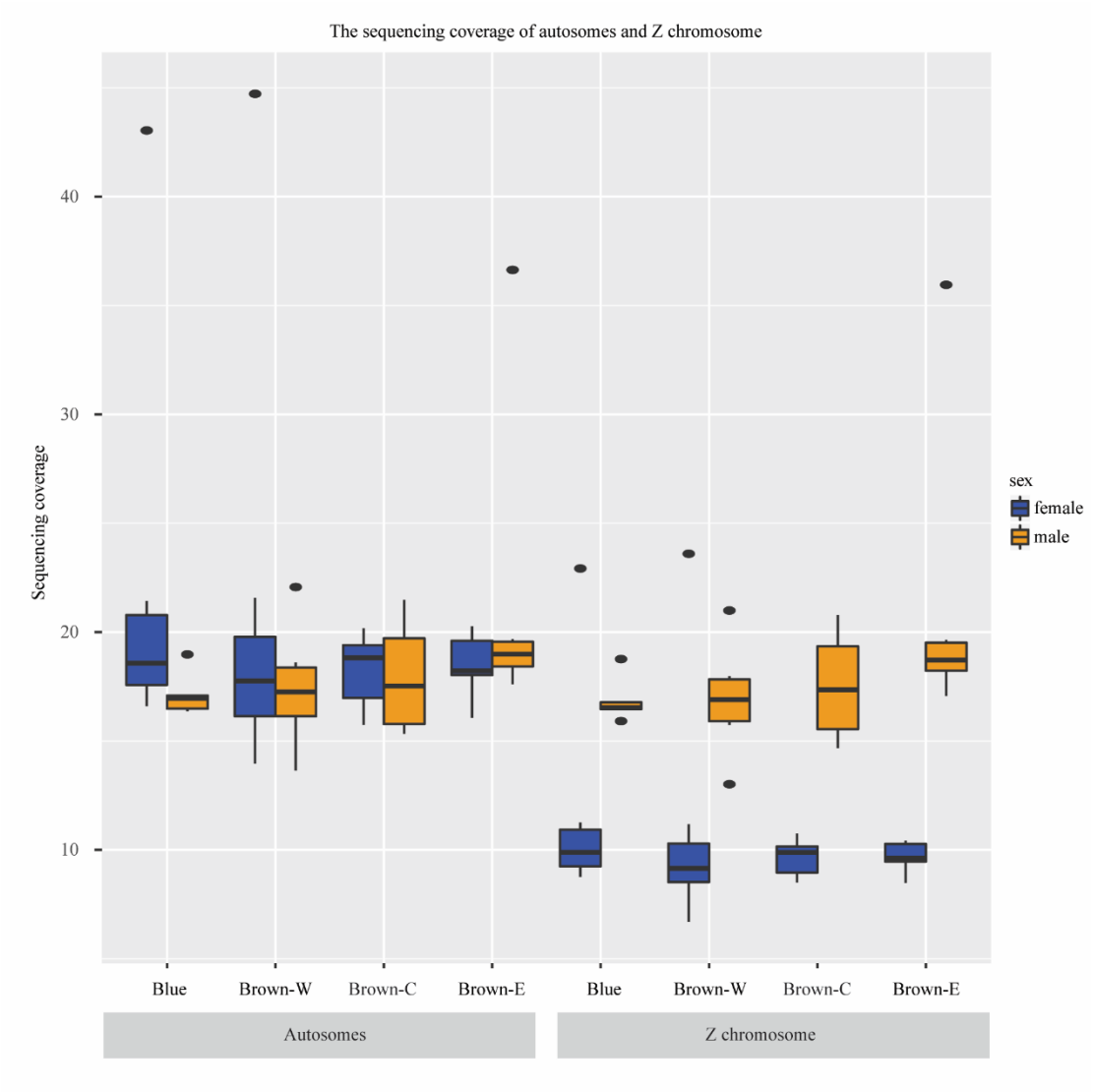


Fig. S20. Sequencing coverage of males and females. Blue boxes indicate the summary of the female individuals, orange boxes indicate the summary of the male individuals. In the box plots, the bold black line represents the median, and the boxes limit the 25$^{th}$ and 75$^{th}$ percentiles of the distributions, while the points are the outlier values. The label under the plots indicates the population symbol and genomic part.

Dataset S1: Completeness evaluation results.

| | Draft genome |
|---|---|
| Complete and single-copy BUSCOs (S) | 4624 (94.08%) |
| Complete and duplicated BUSCOs (D) | 52 (1.06%) |
| Fragmented BUSCOs (F) | 134 (2.73%) |
| Missing BUSCOs (M) | 105 (2.14%) |
| Total BUSCO groups searched | 4915 |

Dataset S2: Summary of the genetic diversity (heterozygous SNP rate) of inbreeding and outbreeding birds on an autosome scale. The genetic diversity of *Crossoptilon mantchuricum* and *Crossoptilon auritum* is the average value within each isolated population. The genetic diversity of other organisms is the lowest value in the corresponding reported population.

| Species | Common_Name | Class | IUCN status | Heterozygous SNP rate | Seq_Type | Source DOI |
|---|---|---|---|---|---|---|
| *Crossoptilon mantchuricum* | Brown eared pheasant (Western) | Aves | Vulnerable | 7.33E-05 | genome-wide | Cureent study |
| *Crossoptilon mantchuricum* | Brown eared pheasant (Eastern) | Aves | Vulnerable | 8.73E-05 | genome-wide | Cureent study |
| *Crossoptilon mantchuricum* | Brown eared pheasant (Center) | Aves | Vulnerable | 1.37E-04 | genome-wide | Cureent study |
| *Haliaeetus albicilla* | White tailed eagle | Aves | Least Concern | 4.00E-04 | genome-wide | 10.1186/s13059-014-0557-1 |
| *Haliaeetus leucocephalus* | Bald eagle | Aves | Least Concern | 4.30E-04 | genome-wide | 10.1186/s13059-014-0557-1 |
| *Nipponia nippon* | Crested ibis | Aves | Endangered | 4.30E-04 | genome-wide | 10.1186/s13059-014-0557-1 |
| *Pelecanus crispus* | Dalmatian pelican | Aves | Near Threatened | 6.00E-04 | genome-wide | 10.1186/s13059-014-0557-1 |
| *Falco peregrinus* | Peregrine falcon | Aves | Least Concern | 7.00E-04 | genome-wide | 10.1038/ng.2588 |
| *Aptenodytes patagonicus* | King penguin | Aves | Least Concern | 7.20E-04 | RNAseq | 10.1038/nature13685 |
| *Eudyptes moseleyi* | Northern rockhopper penguin | Aves | Endangered | 7.97E-04 | RNAseq | 10.1038/nature13685 |
| *Falco cherrug* | Saker falcon | Aves | Endangered | 8.00E-04 | genome-wide | 10.1038/ng.2588 |
| *Crossoptilon auritum* | Blue eared pheasant | Aves | Least Concern | 8.25E-04 | genome-wide | Cureent study |
| *Nestor notabilis* | Kea | Aves | Endangered | 9.10E-04 | genome-wide | 10.1186/s13059-014-0557-1 |
| *Eudyptes chrysocome filholi* | Eastern rockhopper penguin | Aves | Vulnerable | 1.14E-03 | RNAseq | 10.1038/nature13685 |
| *Ectopistes migratorius* | Passenger pigeon | Aves | Extinct | 1.20E-03 | genome-wide | 10.1073/pnas.1401526111 |
| *Cyanistes caeruleus* | Eurasian blue tit | Aves | Least Concern | 1.27E-03 | RNAseq | 10.1038/nature13685 |
| *Phalacrocorax carbo* | Great black cormorant | Aves | Least Concern | 1.39E-03 | genome-wide | 10.1186/s13059-014-0557-1 |
| *Taeniopygia guttata* | Zebra finch | Aves | Least Concern | 1.40E-03 | genome-wide | 10.1038/nature08819 |

| | | | | | | |
|---|---|---|---|---|---|---|
| *Apteryx mantelli* | Kiwi | Aves | Vulnerable | 1.50E-03 | genome-wide | 10.1186/s13059-015-0711-4 |
| *Meleagris gallopavo* | Wild turkey | Aves | Least Concern | 2.37E-03 | genome-wide | 10.1371/journal.pbio.1002112 |
| *Egretta garzetta* | Little egret | Aves | Least Concern | 2.51E-03 | genome-wide | 10.1186/s13059-014-0557-1 |
| *Anas platyrhynchos* | Mallard | Aves | Least Concern | 2.61E-03 | genome-wide | 10.1038/ng.2657 |
| *Ficedula albicollis* | Collared flycatcher | Aves | Least Concern | 3.80E-03 | genome-wide | 10.1371/journal.pbio.1002112 |
| *Melopsittacus undulatus* | Budgerigar | Aves | Least Concern | 4.31E-03 | genome-wide | 10.1186/s13059-014-0557-1 |
| *Gallus gallus* | Chicken | Aves | Least Concern | 5.88E-03 | genome-wide | 10.1371/journal.pbio.1002112 |

Dataset S3: Genetic diversity of the zero-fold degenerate sites and four-fold degenerate sites. The numbers in brackets are 95% confidence intervals, which were obtained from bootstrapping 1,000 times.

| Site Class | Population | $\Theta_\pi$ (%), 95% CI | $\Theta_w$ (%), 95% CI | $\Theta_\pi$ (zero-fold) / $\Theta_\pi$ (fold-fold) |
|---|---|---|---|---|
| zero-fold | Blue | 0.030145% [0.030136%, 0.030154%] | 0.020448% [0.020442%, 0.020453%] | 0.273340 [0.273220, 0.273459] |
| | Brown-W | 0.002670% [0.002666%, 0.002675%] | 0.002237% [0.002234%, 0.002240%] | 0.308766 [0.307968, 0.309564] |
| | Brown-C | 0.005474% [0.005467%, 0.005481%] | 0.004528% [0.004523%, 0.004533%] | 0.318080 [0.317500, 0.318661] |
| | Brown-E | 0.003683% [0.003678%, 0.003689%] | 0.002817% [0.002813%, 0.002821%] | 0.369310 [0.368405, 0.370215] |
| four-fold | Blue | 0.110287% [0.110255%, 0.110320%] | 0.074654% [0.074636%, 0.074672%] | |
| | Brown-W | 0.008657% [0.008640%, 0.008675%] | 0.006903% [0.006891%, 0.006916%] | |
| | Brown-C | 0.017218% [0.017194%, 0.017242%] | 0.014164% [0.014145%, 0.014182%] | |
| | Brown-E | 0.009983% [0.009964%, 0.010001%] | 0.007687% [0.007673%, 0.007701%] | |

Dataset S4: The derived loss-of-function mutations in the potential adaptive genes.

| Gene ID | The frequency of derived loss-of-function (LOF) mutations | | | | Protein ID | Protein name | The site of amino acid substitution | Function |
|---|---|---|---|---|---|---|---|---|
| | Blue | Brown-W | Brown-C | Brown-E | | | | |
| EARP_00000097 | 0.8 | 0 | 0 | 0 | EARP_00000097-RA | helix-turn-helix domain-containing protein | Q552* | regulate gene expression |
| EARP_00005078 | 0.1 | 1 | 1 | 1 | EARP_00005078-RB | ring finger protein 146 | K361* | facilitate DNA repair and protect against cell death |

Dataset S5: The derived missense mutations in the potential adaptive genes. A PROVEAN score less than -2.5 indicates that the corresponding derived missense mutations were deleterious. Blue represents *Crossoptilon auritum* , while Brown-W, Brown-C, and Brown-E represent the Western, Central, and Eastern populations of *Crossoptilon mantchuricum* , respectively.

| Protenin ID | The site of amino acid substitution | Frequency | | | | Proven scores | Unique fixed to *C. mantchuricum* ? | Unique fixed to *C. auritum* ? |
|---|---|---|---|---|---|---|---|---|
| | | Blue | Brown-W | Brown-C | Brown-E | | | |
| EARP_00000044-RA | D411N | 0.40 | 0.00 | 0.00 | 0.00 | 0.160 | no | no |
| EARP_00000045-RA | R101G | 0.00 | 1.00 | 1.00 | 1.00 | 0.867 | yes | no |
| EARP_00000097-RA | A979T | 0.70 | 0.00 | 0.00 | 0.00 | -4.000 | no | no |
| EARP_00000097-RA | C1895Y | 1.00 | 1.00 | 1.00 | 1.00 | -11.000 | no | no |
| EARP_00000097-RA | D2118G | 0.00 | 1.00 | 1.00 | 1.00 | -7.000 | yes | no |
| EARP_00000097-RA | D2650G | 0.80 | 1.00 | 1.00 | 0.00 | -7.000 | no | no |
| EARP_00000097-RA | D28V | 0.60 | 0.00 | 0.00 | 0.00 | -9.000 | no | no |
| EARP_00000097-RA | E631K | 0.60 | 0.00 | 0.00 | 0.00 | -4.000 | no | no |
| EARP_00000097-RA | E63V | 0.50 | 1.00 | 1.00 | 1.00 | -7.000 | no | no |
| EARP_00000097-RA | F19L | 0.20 | 1.00 | 1.00 | 1.00 | -6.000 | no | no |
| EARP_00000097-RA | F2851S | 0.40 | 1.00 | 1.00 | 1.00 | -8.000 | no | no |
| EARP_00000097-RA | F303Y | 0.70 | 1.00 | 1.00 | 1.00 | -3.000 | no | no |
| EARP_00000097-RA | G1018D | 0.00 | 1.00 | 1.00 | 0.00 | -7.000 | yes | no |
| EARP_00000097-RA | G39R | 0.10 | 1.00 | 1.00 | 1.00 | -8.000 | no | no |
| EARP_00000097-RA | L2621F | 0.00 | 1.00 | 1.00 | 0.00 | -4.000 | yes | no |
| EARP_00000097-RA | N777S | 1.00 | 1.00 | 1.00 | 1.00 | -5.000 | no | no |
| EARP_00000097-RA | N785S | 1.00 | 1.00 | 1.00 | 1.00 | -5.000 | no | no |
| EARP_00000097-RA | P1235L | 0.00 | 1.00 | 1.00 | 1.00 | -10.000 | yes | no |
| EARP_00000097-RA | Q851K | 0.00 | 1.00 | 1.00 | 1.00 | -4.000 | yes | no |
| EARP_00000097-RA | R29G | 0.50 | 0.00 | 0.00 | 0.00 | -7.000 | no | no |
| EARP_00000097-RA | R29S | 0.50 | 0.00 | 0.00 | 0.00 | -6.000 | no | no |
| EARP_00000097-RA | R364H | 0.80 | 0.00 | 0.00 | 0.00 | -5.000 | no | no |
| EARP_00000097-RA | R374C | 0.80 | 0.00 | 0.00 | 0.00 | -8.000 | no | no |
| EARP_00000097-RA | S1875P | 0.90 | 1.00 | 1.00 | 1.00 | -5.000 | no | no |
| EARP_00000097-RA | S1899F | 0.40 | 0.00 | 0.00 | 0.00 | -6.000 | no | no |
| EARP_00000097-RA | T1451I | 0.90 | 1.00 | 1.00 | 0.00 | -6.000 | no | no |
| EARP_00000097-RA | T2466A | 0.00 | 1.00 | 1.00 | 0.00 | -5.000 | yes | no |
| EARP_00000097-RA | T388S | 0.40 | 1.00 | 1.00 | 1.00 | -4.000 | no | no |
| EARP_00000097-RA | V295I | 0.00 | 1.00 | 1.00 | 1.00 | -1.000 | yes | no |
| EARP_00000097-RA | W1433C | 0.70 | 0.00 | 0.00 | 1.00 | -13.000 | no | no |
| EARP_00000193-RA | V109A | 0.30 | 1.00 | 1.00 | 0.00 | -4.000 | no | no |
| EARP_00000985-RA | P8L | 1.00 | 0.00 | 0.00 | 0.00 | -0.662 | no | yes |
| EARP_00000986-RA | N62S | 1.00 | 0.00 | 0.00 | 0.00 | -0.005 | no | yes |

| | | | | | | | | |
|---|---|---|---|---|---|---|---|---|
| EARP_00000987-RA | R94Q | 0.00 | 1.00 | 1.00 | 1.00 | 2.941 | yes | no |
| EARP_00000987-RA | S28G | 1.00 | 0.00 | 0.00 | 0.00 | 3.198 | no | yes |
| EARP_00000989-RA | H1599N | 0.00 | 0.00 | 0.00 | 0.50 | -5.304 | no | no |
| EARP_00000989-RA | M2378I | 1.00 | 0.00 | 0.00 | 0.00 | -0.534 | no | yes |
| EARP_00000989-RA | S2400I | 1.00 | 0.00 | 0.00 | 0.00 | -1.674 | no | yes |
| EARP_00002145-RB | R43G | 0.70 | 1.00 | 1.00 | 1.00 | -7.000 | no | no |
| EARP_00002148-RA | K24E | 0.70 | 0.00 | 0.00 | 0.00 | -4.000 | no | no |
| EARP_00002148-RA | R38H | 0.60 | 0.00 | 0.00 | 0.00 | -5.000 | no | no |
| EARP_00002233-RA | S134N | 0.90 | 0.00 | 0.00 | 0.00 | -1.428 | no | no |
| EARP_00002234-RB | A1163T | 1.00 | 0.00 | 0.00 | 0.00 | -2.246 | no | yes |
| EARP_00002234-RB | L1777P | 0.00 | 1.00 | 1.00 | 1.00 | 0.517 | yes | no |
| EARP_00002634-RB | G162S | 0.70 | 0.00 | 0.00 | 0.00 | 0.906 | no | no |
| EARP_00002634-RB | T32I | 1.00 | 0.00 | 0.00 | 0.00 | 0.037 | no | yes |
| EARP_00003544-RA | A1335T | 0.10 | 1.00 | 1.00 | 1.00 | 3.314 | no | no |
| EARP_00003544-RA | L1630P | 0.10 | 1.00 | 1.00 | 1.00 | 0.083 | no | no |
| EARP_00003544-RA | S932P | 0.20 | 1.00 | 1.00 | 1.00 | 2.139 | no | no |
| EARP_00003544-RA | V988I | 0.70 | 0.00 | 0.00 | 0.00 | 0.255 | no | no |
| EARP_00003545-RC | T48A | 0.90 | 1.00 | 1.00 | 1.00 | 0.433 | no | no |
| EARP_00003547-RA | H651Q | 0.70 | 0.00 | 0.00 | 0.00 | 0.401 | no | no |
| EARP_00003548-RB | K103E | 0.00 | 1.00 | 1.00 | 1.00 | 0.389 | yes | no |
| EARP_00003548-RB | Y122D | 0.00 | 1.00 | 1.00 | 1.00 | 2.078 | yes | no |
| EARP_00005078-RB | G339R | 0.20 | 1.00 | 1.00 | 1.00 | -8.000 | no | no |
| EARP_00005078-RB | H401R | 0.10 | 1.00 | 1.00 | 1.00 | -8.000 | no | no |
| EARP_00005078-RB | H401Y | 1.00 | 0.00 | 0.00 | 0.00 | -6.000 | no | yes |
| EARP_00005078-RB | N337S | 0.20 | 1.00 | 1.00 | 1.00 | -5.000 | no | no |
| EARP_00005078-RB | Q247R | 0.00 | 1.00 | 1.00 | 1.00 | -4.000 | yes | no |
| EARP_00005078-RB | R141W | 1.00 | 0.00 | 0.00 | 0.00 | -2.000 | no | yes |
| EARP_00005078-RB | R444G | 1.00 | 0.00 | 0.00 | 0.00 | -1.000 | no | yes |
| EARP_00005078-RB | S142F | 0.00 | 0.00 | 0.25 | 0.88 | -6.000 | no | no |
| EARP_00005078-RB | T362I | 0.10 | 1.00 | 1.00 | 1.00 | -6.000 | no | no |
| EARP_00005078-RB | V132M | 1.00 | 0.00 | 0.00 | 0.00 | -3.000 | no | yes |
| EARP_00006312-RA | A162P | 0.80 | 0.00 | 0.00 | 0.00 | -5.000 | no | no |
| EARP_00006312-RA | W409L | 0.40 | 0.00 | 0.00 | 0.00 | -13.000 | no | no |
| EARP_00006312-RA | Y714H | 0.20 | 1.00 | 1.00 | 1.00 | -5.000 | no | no |
| EARP_00006313-RA | V812A | 0.40 | 1.00 | 1.00 | 1.00 | -4.000 | no | no |
| EARP_00006344-RA | G7D | 0.70 | 0.00 | 0.00 | 0.00 | -7.000 | no | no |
| EARP_00006349-RB | I201V | 0.60 | 0.00 | 0.00 | 0.00 | 0.427 | no | no |
| EARP_00006349-RB | V326A | 0.80 | 0.00 | 0.00 | 0.00 | -0.455 | no | no |
| EARP_00006356-RA | A95T | 0.00 | 1.00 | 1.00 | 0.75 | -0.252 | yes | no |
| EARP_00006357-RC | V86L | 0.00 | 1.00 | 1.00 | 1.00 | 0.494 | yes | no |
| EARP_00006614-RD | E383K | 1.00 | 0.00 | 0.00 | 0.00 | -1.865 | no | yes |

| | | | | | | | | |
|---|---|---|---|---|---|---|---|---|
| EARP_00007488-RA | I62V | 1.00 | 1.00 | 1.00 | 1.00 | 0.054 | no | no |
| EARP_00007490-RA | E1110K | 0.00 | 0.00 | 1.00 | 0.00 | -0.487 | yes | no |
| EARP_00007490-RA | V5M | 0.40 | 0.00 | 0.00 | 0.00 | -0.106 | no | no |
| EARP_00007491-RA | R77S | 0.00 | 1.00 | 1.00 | 1.00 | -6.000 | yes | no |
| EARP_00007492-RB | G579R | 0.70 | 0.00 | 0.00 | 0.00 | -7.828 | no | no |
| EARP_00007492-RB | H1120N | 1.00 | 0.00 | 0.00 | 0.00 | -1.144 | no | yes |
| EARP_00007492-RB | L479P | 0.00 | 1.00 | 1.00 | 1.00 | 3.457 | yes | no |
| EARP_00007492-RB | P353H | 0.00 | 1.00 | 1.00 | 1.00 | 1.750 | yes | no |
| EARP_00007492-RB | R559G | 0.00 | 1.00 | 1.00 | 1.00 | 3.443 | yes | no |
| EARP_00007492-RB | V418E | 1.00 | 0.00 | 0.00 | 0.00 | -5.531 | no | yes |
| EARP_00007494-RB | L12V | 1.00 | 1.00 | 1.00 | 1.00 | -0.313 | no | no |
| EARP_00007509-RD | L543P | 0.00 | 1.00 | 1.00 | 1.00 | 1.766 | yes | no |
| EARP_00007509-RD | M56L | 0.00 | 1.00 | 1.00 | 1.00 | 1.702 | yes | no |
| EARP_00007510-RC | A6V | 1.00 | 0.00 | 0.00 | 0.00 | -0.138 | no | yes |
| EARP_00007511-RA | E41K | 1.00 | 0.00 | 0.00 | 0.00 | -4.000 | no | yes |
| EARP_00007511-RC | G1815D | 0.00 | 0.36 | 0.13 | 1.00 | 0.107 | yes | no |
| EARP_00008168-RA | L1075F | 0.00 | 1.00 | 1.00 | 1.00 | 1.431 | yes | no |
| EARP_00008168-RA | L1144S | 0.00 | 1.00 | 1.00 | 1.00 | 0.786 | yes | no |
| EARP_00008598-RA | D338E | 0.90 | 0.00 | 0.00 | 0.00 | 0.255 | no | no |
| EARP_00008600-RA | V4M | 0.60 | 1.00 | 1.00 | 1.00 | 1.026 | no | no |
| EARP_00008602-RC | A34V | 0.70 | 0.00 | 0.00 | 0.00 | -0.068 | no | no |
| EARP_00008602-RA | G51R | 0.50 | 0.00 | 0.00 | 0.00 | 0.355 | no | no |
| EARP_00008602-RC | L22W | 0.10 | 1.00 | 1.00 | 1.00 | -0.259 | no | no |
| EARP_00008602-RC | T26A | 0.50 | 0.00 | 0.00 | 0.00 | -0.357 | no | no |
| EARP_00008602-RA | Y78C | 0.10 | 1.00 | 1.00 | 1.00 | -0.378 | no | no |
| EARP_00008602-RA | Y78H | 0.10 | 1.00 | 1.00 | 1.00 | 0.000 | no | no |
| EARP_00008603-RB | I842V | 0.70 | 0.00 | 0.00 | 0.00 | 0.452 | no | no |
| EARP_00008603-RB | T311I | 0.00 | 1.00 | 0.25 | 0.00 | 3.975 | yes | no |
| EARP_00008603-RB | V382M | 0.20 | 0.00 | 0.00 | 1.00 | -1.846 | no | no |
| EARP_00009935-RA | F57S | 0.30 | 1.00 | 1.00 | 1.00 | -8.000 | no | no |
| EARP_00009935-RA | V65M | 0.90 | 0.00 | 0.00 | 0.00 | -3.000 | no | no |
| EARP_00010173-RA | A428V | 0.00 | 1.00 | 0.50 | 0.00 | -2.152 | yes | no |
| EARP_00010175-RB | G285E | 1.00 | 0.00 | 0.00 | 0.00 | 0.133 | no | yes |
| EARP_00010175-RB | T949I | 1.00 | 0.00 | 0.00 | 0.00 | -0.011 | no | yes |
| EARP_00011418-RA | L1448M | 0.00 | 0.00 | 0.88 | 0.00 | 1.408 | no | no |
| EARP_00011419-RB | T208A | 0.70 | 0.00 | 0.00 | 0.00 | 0.000 | no | no |
| EARP_00011419-RB | T446A | 0.70 | 0.00 | 0.00 | 0.00 | -0.356 | no | no |
| EARP_00011586-RC | G208A | 0.00 | 1.00 | 1.00 | 0.00 | 0.214 | yes | no |
| EARP_00011586-RC | V33I | 0.10 | 0.00 | 0.00 | 1.00 | -0.297 | no | no |
| EARP_00012749-RA | M467T | 1.00 | 0.00 | 0.00 | 0.00 | 0.574 | no | yes |
| EARP_00012749-RA | S3Y | 0.80 | 0.00 | 0.00 | 0.00 | -1.320 | no | no |

| | | | | | | | | |
|---|---|---|---|---|---|---|---|---|
| EARP_00012844-RA | T1112P | 0.00 | 1.00 | 1.00 | 1.00 | -0.129 | yes | no |
| EARP_00012844-RA | T1198A | 0.00 | 1.00 | 1.00 | 1.00 | 0.431 | yes | no |
| EARP_00012846-RA | S376N | 0.60 | 0.00 | 0.00 | 0.00 | 0.303 | no | no |
| EARP_00012846-RA | V1344E | 0.00 | 1.00 | 1.00 | 1.00 | 1.988 | yes | no |
| EARP_00012848-RA | P104S | 0.20 | 0.00 | 1.00 | 0.00 | -4.667 | no | no |
| EARP_00012944-RA | L33F | 0.00 | 1.00 | 1.00 | 1.00 | -0.391 | yes | no |
| EARP_00013131-RA | R511Q | 0.70 | 0.00 | 0.00 | 0.00 | 0.000 | no | no |
| EARP_00013132-RA | I120V | 1.00 | 0.00 | 0.00 | 0.00 | 1.000 | no | yes |
| EARP_00013132-RA | L474S | 0.00 | 1.00 | 1.00 | 1.00 | 6.000 | yes | no |
| EARP_00013132-RA | M332V | 0.00 | 1.00 | 1.00 | 1.00 | 3.000 | yes | no |
| EARP_00013133-RA | P1884S | 0.80 | 0.00 | 0.00 | 0.00 | 0.337 | no | no |
| EARP_00013133-RA | S1767L | 0.80 | 0.00 | 0.00 | 0.00 | -1.419 | no | no |
| EARP_00013133-RA | T2351A | 1.00 | 0.00 | 0.00 | 0.00 | -0.568 | no | yes |
| EARP_00013133-RA | V2114A | 0.80 | 0.00 | 0.13 | 0.00 | 0.655 | no | no |
| EARP_00013134-RA | T711I | 0.00 | 1.00 | 1.00 | 1.00 | -0.500 | yes | no |
| EARP_00013135-RA | T488K | 0.40 | 0.00 | 0.00 | 0.00 | -6.000 | no | no |
| EARP_00013137-RA | I205M | 0.00 | 1.00 | 1.00 | 1.00 | 1.217 | yes | no |
| EARP_00013138-RA | T664A | 0.60 | 1.00 | 1.00 | 1.00 | -2.663 | no | no |
| EARP_00013139-RA | E1834K | 0.40 | 0.00 | 0.00 | 0.00 | -0.870 | no | no |
| EARP_00013139-RA | H1168Q | 0.40 | 0.00 | 0.00 | 0.00 | 1.333 | no | no |
| EARP_00013139-RA | I742V | 0.80 | 1.00 | 1.00 | 1.00 | 0.467 | no | no |
| EARP_00013139-RA | Q44R | 0.00 | 1.00 | 1.00 | 1.00 | -0.391 | yes | no |
| EARP_00013139-RA | T1428A | 0.50 | 0.00 | 0.00 | 0.00 | -0.216 | no | no |
| EARP_00013142-RA | T43S | 1.00 | 0.00 | 0.00 | 0.00 | -4.000 | no | yes |
| EARP_00013786-RA | F42S | 0.00 | 1.00 | 1.00 | 1.00 | 1.747 | yes | no |
| EARP_00014053-RA | R263C | 0.00 | 0.00 | 0.13 | 0.50 | -3.196 | no | no |
| EARP_00014072-RA | Y80F | 0.70 | 1.00 | 0.88 | 1.00 | -0.948 | no | no |
| EARP_00014073-RD | R56H | 1.00 | 0.00 | 0.00 | 0.00 | -5.000 | no | yes |
| EARP_00014240-RA | V119M | 0.10 | 1.00 | 1.00 | 1.00 | -0.100 | no | no |
| EARP_00014598-RB | E7K | 1.00 | 0.00 | 0.00 | 0.00 | -0.036 | no | yes |
| EARP_00014598-RB | V1549I | 0.00 | 1.00 | 1.00 | 1.00 | -0.021 | yes | no |
| EARP_00015100-RA | A116E | 0.00 | 1.00 | 1.00 | 1.00 | 0.886 | yes | no |
| EARP_00015100-RA | E97D | 0.90 | 0.00 | 0.00 | 0.00 | -0.202 | no | no |
| EARP_00015100-RA | G177D | 1.00 | 0.00 | 0.00 | 0.00 | 1.921 | no | yes |
| EARP_00015100-RA | L9P | 0.00 | 1.00 | 1.00 | 1.00 | -0.022 | yes | no |
| EARP_00015807-RA | L58V | 0.00 | 1.00 | 1.00 | 1.00 | -3.000 | yes | no |
| EARP_00015807-RA | L78P | 0.10 | 1.00 | 1.00 | 1.00 | -7.000 | no | no |
| EARP_00015808-RA | C10R | 1.00 | 0.00 | 0.00 | 0.00 | 0.349 | no | yes |
| EARP_00015808-RA | H23Y | 0.00 | 1.00 | 1.00 | 1.00 | -0.193 | yes | no |
| EARP_00015808-RA | L484P | 0.00 | 1.00 | 1.00 | 1.00 | 3.432 | yes | no |
| EARP_00016036-RA | P908S | 0.00 | 1.00 | 1.00 | 0.50 | 1.395 | yes | no |

| | | | | | | | | |
|---|---|---|---|---|---|---|---|---|
| EARP_00016471-RA | E1545K | 0.90 | 1.00 | 1.00 | 1.00 | 0.792 | no | no |
| EARP_00016471-RA | Q1996H | 0.50 | 1.00 | 1.00 | 1.00 | -0.655 | no | no |
| EARP_00016471-RA | V4I | 0.00 | 1.00 | 1.00 | 1.00 | -0.355 | yes | no |
| EARP_00017025-RF | A628G | 0.00 | 1.00 | 1.00 | 1.00 | -0.100 | yes | no |
| EARP_00017025-RF | R140H | 0.70 | 0.00 | 0.00 | 0.00 | -0.158 | no | no |
| EARP_00017027-RB | S286P | 0.70 | 0.00 | 0.00 | 0.00 | -0.730 | no | no |
| EARP_00017032-RA | V374I | 1.00 | 0.00 | 0.00 | 0.00 | 0.314 | no | yes |
| EARP_00017036-RA | E450D | 0.10 | 1.00 | 1.00 | 1.00 | -1.894 | no | no |
| EARP_00017036-RA | R488C | 0.90 | 0.00 | 0.00 | 0.00 | 0.244 | no | no |
| EARP_00017036-RA | V85I | 0.20 | 1.00 | 1.00 | 1.00 | 0.964 | no | no |
| EARP_00017037-RD | T735A | 0.30 | 1.00 | 1.00 | 1.00 | 0.873 | no | no |
| EARP_00017072-RA | Q136R | 0.00 | 1.00 | 1.00 | 1.00 | -0.347 | yes | no |
| EARP_00017811-RA | L136I | 0.40 | 1.00 | 1.00 | 1.00 | 0.386 | no | no |
| EARP_00017811-RA | M336I | 1.00 | 1.00 | 1.00 | 0.00 | -1.846 | no | no |
| EARP_00017811-RA | V1139A | 1.00 | 1.00 | 1.00 | 1.00 | 0.466 | no | no |

Dataset S6: Genetic diversity of the potential adaptive genes. The genetic diversity is the average value of sites-pi within each gene. Blue represents *Crossoptilon auritum* . Brown-W, Brown-C, and Brown-E represent the Western, Central, and Eastern populations of *Crossoptilon mantchuricum* , respectively.

| Gene ID | Genetic diversity (Π) | | | |
|---|---|---|---|---|
| | Blue | Brown-W | Brown-C | Brown-E |
| EARP_00000007 | 0.00 | 0.00 | 0.00 | 0.00 |
| EARP_00000044 | 0.49 | 0.00 | 0.00 | 0.00 |
| EARP_00000045 | 0.18 | 0.02 | 0.02 | 0.04 |
| EARP_00000046 | 0.17 | 0.03 | 0.02 | 0.11 |
| EARP_00000047 | 0.24 | 0.02 | 0.02 | 0.09 |
| EARP_00000048 | 0.00 | 0.00 | 0.00 | 0.00 |
| EARP_00000097 | 0.32 | 0.00 | 0.01 | 0.00 |
| EARP_00000191 | 0.05 | 0.52 | 0.46 | 0.12 |
| EARP_00000192 | 0.29 | 0.00 | 0.00 | 0.06 |
| EARP_00000193 | 0.20 | 0.07 | 0.07 | 0.04 |
| EARP_00000194 | 0.29 | 0.00 | 0.00 | 0.00 |
| EARP_00009935 | 0.31 | 0.00 | 0.00 | 0.00 |
| EARP_00010171 | 0.00 | 0.00 | 0.00 | 0.00 |
| EARP_00010172 | 0.48 | 0.00 | 0.00 | 0.00 |
| EARP_00010173 | 0.21 | 0.03 | 0.03 | 0.00 |
| EARP_00010174 | 0.10 | 0.00 | 0.00 | 0.00 |
| EARP_00010175 | 0.23 | 0.02 | 0.02 | 0.00 |
| EARP_00002145 | 0.34 | 0.00 | 0.01 | 0.01 |
| EARP_00002146 | 0.18 | 0.00 | 0.00 | 0.00 |
| EARP_00002147 | 0.02 | 0.00 | 0.15 | 0.00 |
| EARP_00002148 | 0.51 | 0.00 | 0.00 | 0.00 |
| EARP_00002231 | 0.15 | 0.00 | 0.05 | 0.21 |
| EARP_00002232 | 0.25 | 0.00 | 0.06 | 0.05 |
| EARP_00002233 | 0.32 | 0.00 | 0.05 | 0.05 |
| EARP_00002234 | 0.15 | 0.00 | 0.06 | 0.05 |
| EARP_00002248 | 0.17 | 0.03 | 0.04 | 0.01 |
| EARP_00002249 | 0.31 | 0.00 | 0.00 | 0.01 |
| EARP_00002250 | 0.30 | 0.00 | 0.00 | 0.00 |
| EARP_00011416 | 0.30 | 0.00 | 0.00 | 0.01 |
| EARP_00011418 | 0.14 | 0.00 | 0.00 | 0.00 |
| EARP_00011419 | 0.40 | 0.00 | 0.00 | 0.00 |
| EARP_00011420 | 0.26 | 0.00 | 0.00 | 0.00 |
| EARP_00011586 | 0.19 | 0.00 | 0.00 | 0.00 |
| EARP_00011725 | 0.36 | 0.00 | 0.06 | 0.00 |
| EARP_00002633 | 0.28 | 0.00 | 0.00 | 0.00 |
| EARP_00002634 | 0.30 | 0.00 | 0.00 | 0.00 |
| EARP_00002780 | 0.25 | 0.00 | 0.00 | 0.03 |

| | | | | |
|---|---|---|---|---|
| EARP_00002781 | 0.00 | 0.00 | 0.00 | 0.00 |
| EARP_00002782 | 0.23 | 0.00 | 0.00 | 0.00 |
| EARP_00002783 | 0.10 | 0.00 | 0.00 | 0.44 |
| EARP_00012228 | 0.00 | 0.00 | 0.00 | 0.00 |
| EARP_00012748 | 0.35 | 0.00 | 0.00 | 0.01 |
| EARP_00012749 | 0.26 | 0.00 | 0.03 | 0.02 |
| EARP_00012844 | 0.32 | 0.01 | 0.00 | 0.00 |
| EARP_00012845 | 0.00 | 0.00 | 0.00 | 0.00 |
| EARP_00012846 | 0.19 | 0.00 | 0.00 | 0.00 |
| EARP_00012847 | 0.28 | 0.00 | 0.00 | 0.00 |
| EARP_00012848 | 0.22 | 0.01 | 0.10 | 0.00 |
| EARP_00012849 | 0.00 | 0.00 | 0.00 | 0.00 |
| EARP_00012850 | 0.23 | 0.00 | 0.08 | 0.00 |
| EARP_00012816 | 0.19 | 0.00 | 0.00 | 0.00 |
| EARP_00012944 | 0.29 | 0.00 | 0.00 | 0.00 |
| EARP_00012945 | 0.18 | 0.00 | 0.00 | 0.00 |
| EARP_00012946 | 0.00 | 0.00 | 0.00 | 0.00 |
| EARP_00013130 | 0.28 | 0.00 | 0.03 | 0.00 |
| EARP_00013131 | 0.26 | 0.00 | 0.02 | 0.00 |
| EARP_00013132 | 0.00 | 0.00 | 0.00 | 0.00 |
| EARP_00013133 | 0.20 | 0.00 | 0.02 | 0.00 |
| EARP_00013134 | 0.18 | 0.00 | 0.01 | 0.00 |
| EARP_00013135 | 0.23 | 0.00 | 0.02 | 0.00 |
| EARP_00013136 | 0.00 | 0.00 | 0.00 | 0.00 |
| EARP_00013137 | 0.07 | 0.00 | 0.05 | 0.00 |
| EARP_00013138 | 0.31 | 0.00 | 0.02 | 0.00 |
| EARP_00013139 | 0.41 | 0.00 | 0.01 | 0.00 |
| EARP_00013142 | 0.28 | 0.01 | 0.01 | 0.00 |
| EARP_00003307 | 0.38 | 0.00 | 0.00 | 0.01 |
| EARP_00013446 | 0.31 | 0.00 | 0.00 | 0.00 |
| EARP_00013447 | 0.17 | 0.00 | 0.00 | 0.00 |
| EARP_00013448 | 0.13 | 0.00 | 0.00 | 0.00 |
| EARP_00013449 | 0.30 | 0.00 | 0.00 | 0.00 |
| EARP_00013450 | 0.28 | 0.00 | 0.00 | 0.00 |
| EARP_00003347 | 0.41 | 0.00 | 0.00 | 0.00 |
| EARP_00003349 | 0.09 | 0.00 | 0.00 | 0.04 |
| EARP_00013785 | 0.21 | 0.00 | 0.05 | 0.00 |
| EARP_00013786 | 0.15 | 0.00 | 0.00 | 0.00 |
| EARP_00013787 | 0.36 | 0.00 | 0.05 | 0.00 |
| EARP_00000455 | 0.14 | 0.00 | 0.00 | 0.00 |
| EARP_00003474 | 0.00 | 0.00 | 0.00 | 0.00 |
| EARP_00013794 | 0.22 | 0.00 | 0.00 | 0.02 |
| EARP_00014053 | 0.21 | 0.00 | 0.01 | 0.05 |
| EARP_00014054 | 0.44 | 0.00 | 0.00 | 0.00 |

| | | | | |
|---|---|---|---|---|
| EARP_00014069 | 0.27 | 0.00 | 0.02 | 0.00 |
| EARP_00014070 | 0.00 | 0.00 | 0.00 | 0.00 |
| EARP_00014071 | 0.22 | 0.00 | 0.17 | 0.00 |
| EARP_00014072 | 0.32 | 0.00 | 0.41 | 0.00 |
| EARP_00014073 | 0.14 | 0.05 | 0.05 | 0.04 |
| EARP_00014074 | 0.11 | 0.03 | 0.34 | 0.17 |
| EARP_00014075 | 0.00 | 0.00 | 0.50 | 0.23 |
| EARP_00003544 | 0.40 | 0.00 | 0.00 | 0.00 |
| EARP_00003545 | 0.33 | 0.00 | 0.00 | 0.00 |
| EARP_00003546 | 0.25 | 0.00 | 0.00 | 0.00 |
| EARP_00003547 | 0.32 | 0.01 | 0.02 | 0.00 |
| EARP_00003548 | 0.18 | 0.04 | 0.10 | 0.00 |
| EARP_00003549 | 0.20 | 0.00 | 0.00 | 0.00 |
| EARP_00003550 | 0.17 | 0.29 | 0.07 | 0.00 |
| EARP_00014238 | 0.20 | 0.00 | 0.03 | 0.01 |
| EARP_00014239 | 0.25 | 0.02 | 0.03 | 0.01 |
| EARP_00014240 | 0.14 | 0.00 | 0.01 | 0.00 |
| EARP_00014241 | 0.07 | 0.00 | 0.00 | 0.00 |
| EARP_00014242 | 0.19 | 0.00 | 0.00 | 0.00 |
| EARP_00014598 | 0.18 | 0.00 | 0.06 | 0.00 |
| EARP_00014599 | 0.36 | 0.00 | 0.10 | 0.00 |
| EARP_00014600 | 0.32 | 0.01 | 0.00 | 0.00 |
| EARP_00014601 | 0.25 | 0.00 | 0.00 | 0.00 |
| EARP_00015100 | 0.10 | 0.01 | 0.02 | 0.00 |
| EARP_00015101 | 0.25 | 0.01 | 0.02 | 0.02 |
| EARP_00015102 | 0.36 | 0.00 | 0.00 | 0.00 |
| EARP_00015103 | 0.36 | 0.00 | 0.00 | 0.00 |
| EARP_00003923 | 0.35 | 0.00 | 0.03 | 0.00 |
| EARP_00015598 | 0.00 | 0.00 | 0.00 | 0.00 |
| EARP_00015599 | 0.00 | 0.00 | 0.00 | 0.00 |
| EARP_00015806 | 0.28 | 0.22 | 0.00 | 0.18 |
| EARP_00015807 | 0.24 | 0.03 | 0.00 | 0.01 |
| EARP_00015808 | 0.23 | 0.00 | 0.00 | 0.00 |
| EARP_00016029 | 0.06 | 0.12 | 0.18 | 0.13 |
| EARP_00016030 | 0.00 | 0.00 | 0.00 | 0.00 |
| EARP_00016031 | 0.19 | 0.00 | 0.00 | 0.00 |
| EARP_00016032 | 0.13 | 0.10 | 0.13 | 0.13 |
| EARP_00016033 | 0.14 | 0.09 | 0.08 | 0.13 |
| EARP_00016034 | 0.13 | 0.12 | 0.18 | 0.00 |
| EARP_00016035 | 0.19 | 0.00 | 0.00 | 0.00 |
| EARP_00016036 | 0.09 | 0.04 | 0.06 | 0.20 |
| EARP_00016102 | 0.12 | 0.00 | 0.00 | 0.00 |
| EARP_00000574 | 0.10 | 0.00 | 0.00 | 0.00 |
| EARP_00000596 | 0.16 | 0.00 | 0.05 | 0.03 |

| | | | | |
|---|---|---|---|---|
| EARP_00000597 | 0.25 | 0.04 | 0.04 | 0.04 |
| EARP_00000598 | 0.00 | 0.00 | 0.00 | 0.00 |
| EARP_00004745 | 0.26 | 0.00 | 0.01 | 0.03 |
| EARP_00004746 | 0.31 | 0.00 | 0.00 | 0.53 |
| EARP_00016471 | 0.33 | 0.00 | 0.01 | 0.00 |
| EARP_00016472 | 0.31 | 0.00 | 0.00 | 0.00 |
| EARP_00016473 | 0.27 | 0.00 | 0.00 | 0.00 |
| EARP_00016474 | 0.22 | 0.00 | 0.00 | 0.00 |
| EARP_00016475 | 0.27 | 0.00 | 0.02 | 0.00 |
| EARP_00017025 | 0.32 | 0.00 | 0.00 | 0.00 |
| EARP_00017026 | 0.41 | 0.00 | 0.00 | 0.00 |
| EARP_00017027 | 0.27 | 0.00 | 0.00 | 0.02 |
| EARP_00017028 | 0.34 | 0.00 | 0.00 | 0.00 |
| EARP_00017029 | 0.16 | 0.00 | 0.00 | 0.02 |
| EARP_00017030 | 0.02 | 0.00 | 0.00 | 0.00 |
| EARP_00017031 | 0.30 | 0.00 | 0.00 | 0.00 |
| EARP_00017032 | 0.37 | 0.00 | 0.00 | 0.00 |
| EARP_00017033 | 0.38 | 0.00 | 0.00 | 0.05 |
| EARP_00017034 | 0.13 | 0.00 | 0.20 | 0.00 |
| EARP_00017035 | 0.00 | 0.00 | 0.00 | 0.00 |
| EARP_00017036 | 0.25 | 0.00 | 0.00 | 0.00 |
| EARP_00017037 | 0.27 | 0.00 | 0.03 | 0.02 |
| EARP_00017038 | 0.04 | 0.00 | 0.05 | 0.00 |
| EARP_00017066 | 0.20 | 0.00 | 0.01 | 0.00 |
| EARP_00017067 | 0.26 | 0.00 | 0.06 | 0.00 |
| EARP_00017068 | 0.18 | 0.00 | 0.00 | 0.00 |
| EARP_00017069 | 0.39 | 0.00 | 0.01 | 0.00 |
| EARP_00017070 | 0.34 | 0.00 | 0.01 | 0.00 |
| EARP_00017071 | 0.29 | 0.00 | 0.00 | 0.00 |
| EARP_00017072 | 0.37 | 0.01 | 0.01 | 0.00 |
| EARP_00005078 | 0.17 | 0.00 | 0.08 | 0.16 |
| EARP_00005079 | 0.13 | 0.00 | 0.00 | 0.00 |
| EARP_00005080 | 0.30 | 0.00 | 0.00 | 0.00 |
| EARP_00017302 | 0.43 | 0.00 | 0.00 | 0.00 |
| EARP_00017303 | 0.24 | 0.00 | 0.00 | 0.07 |
| EARP_00017606 | 0.00 | 0.00 | 0.00 | 0.00 |
| EARP_00017607 | 0.09 | 0.00 | 0.00 | 0.00 |
| EARP_00017698 | 0.00 | 0.00 | 0.00 | 0.00 |
| EARP_00017699 | 0.25 | 0.00 | 0.00 | 0.00 |
| EARP_00017707 | 0.44 | 0.00 | 0.00 | 0.00 |
| EARP_00017708 | 0.17 | 0.05 | 0.14 | 0.00 |
| EARP_00017709 | 0.24 | 0.02 | 0.05 | 0.00 |
| EARP_00017809 | 0.10 | 0.00 | 0.00 | 0.01 |
| EARP_00017810 | 0.06 | 0.00 | 0.00 | 0.00 |

| | | | | |
|---|---|---|---|---|
| EARP_00017811 | 0.08 | 0.00 | 0.00 | 0.00 |
| EARP_00017812 | 0.10 | 0.00 | 0.00 | 0.00 |
| EARP_00006312 | 0.33 | 0.00 | 0.03 | 0.00 |
| EARP_00006313 | 0.31 | 0.00 | 0.03 | 0.00 |
| EARP_00006329 | 0.36 | 0.00 | 0.00 | 0.00 |
| EARP_00006344 | 0.34 | 0.00 | 0.11 | 0.00 |
| EARP_00006349 | 0.23 | 0.00 | 0.01 | 0.27 |
| EARP_00006350 | 0.31 | 0.00 | 0.03 | 0.06 |
| EARP_00006351 | 0.26 | 0.00 | 0.00 | 0.02 |
| EARP_00006352 | 0.00 | 0.00 | 0.00 | 0.00 |
| EARP_00006353 | 0.04 | 0.00 | 0.02 | 0.43 |
| EARP_00006354 | 0.17 | 0.00 | 0.00 | 0.33 |
| EARP_00006355 | 0.14 | 0.00 | 0.01 | 0.15 |
| EARP_00006356 | 0.28 | 0.00 | 0.03 | 0.17 |
| EARP_00006357 | 0.19 | 0.00 | 0.13 | 0.00 |
| EARP_00000889 | 0.23 | 0.00 | 0.00 | 0.26 |
| EARP_00006613 | 0.25 | 0.00 | 0.02 | 0.00 |
| EARP_00006614 | 0.24 | 0.00 | 0.02 | 0.00 |
| EARP_00006615 | 0.00 | 0.00 | 0.00 | 0.00 |
| EARP_00006616 | 0.38 | 0.00 | 0.00 | 0.00 |
| EARP_00018561 | 0.11 | 0.00 | 0.00 | 0.00 |
| EARP_00018562 | 0.26 | 0.00 | 0.00 | 0.00 |
| EARP_00018563 | 0.00 | 0.00 | 0.00 | 0.00 |
| EARP_00018564 | 0.00 | 0.00 | 0.00 | 0.00 |
| EARP_00006824 | 0.34 | 0.06 | 0.06 | 0.00 |
| EARP_00006825 | 0.19 | 0.07 | 0.08 | 0.00 |
| EARP_00000981 | 0.28 | 0.28 | 0.13 | 0.11 |
| EARP_00000982 | 0.26 | 0.00 | 0.00 | 0.04 |
| EARP_00000983 | 0.13 | 0.07 | 0.03 | 0.00 |
| EARP_00000984 | 0.17 | 0.03 | 0.01 | 0.01 |
| EARP_00000985 | 0.00 | 0.00 | 0.00 | 0.00 |
| EARP_00000986 | 0.12 | 0.08 | 0.04 | 0.07 |
| EARP_00000987 | 0.14 | 0.04 | 0.02 | 0.03 |
| EARP_00000988 | 0.13 | 0.00 | 0.00 | 0.04 |
| EARP_00000989 | 0.14 | 0.03 | 0.02 | 0.02 |
| EARP_00000990 | 0.20 | 0.03 | 0.01 | 0.02 |
| EARP_00007488 | 0.38 | 0.00 | 0.04 | 0.00 |
| EARP_00007489 | 0.35 | 0.00 | 0.09 | 0.00 |
| EARP_00007490 | 0.29 | 0.01 | 0.04 | 0.00 |
| EARP_00007491 | 0.16 | 0.00 | 0.03 | 0.00 |
| EARP_00007492 | 0.13 | 0.00 | 0.03 | 0.00 |
| EARP_00007493 | 0.24 | 0.00 | 0.02 | 0.00 |
| EARP_00007494 | 0.27 | 0.00 | 0.02 | 0.00 |
| EARP_00007499 | 0.28 | 0.03 | 0.08 | 0.00 |

| | | | | |
|---|---|---|---|---|
| EARP_00007507 | 0.14 | 0.14 | 0.06 | 0.00 |
| EARP_00007508 | 0.00 | 0.00 | 0.00 | 0.00 |
| EARP_00007509 | 0.07 | 0.01 | 0.03 | 0.00 |
| EARP_00007510 | 0.14 | 0.01 | 0.00 | 0.00 |
| EARP_00007511 | 0.04 | 0.01 | 0.02 | 0.00 |
| EARP_00007512 | 0.06 | 0.01 | 0.02 | 0.00 |
| EARP_00007520 | 0.00 | 0.00 | 0.00 | 0.00 |
| EARP_00007521 | 0.20 | 0.00 | 0.01 | 0.00 |
| EARP_00007522 | 0.20 | 0.00 | 0.00 | 0.00 |
| EARP_00007523 | 0.15 | 0.09 | 0.11 | 0.00 |
| EARP_00018845 | 0.52 | 0.00 | 0.00 | 0.00 |
| EARP_00018891 | 0.48 | 0.00 | 0.00 | 0.00 |
| EARP_00018892 | 0.00 | 0.00 | 0.00 | 0.00 |
| EARP_00018893 | 0.46 | 0.00 | 0.00 | 0.00 |
| EARP_00018894 | 0.37 | 0.00 | 0.00 | 0.00 |
| EARP_00018895 | 0.00 | 0.00 | 0.00 | 0.00 |
| EARP_00018896 | 0.47 | 0.00 | 0.00 | 0.00 |
| EARP_00018902 | 0.05 | 0.00 | 0.00 | 0.00 |
| EARP_00008168 | 0.23 | 0.00 | 0.16 | 0.00 |
| EARP_00008169 | 0.09 | 0.00 | 0.02 | 0.00 |
| EARP_00008170 | 0.00 | 0.00 | 0.00 | 0.00 |
| EARP_00008578 | 0.19 | 0.08 | 0.06 | 0.00 |
| EARP_00008598 | 0.33 | 0.00 | 0.01 | 0.00 |
| EARP_00008599 | 0.31 | 0.00 | 0.02 | 0.00 |
| EARP_00008600 | 0.24 | 0.00 | 0.07 | 0.00 |
| EARP_00008601 | 0.37 | 0.00 | 0.02 | 0.00 |
| EARP_00008602 | 0.21 | 0.00 | 0.09 | 0.00 |
| EARP_00008603 | 0.29 | 0.00 | 0.06 | 0.00 |
| EARP_00008888 | 0.23 | 0.09 | 0.02 | 0.10 |
| EARP_00011127 | 0.00 | 0.00 | 0.00 | 0.00 |
| EARP_00011128 | 0.00 | 0.00 | 0.00 | 0.00 |
| EARP_00011129 | 0.15 | 0.03 | 0.01 | 0.00 |
| EARP_00011680 | 0.05 | 0.00 | 0.00 | 0.00 |
| EARP_00011865 | 0.12 | 0.00 | 0.01 | 0.03 |
| EARP_00011866 | 0.05 | 0.00 | 0.00 | 0.00 |
| EARP_00011867 | 0.15 | 0.00 | 0.00 | 0.00 |
| EARP_00011868 | 0.02 | 0.00 | 0.00 | 0.05 |
| EARP_00011869 | 0.07 | 0.00 | 0.00 | 0.00 |
| EARP_00012502 | 0.00 | 0.00 | 0.00 | 0.05 |
| EARP_00012505 | 0.16 | 0.00 | 0.00 | 0.00 |
| EARP_00012506 | 0.00 | 0.00 | 0.00 | 0.00 |
| EARP_00012507 | 0.00 | 0.00 | 0.00 | 0.00 |
| EARP_00012508 | 0.07 | 0.00 | 0.00 | 0.00 |
| EARP_00012509 | 0.22 | 0.00 | 0.00 | 0.00 |

| | | | | |
|---|---|---|---|---|
| EARP_00012510 | 0.10 | 0.00 | 0.00 | 0.01 |
| EARP_00012511 | 0.18 | 0.04 | 0.07 | 0.01 |
| EARP_00012512 | 0.20 | 0.00 | 0.00 | 0.00 |
| EARP_00012513 | 0.13 | 0.00 | 0.00 | 0.01 |
| EARP_00012514 | 0.31 | 0.00 | 0.00 | 0.00 |
| EARP_00012515 | 0.07 | 0.00 | 0.00 | 0.00 |
| EARP_00012516 | 0.01 | 0.00 | 0.00 | 0.00 |
| EARP_00012517 | 0.05 | 0.00 | 0.00 | 0.01 |
| EARP_00012518 | 0.07 | 0.00 | 0.00 | 0.00 |
| EARP_00012519 | 0.12 | 0.00 | 0.00 | 0.00 |
| EARP_00012520 | 0.13 | 0.00 | 0.00 | 0.00 |
| EARP_00012521 | 0.09 | 0.00 | 0.00 | 0.01 |
| EARP_00013700 | 0.20 | 0.00 | 0.00 | 0.00 |
| EARP_00013701 | 0.22 | 0.00 | 0.00 | 0.00 |
| EARP_00013702 | 0.00 | 0.00 | 0.00 | 0.00 |
| EARP_00013703 | 0.02 | 0.00 | 0.00 | 0.00 |
| EARP_00013704 | 0.12 | 0.07 | 0.06 | 0.03 |
| EARP_00014256 | 0.10 | 0.00 | 0.00 | 0.00 |
| EARP_00014257 | 0.12 | 0.00 | 0.01 | 0.01 |
| EARP_00014258 | 0.10 | 0.00 | 0.00 | 0.02 |
| EARP_00014259 | 0.12 | 0.00 | 0.01 | 0.02 |
| EARP_00014269 | 0.37 | 0.00 | 0.00 | 0.00 |
| EARP_00014270 | 0.32 | 0.17 | 0.18 | 0.18 |
| EARP_00015298 | 0.22 | 0.00 | 0.00 | 0.00 |
| EARP_00015299 | 0.10 | 0.00 | 0.00 | 0.00 |
| EARP_00015303 | 0.21 | 0.00 | 0.01 | 0.00 |
| EARP_00015304 | 0.05 | 0.00 | 0.00 | 0.03 |
| EARP_00015305 | 0.14 | 0.00 | 0.00 | 0.01 |
| EARP_00015306 | 0.11 | 0.00 | 0.00 | 0.00 |
| EARP_00015426 | 0.27 | 0.00 | 0.00 | 0.01 |
| EARP_00005020 | 0.34 | 0.00 | 0.00 | 0.00 |
| EARP_00005021 | 0.00 | 0.00 | 0.00 | 0.00 |
| EARP_00005022 | 0.05 | 0.00 | 0.04 | 0.00 |
| EARP_00005028 | 0.06 | 0.01 | 0.02 | 0.00 |
| EARP_00017436 | 0.00 | 0.00 | 0.00 | 0.00 |
| EARP_00017437 | 0.05 | 0.00 | 0.00 | 0.02 |
| EARP_00017591 | 0.12 | 0.01 | 0.01 | 0.01 |
| EARP_00017592 | 0.08 | 0.00 | 0.00 | 0.00 |
| EARP_00017593 | 0.28 | 0.31 | 0.30 | 0.24 |
| EARP_00006966 | 0.17 | 0.00 | 0.00 | 0.00 |
| EARP_00006967 | 0.10 | 0.00 | 0.00 | 0.00 |
| EARP_00008636 | 0.20 | 0.00 | 0.00 | 0.01 |
| EARP_00008638 | 0.00 | 0.00 | 0.00 | 0.00 |
| EARP_00008639 | 0.07 | 0.00 | 0.00 | 0.00 |

| | | | | |
|---|---|---|---|---|
| EARP_00008640 | 0.00 | 0.00 | 0.00 | 0.00 |
| EARP_00008641 | 0.00 | 0.00 | 0.00 | 0.00 |
| EARP_00008643 | 0.26 | 0.00 | 0.00 | 0.02 |
| EARP_00008644 | 0.10 | 0.18 | 0.20 | 0.00 |
| EARP_00008645 | 0.08 | 0.00 | 0.00 | 0.00 |
| EARP_00008646 | 0.08 | 0.00 | 0.00 | 0.00 |
| EARP_00009516 | 0.31 | 0.00 | 0.02 | 0.00 |
| Average | 0.19 | 0.01 | 0.03 | 0.02 |

Dataset S7: Likelihood analysis of different evolutionary scenarios. In the models, S represents consistent small population size, D represents population decline, I indicates that there was no gene flow between adjacent populations, WCE indicates that there was gene flow between adjacent populations, CW indicates that the gene flow only existed between the Western and Central populations, CE indicates that migration only occurred between the Central and Eastern populations, and IN indicates that inbreeding occurred. The likelihood (ln) was estimated using fastsimcoal26. d represents the number of parameters in the different models. AIC represents the Akaike information criterion. w represents Akaike weight.

| Models | ln(Likelihood) | d | $AIC_i$ | $\Delta_i$ | $w_i$ |
|---|---|---|---|---|---|
| S+I | -47915.76 | 9.00 | 95849.52 | 6566.44 | 0.00 |
| S+WCE | -45039.69 | 23.00 | 90125.37 | 842.30 | 0.00 |
| S+CW | -45231.52 | 16.00 | 90495.04 | 1211.96 | 0.00 |
| S+CE | -44783.52 | 16.00 | 89599.04 | 315.97 | 0.00 |
| D+I | -44617.25 | 28.00 | 89290.49 | 7.42 | 0.02 |
| D+WCE | -54029.39 | 34.00 | 108126.79 | 18843.71 | 0.00 |
| D+CW | -44689.21 | 31.00 | 89440.41 | 157.34 | 0.00 |
| D+CE | -44653.58 | 31.00 | 89369.16 | 86.09 | 0.00 |
| S+I+IN | -47926.01 | 12.00 | 95876.01 | 6592.94 | 0.00 |
| S+WCE+IN | -45031.20 | 26.00 | 90114.40 | 831.32 | 0.00 |
| S+CW+IN | -45232.04 | 19.00 | 90502.07 | 1219.00 | 0.00 |
| S+CE+IN | -44771.16 | 19.00 | 89580.32 | 297.25 | 0.00 |
| D+I+IN | -44610.54 | 31.00 | 89283.07 | 0.00 | 0.98 |
| D+WCE+IN | -47953.29 | 37.00 | 95980.58 | 6697.50 | 0.00 |
| D+CW+IN | -44692.62 | 34.00 | 89453.24 | 170.16 | 0.00 |
| D+CE+IN | -44657.87 | 34.00 | 89383.75 | 100.67 | 0.00 |

Dataset S8: Model probability estimated in Migrate-N. Brown-W, Brown-C, and Brown-E indicate the Western, Central, and Eastern populations of *Crossoptilon mantchuricum* , respectively. ml is the marginal likelihood. bf is the Bayes factor.

| Model | Log(ml) | Log(bf) | Model-probability | Custom migration model |
|---|---|---|---|---|
| Migration between adjacent populations | -1403.43 | -7.87 | 0.0004 | Brown-W, Brown-C, Brown-E={**0 *** 0**} |
| Migration between Brown-W and Brown-C | -1402.01 | -6.45 | 0.0015 | Brown-W, Brown-C, Brown-E={**0 **0 00*} |
| Migration between Brown-C and Brown-E | -1398.59 | -3.03 | 0.046 | Brown-W, Brown-C, Brown-E={*00 0** 0**} |
| Isolation | -1395.56 | 0 | 0.9521 | Brown-W, Brown-C, Brown-E={*00 0*0 00*} |

Dataset S9: Sample information, coverage, and mapping rate. The asterisks mark the individuals that were excluded from the population genetic analysis because they had a close relationship (duplicate/MZ twin, 1st-degree) with at least one individual in the corresponding population. The sequence data of all individuals were deposited in the National Genomics Data Center (https://bigd.big.ac.cn/?lang=en). Readers can use the accession number to find the data in the National Genomics Data Center Datavases.

| Species | Location | Tissue type | Gender | Sample index | Sample ID | Sequencing type | Sequencing coverage (×) | Mapping rate | Accession number |
|---|---|---|---|---|---|---|---|---|---|
| *C. auritum* | Gansu | Blood | Female | 1 | CA00 | Re-sequencing | 41.57 | 98.53% | SAMC226688 |
| *C. auritum* | Gansu | Blood | Female | 2 | CA01 | Re-sequencing | 16.03 | 97.86% | SAMC226689 |
| *C. auritum* | Gansu | Blood | Male | 3 | CA02 | Re-sequencing | 17.06 | 98.48% | SAMC226690 |
| *C. auritum* | Gansu | Blood | Female | 4 | CA03* | Re-sequencing | 16.73 | 98.24% | SAMC226691 |
| *C. auritum* | Gansu | Blood | Female | 5 | CA04 | Re-sequencing | 20.68 | 98.49% | SAMC226692 |
| *C. auritum* | Gansu | Blood | Female | 6 | CA05 | Re-sequencing | 17.67 | 98.05% | SAMC226693 |
| *C. auritum* | Gansu | Blood | Male | 7 | CA06 | Re-sequencing | 18.96 | 98.58% | SAMC226694 |
| *C. auritum* | Gansu | Blood | Male | 8 | CA07 | Re-sequencing | 16.48 | 98.74% | SAMC226695 |
| *C. auritum* | Gansu | Blood | Male | 9 | CA08 | Re-sequencing | 16.33 | 98.68% | SAMC226696 |
| *C. auritum* | Gansu | Blood | Male | 10 | CA09 | Re-sequencing | 16.93 | 98.54% | SAMC226697 |
| *C. auritum* | Gansu | Blood | Female | 11 | CA10 | Re-sequencing | 18.20 | 98.09% | SAMC226698 |
| *C. mantchuricum* | Shaanxi(Western population) | Blood | Female | 12 | CMAA00 | Re-sequencing | 43.17 | 98.59% | SAMC226699 |
| *C. mantchuricum* | Shaanxi(Western population) | Blood | Female | 13 | CMAA01 | Re-sequencing | 15.60 | 98.54% | SAMC226700 |

| | | | | | | | | | |
|---|---|---|---|---|---|---|---|---|---|
| *C. mantchuricum* | Shaanxi(Western population) | Blood | Male | 14 | CMAA02 | Re-sequencing | 15.89 | 98.65% | SAMC226701 |
| *C. mantchuricum* | Shaanxi(Western population) | Muscle | Female | 15 | CMAA03 | Re-sequencing | 15.31 | 97.56% | SAMC226702 |
| *C. mantchuricum* | Shaanxi(Western population) | Blood | Male | 16 | CMAA04* | Re-sequencing | 17.64 | 98.85% | SAMC226703 |
| *C. mantchuricum* | Shaanxi(Western population) | Blood | Female | 17 | CMAA05 | Re-sequencing | 18.86 | 97.42% | SAMC226704 |
| *C. mantchuricum* | Shaanxi(Western population) | Blood | Male | 18 | CMAA06 | Re-sequencing | 18.56 | 93.89% | SAMC226705 |
| *C. mantchuricum* | Shaanxi(Western population) | Blood | Female | 19 | CMAA07* | Re-sequencing | 16.07 | 95.51% | SAMC226706 |
| *C. mantchuricum* | Shaanxi(Western population) | Blood | Female | 20 | CMAA08 | Re-sequencing | 20.81 | 98.60% | SAMC226707 |
| *C. mantchuricum* | Shaanxi(Western population) | Blood | Female | 21 | CMAA09* | Re-sequencing | 15.53 | 98.75% | SAMC226708 |
| *C. mantchuricum* | Shaanxi(Western population) | Blood | Female | 22 | CMAA10 | Re-sequencing | 13.42 | 86.63% | SAMC226709 |
| *C. mantchuricum* | Shaanxi(Western population) | Blood | Male | 23 | CMAA11* | Re-sequencing | 21.99 | 96.29% | SAMC226710 |
| *C. mantchuricum* | Shaanxi(Western population) | Blood | Female | 24 | CMAA12* | Re-sequencing | 19.77 | 96.96% | SAMC226711 |
| *C. mantchuricum* | Shaanxi(Western population) | Blood | Female | 25 | CMAA13 | Re-sequencing | 18.19 | 97.43% | SAMC226712 |
| *C. mantchuricum* | Shaanxi(Western population) | Blood | Female | 26 | CMAA14 | Re-sequencing | 18.36 | 96.47% | SAMC226713 |
| *C. mantchuricum* | Shaanxi(Western population) | Blood | Female | 27 | CMAA15* | Re-sequencing | 15.59 | 93.59% | SAMC226714 |
| *C. mantchuricum* | Shaanxi(Western population) | Blood | Male | 28 | CMAA16 | Re-sequencing | 16.82 | 97.81% | SAMC226715 |
| *C. mantchuricum* | Shaanxi(Western population) | Blood | Male | 29 | CMAA17* | Re-sequencing | 13.60 | 83.55% | SAMC226716 |
| *C. mantchuricum* | Shanxi(Central population) | Muscle | Male | 30 | CMA04* | Re-sequencing | 15.94 | 98.39% | SAMC226717 |

| | | | | | | | | | |
|---|---|---|---|---|---|---|---|---|---|
| *C. mantchuricum* | Shanxi(Central population) | Blood | Female | 31 | CMA08 | Re-sequencing | 15.21 | 98.24% | SAMC226718 |
| *C. mantchuricum* | Shanxi(Central population) | Muscle | Female | 32 | CMA09 | Re-sequencing | 19.23 | 97.51% | SAMC226719 |
| *C. mantchuricum* | Shanxi(Central population) | Liver | Female | 33 | CMA10* | Re-sequencing | 16.77 | 97.81% | SAMC226720 |
| *C. mantchuricum* | Shanxi(Central population) | Muscle | Female | 34 | CMA11 | Re-sequencing | 19.53 | 96.86% | SAMC226721 |
| *C. mantchuricum* | Shanxi(Central population) | Liver | Female | 35 | CMA12 | Re-sequencing | 18.26 | 97.80% | SAMC226722 |
| *C. mantchuricum* | Shanxi(Central population) | Liver | Male | 36 | CMA13 | Re-sequencing | 21.46 | 97.98% | SAMC226723 |
| *C. mantchuricum* | Shanxi(Central population) | Liver | Male | 37 | CMA14 | Re-sequencing | 19.13 | 98.39% | SAMC226724 |
| *C. mantchuricum* | Shanxi(Central population) | Liver | Female | 38 | CMA15* | Re-sequencing | 18.19 | 97.54% | SAMC226725 |
| *C. mantchuricum* | Shanxi(Central population) | Muscle | Female | 39 | CMA16 | Re-sequencing | 16.03 | 97.79% | SAMC226726 |
| *C. mantchuricum* | Shanxi(Central population) | Muscle | Male | 40 | CMA18 | Re-sequencing | 15.32 | 97.62% | SAMC226727 |
| *C. mantchuricum* | Hebei(Eastern population) | Blood | Male | 41 | CMH00 | Re-sequencing | 36.59 | 98.26% | SAMC226728 |
| *C. mantchuricum* | Hebei(Eastern population) | Blood | Female | 42 | CMH01 | Re-sequencing | 17.40 | 98.53% | SAMC226729 |
| *C. mantchuricum* | Hebei(Eastern population) | Blood | Male | 43 | CMH02 | Re-sequencing | 19.22 | 98.65% | SAMC226730 |
| *C. mantchuricum* | Hebei(Eastern population) | Blood | Female | 44 | CMH03 | Re-sequencing | 19.54 | 98.12% | SAMC226731 |
| *C. mantchuricum* | Hebei(Eastern population) | Muscle | Male | 45 | CMH04* | Re-sequencing | 18.79 | 97.85% | SAMC226732 |
| *C. mantchuricum* | Hebei(Eastern population) | Blood | Male | 46 | CMH05 | Re-sequencing | 18.30 | 98.63% | SAMC226733 |
| *C. mantchuricum* | Hebei(Eastern population) | Muscle | Male | 47 | CMH06 | Re-sequencing | 19.69 | 97.85% | SAMC226734 |

| | | | | | | | | | |
|---|---|---|---|---|---|---|---|---|---|
| *C. mantchuricum* | Hebei(Eastern population) | Blood | Female | 48 | CMH07* | Re-sequencing | 17.60 | 98.34% | SAMC226735 |
| *C. mantchuricum* | Hebei(Eastern population) | Blood | Female | 49 | CMH08 | Re-sequencing | 15.51 | 97.95% | SAMC226736 |
| *C. mantchuricum* | Hebei(Eastern population) | Blood | Female | 50 | CMH09 | Re-sequencing | 18.92 | 98.19% | SAMC226737 |
| *C. mantchuricum* | Hebei(Eastern population) | Muscle | Male | 51 | CMH12* | Re-sequencing | 17.60 | 97.77% | SAMC226738 |
| *C. mantchuricum* | Shanxi(Central population) | Blood | Female | 52 | CMA00* | De novo sequencing | 201.75 | N | SAMC226739 |

Dataset S10: The relationship of each sample in each population inferred by the King program. Blue indicates *Crossoptilon auritum* . Brown-W, Brown-C, and Brown-E indicate the Western, Central, and Eastern populations of *Crossoptilon mantchuricum* , respectively. ID1: The first individual of the pair; ID2: The second individual of the pair; N_SNP: The number of SNPS that do not have missing SNPS in either of the individuals; HetHet: Percentage of SNPs with double heterozygotes; IBS0: Proportion of SNPs with 0-IBS (identical-by-state); Kinship: Kinship coefficient estimated by the program. The asterisks mark the individuals that were excluded in the downstream analysis.

| Population | ID1 | ID2 | N_SNP | HetHet | IBS0 | Kinship |
|---|---|---|---|---|---|---|
| Blue | CA00 | CA1 | 2275444 | 15.29% | 8.02% | -0.06 |
| Blue | CA00 | CA10 | 2275444 | 12.22% | 12.15% | -0.20 |
| Blue | CA00 | CA2 | 2275444 | 13.75% | 7.01% | 0.00 |
| Blue | CA00 | CA3* | 2275444 | 13.94% | 7.15% | -0.01 |
| Blue | CA00 | CA4 | 2275444 | 11.88% | 12.58% | -0.23 |
| Blue | CA00 | CA5 | 2275444 | 12.65% | 9.10% | -0.10 |
| Blue | CA00 | CA6 | 2275444 | 12.14% | 12.50% | -0.22 |
| Blue | CA00 | CA7 | 2275444 | 11.95% | 12.38% | -0.21 |
| Blue | CA00 | CA8 | 2275444 | 12.02% | 12.52% | -0.22 |
| Blue | CA00 | CA9 | 2275444 | 12.15% | 12.33% | -0.21 |
| Blue | CA1 | CA10 | 2275444 | 15.29% | 7.84% | -0.06 |
| Blue | CA1 | CA2 | 2275444 | 15.24% | 7.92% | -0.06 |
| Blue | CA1 | CA3* | 2275444 | 17.07% | 0.30% | 0.21 |
| Blue | CA1 | CA4 | 2275444 | 14.83% | 8.22% | -0.09 |
| Blue | CA1 | CA5 | 2275444 | 14.68% | 8.77% | -0.11 |
| Blue | CA1 | CA6 | 2275444 | 15.06% | 8.01% | -0.08 |
| Blue | CA1 | CA7 | 2275444 | 15.06% | 8.17% | -0.08 |
| Blue | CA1 | CA8 | 2275444 | 14.94% | 8.36% | -0.09 |
| Blue | CA1 | CA9 | 2275444 | 15.15% | 7.82% | -0.07 |
| Blue | CA10 | CA2 | 2275444 | 12.19% | 12.07% | -0.19 |
| Blue | CA10 | CA3* | 2275444 | 12.59% | 12.35% | -0.20 |
| Blue | CA10 | CA4 | 2275444 | 13.34% | 7.26% | -0.03 |
| Blue | CA10 | CA5 | 2275444 | 12.04% | 11.43% | -0.18 |
| Blue | CA10 | CA6 | 2275444 | 13.54% | 7.25% | -0.02 |
| Blue | CA10 | CA7 | 2275444 | 13.39% | 7.44% | -0.03 |
| Blue | CA10 | CA8 | 2275444 | 13.30% | 7.30% | -0.03 |
| Blue | CA10 | CA9 | 2275444 | 13.39% | 7.49% | -0.03 |
| Blue | CA2 | CA3* | 2275444 | 13.73% | 7.19% | -0.02 |
| Blue | CA2 | CA4 | 2275444 | 12.00% | 12.38% | -0.22 |
| Blue | CA2 | CA5 | 2275444 | 12.55% | 9.02% | -0.10 |
| Blue | CA2 | CA6 | 2275444 | 12.05% | 12.22% | -0.21 |
| Blue | CA2 | CA7 | 2275444 | 12.16% | 12.21% | -0.20 |
| Blue | CA2 | CA8 | 2275444 | 11.95% | 12.25% | -0.21 |
| Blue | CA2 | CA9 | 2275444 | 12.20% | 12.12% | -0.20 |
| Blue | CA3* | CA4 | 2275444 | 12.33% | 12.66% | -0.23 |
| Blue | CA3* | CA5 | 2275444 | 12.95% | 9.17% | -0.10 |
| Blue | CA3* | CA6 | 2275444 | 12.36% | 12.56% | -0.22 |
| Blue | CA3* | CA7 | 2275444 | 12.51% | 12.56% | -0.22 |
| Blue | CA3* | CA8 | 2275444 | 12.39% | 12.66% | -0.23 |
| Blue | CA3* | CA9 | 2275444 | 12.57% | 12.53% | -0.21 |
| Blue | CA4 | CA5 | 2275444 | 11.66% | 11.95% | -0.20 |

| | | | | | | |
|---|---|---|---|---|---|---|
| Blue | CA4 | CA6 | 2275444 | 13.02% | 7.41% | -0.03 |
| Blue | CA4 | CA7 | 2275444 | 13.20% | 7.05% | -0.02 |
| Blue | CA4 | CA8 | 2275444 | 13.06% | 7.44% | -0.03 |
| Blue | CA4 | CA9 | 2275444 | 13.01% | 7.46% | -0.03 |
| Blue | CA5 | CA6 | 2275444 | 11.78% | 11.62% | -0.18 |
| Blue | CA5 | CA7 | 2275444 | 11.91% | 11.58% | -0.18 |
| Blue | CA5 | CA8 | 2275444 | 11.73% | 11.61% | -0.19 |
| Blue | CA5 | CA9 | 2275444 | 11.96% | 11.63% | -0.18 |
| Blue | CA6 | CA7 | 2275444 | 13.28% | 7.55% | -0.03 |
| Blue | CA6 | CA8 | 2275444 | 13.00% | 7.30% | -0.03 |
| Blue | CA6 | CA9 | 2275444 | 13.17% | 7.09% | -0.02 |
| Blue | CA7 | CA8 | 2275444 | 13.15% | 7.40% | -0.03 |
| Blue | CA7 | CA9 | 2275444 | 13.46% | 6.85% | 0.00 |
| Blue | CA8 | CA9 | 2275444 | 13.21% | 7.50% | -0.03 |
| Brown-W | CMAA00 | CMAA1 | 2275444 | 0.98% | 0.53% | -0.03 |
| Brown-W | CMAA00 | CMAA10 | 2275444 | 0.79% | 0.61% | -0.20 |
| Brown-W | CMAA00 | CMAA11* | 2275444 | 1.24% | 0.20% | 0.14 |
| Brown-W | CMAA00 | CMAA12* | 2275444 | 1.02% | 0.69% | -0.09 |
| Brown-W | CMAA00 | CMAA13 | 2275444 | 1.16% | 0.34% | 0.05 |
| Brown-W | CMAA00 | CMAA14 | 2275444 | 1.39% | 0.43% | 0.07 |
| Brown-W | CMAA00 | CMAA15* | 2275444 | 1.33% | 0.40% | 0.07 |
| Brown-W | CMAA00 | CMAA16 | 2275444 | 1.26% | 0.27% | 0.09 |
| Brown-W | CMAA00 | CMAA17* | 2275444 | 1.10% | 0.60% | -0.03 |
| Brown-W | CMAA1 | CMAA10 | 2275444 | 1.05% | 0.22% | 0.07 |
| Brown-W | CMAA1 | CMAA11* | 2275444 | 1.06% | 0.45% | 0.02 |
| Brown-W | CMAA1 | CMAA12* | 2275444 | 0.90% | 0.93% | -0.18 |
| Brown-W | CMAA1 | CMAA13 | 2275444 | 0.96% | 0.35% | 0.03 |
| Brown-W | CMAA1 | CMAA14 | 2275444 | 1.19% | 0.44% | 0.02 |
| Brown-W | CMAA1 | CMAA15* | 2275444 | 1.30% | 0.25% | 0.10 |
| Brown-W | CMAA1 | CMAA16 | 2275444 | 1.46% | 0.33% | 0.09 |
| Brown-W | CMAA1 | CMAA17* | 2275444 | 1.07% | 0.49% | 0.01 |
| Brown-W | CMAA10 | CMAA11* | 2275444 | 0.70% | 0.50% | -0.15 |
| Brown-W | CMAA10 | CMAA12* | 2275444 | 0.65% | 0.77% | -0.28 |
| Brown-W | CMAA10 | CMAA13 | 2275444 | 0.76% | 0.60% | -0.15 |
| Brown-W | CMAA10 | CMAA14 | 2275444 | 0.89% | 0.50% | -0.15 |
| Brown-W | CMAA10 | CMAA15* | 2275444 | 0.98% | 0.61% | -0.19 |
| Brown-W | CMAA10 | CMAA16 | 2275444 | 0.96% | 0.48% | -0.15 |
| Brown-W | CMAA10 | CMAA17* | 2275444 | 0.73% | 0.68% | -0.23 |
| Brown-W | CMAA11* | CMAA12* | 2275444 | 0.98% | 0.63% | -0.06 |
| Brown-W | CMAA11* | CMAA13 | 2275444 | 1.40% | 0.05% | 0.23 |
| Brown-W | CMAA11* | CMAA14 | 2275444 | 1.12% | 0.43% | 0.01 |
| Brown-W | CMAA11* | CMAA15* | 2275444 | 1.45% | 0.12% | 0.18 |
| Brown-W | CMAA11* | CMAA16 | 2275444 | 1.57% | 0.22% | 0.16 |
| Brown-W | CMAA11* | CMAA17* | 2275444 | 1.18% | 0.27% | 0.11 |
| Brown-W | CMAA12* | CMAA13 | 2275444 | 0.84% | 0.70% | -0.14 |
| Brown-W | CMAA12* | CMAA14 | 2275444 | 1.03% | 0.65% | -0.09 |
| Brown-W | CMAA12* | CMAA15* | 2275444 | 1.10% | 0.63% | -0.08 |
| Brown-W | CMAA12* | CMAA16 | 2275444 | 1.13% | 0.82% | -0.16 |
| Brown-W | CMAA12* | CMAA17* | 2275444 | 0.82% | 0.98% | -0.22 |
| Brown-W | CMAA13 | CMAA14 | 2275444 | 1.16% | 0.44% | -0.01 |
| Brown-W | CMAA13 | CMAA15* | 2275444 | 1.28% | 0.15% | 0.12 |
| Brown-W | CMAA13 | CMAA16 | 2275444 | 1.33% | 0.26% | 0.08 |
| Brown-W | CMAA13 | CMAA17* | 2275444 | 1.10% | 0.35% | 0.05 |

| | | | | | | |
|---|---|---|---|---|---|---|
| Brown-W | CMAA14 | CMAA15* | 2275444 | 1.27% | 0.43% | 0.06 |
| Brown-W | CMAA14 | CMAA16 | 2275444 | 1.42% | 0.24% | 0.14 |
| Brown-W | CMAA14 | CMAA17* | 2275444 | 1.11% | 0.50% | -0.02 |
| Brown-W | CMAA15* | CMAA16 | 2275444 | 1.73% | 0.02% | 0.26 |
| Brown-W | CMAA15* | CMAA17* | 2275444 | 1.37% | 0.04% | 0.20 |
| Brown-W | CMAA16 | CMAA17* | 2275444 | 1.94% | 0.21% | 0.23 |
| Brown-W | CMAA00 | CMAA2 | 2275444 | 0.62% | 1.05% | -0.65 |
| Brown-W | CMAA00 | CMAA3 | 2275444 | 1.48% | 0.59% | 0.00 |
| Brown-W | CMAA00 | CMAA4* | 2275444 | 1.20% | 0.52% | 0.00 |
| Brown-W | CMAA00 | CMAA5 | 2275444 | 1.33% | 0.63% | -0.01 |
| Brown-W | CMAA00 | CMAA6 | 2275444 | 1.21% | 0.52% | 0.00 |
| Brown-W | CMAA00 | CMAA7* | 2275444 | 0.90% | 0.69% | -0.09 |
| Brown-W | CMAA00 | CMAA8 | 2275444 | 1.52% | 0.60% | 0.04 |
| Brown-W | CMAA00 | CMAA9* | 2275444 | 1.02% | 0.68% | -0.07 |
| Brown-W | CMAA1 | CMAA2 | 2275444 | 0.86% | 0.02% | 0.09 |
| Brown-W | CMAA1 | CMAA3 | 2275444 | 1.08% | 0.58% | -0.09 |
| Brown-W | CMAA1 | CMAA4* | 2275444 | 1.19% | 0.62% | -0.05 |
| Brown-W | CMAA1 | CMAA5 | 2275444 | 0.83% | 0.41% | -0.04 |
| Brown-W | CMAA1 | CMAA6 | 2275444 | 1.20% | 0.62% | -0.05 |
| Brown-W | CMAA1 | CMAA7* | 2275444 | 1.07% | 0.95% | -0.18 |
| Brown-W | CMAA1 | CMAA8 | 2275444 | 1.08% | 0.30% | 0.05 |
| Brown-W | CMAA1 | CMAA9* | 2275444 | 1.10% | 0.61% | -0.05 |
| Brown-W | CMAA10 | CMAA2 | 2275444 | 0.69% | 0.73% | -0.31 |
| Brown-W | CMAA10 | CMAA3 | 2275444 | 1.03% | 0.63% | -0.22 |
| Brown-W | CMAA10 | CMAA4* | 2275444 | 0.82% | 0.57% | -0.20 |
| Brown-W | CMAA10 | CMAA5 | 2275444 | 0.81% | 0.42% | -0.14 |
| Brown-W | CMAA10 | CMAA6 | 2275444 | 0.83% | 0.56% | -0.20 |
| Brown-W | CMAA10 | CMAA7* | 2275444 | 0.79% | 0.99% | -0.38 |
| Brown-W | CMAA10 | CMAA8 | 2275444 | 0.73% | 0.48% | -0.18 |
| Brown-W | CMAA10 | CMAA9* | 2275444 | 0.85% | 0.72% | -0.25 |
| Brown-W | CMAA11* | CMAA2 | 2275444 | 0.71% | 0.75% | -0.42 |
| Brown-W | CMAA11* | CMAA3 | 2275444 | 1.30% | 0.40% | 0.03 |
| Brown-W | CMAA11* | CMAA4* | 2275444 | 1.23% | 0.36% | 0.06 |
| Brown-W | CMAA11* | CMAA5 | 2275444 | 1.20% | 0.38% | 0.05 |
| Brown-W | CMAA11* | CMAA6 | 2275444 | 1.24% | 0.35% | 0.06 |
| Brown-W | CMAA11* | CMAA7* | 2275444 | 1.02% | 0.49% | -0.01 |
| Brown-W | CMAA11* | CMAA8 | 2275444 | 1.37% | 0.47% | 0.05 |
| Brown-W | CMAA11* | CMAA9* | 2275444 | 1.18% | 0.52% | 0.01 |
| Brown-W | CMAA12* | CMAA2 | 2275444 | 0.40% | 1.08% | -0.71 |
| Brown-W | CMAA12* | CMAA3 | 2275444 | 1.00% | 0.67% | -0.14 |
| Brown-W | CMAA12* | CMAA4* | 2275444 | 1.20% | 0.52% | -0.02 |
| Brown-W | CMAA12* | CMAA5 | 2275444 | 1.48% | 0.12% | 0.19 |
| Brown-W | CMAA12* | CMAA6 | 2275444 | 1.21% | 0.52% | -0.02 |
| Brown-W | CMAA12* | CMAA7* | 2275444 | 1.00% | 0.76% | -0.12 |
| Brown-W | CMAA12* | CMAA8 | 2275444 | 1.40% | 0.79% | -0.08 |
| Brown-W | CMAA12* | CMAA9* | 2275444 | 1.26% | 0.69% | -0.05 |
| Brown-W | CMAA13 | CMAA2 | 2275444 | 0.64% | 0.65% | -0.33 |
| Brown-W | CMAA13 | CMAA3 | 2275444 | 1.19% | 0.49% | -0.06 |
| Brown-W | CMAA13 | CMAA4* | 2275444 | 1.08% | 0.51% | -0.06 |
| Brown-W | CMAA13 | CMAA5 | 2275444 | 1.04% | 0.37% | -0.01 |
| Brown-W | CMAA13 | CMAA6 | 2275444 | 1.09% | 0.50% | -0.06 |
| Brown-W | CMAA13 | CMAA7* | 2275444 | 0.80% | 0.62% | -0.14 |
| Brown-W | CMAA13 | CMAA8 | 2275444 | 1.09% | 0.25% | 0.05 |

| | | | | | | |
|---|---|---|---|---|---|---|
| Brown-W | CMAA13 | CMAA9* | 2275444 | 0.98% | 0.46% | -0.04 |
| Brown-W | CMAA14 | CMAA2 | 2275444 | 0.66% | 0.75% | -0.49 |
| Brown-W | CMAA14 | CMAA3 | 2275444 | 1.44% | 0.45% | 0.06 |
| Brown-W | CMAA14 | CMAA4* | 2275444 | 1.25% | 0.60% | 0.01 |
| Brown-W | CMAA14 | CMAA5 | 2275444 | 1.19% | 0.37% | 0.07 |
| Brown-W | CMAA14 | CMAA6 | 2275444 | 1.26% | 0.59% | 0.01 |
| Brown-W | CMAA14 | CMAA7* | 2275444 | 1.26% | 0.88% | -0.11 |
| Brown-W | CMAA14 | CMAA8 | 2275444 | 1.36% | 0.29% | 0.12 |
| Brown-W | CMAA14 | CMAA9* | 2275444 | 1.24% | 0.65% | -0.02 |
| Brown-W | CMAA15* | CMAA2 | 2275444 | 0.81% | 0.54% | -0.33 |
| Brown-W | CMAA15* | CMAA3 | 2275444 | 1.37% | 0.40% | 0.07 |
| Brown-W | CMAA15* | CMAA4* | 2275444 | 1.34% | 0.50% | 0.05 |
| Brown-W | CMAA15* | CMAA5 | 2275444 | 1.57% | 0.55% | 0.07 |
| Brown-W | CMAA15* | CMAA6 | 2275444 | 1.35% | 0.49% | 0.06 |
| Brown-W | CMAA15* | CMAA7* | 2275444 | 1.16% | 0.66% | -0.05 |
| Brown-W | CMAA15* | CMAA8 | 2275444 | 1.28% | 0.31% | 0.10 |
| Brown-W | CMAA15* | CMAA9* | 2275444 | 1.43% | 0.60% | 0.02 |
| Brown-W | CMAA16 | CMAA2 | 2275444 | 1.01% | 0.52% | -0.27 |
| Brown-W | CMAA16 | CMAA3 | 2275444 | 1.50% | 0.44% | 0.08 |
| Brown-W | CMAA16 | CMAA4* | 2275444 | 1.30% | 0.36% | 0.08 |
| Brown-W | CMAA16 | CMAA5 | 2275444 | 1.33% | 0.47% | 0.05 |
| Brown-W | CMAA16 | CMAA6 | 2275444 | 1.31% | 0.36% | 0.09 |
| Brown-W | CMAA16 | CMAA7* | 2275444 | 1.24% | 0.56% | -0.01 |
| Brown-W | CMAA16 | CMAA8 | 2275444 | 1.35% | 0.37% | 0.08 |
| Brown-W | CMAA16 | CMAA9* | 2275444 | 1.28% | 0.64% | -0.03 |
| Brown-W | CMAA17* | CMAA2 | 2275444 | 0.73% | 0.50% | -0.26 |
| Brown-W | CMAA17* | CMAA3 | 2275444 | 1.30% | 0.42% | 0.02 |
| Brown-W | CMAA17* | CMAA4* | 2275444 | 1.13% | 0.70% | -0.09 |
| Brown-W | CMAA17* | CMAA5 | 2275444 | 1.05% | 0.51% | -0.03 |
| Brown-W | CMAA17* | CMAA6 | 2275444 | 1.14% | 0.69% | -0.08 |
| Brown-W | CMAA17* | CMAA7* | 2275444 | 0.79% | 0.79% | -0.16 |
| Brown-W | CMAA17* | CMAA8 | 2275444 | 1.05% | 0.56% | -0.05 |
| Brown-W | CMAA17* | CMAA9* | 2275444 | 0.93% | 0.77% | -0.14 |
| Brown-W | CMAA2 | CMAA3 | 2275444 | 0.78% | 0.84% | -0.56 |
| Brown-W | CMAA2 | CMAA4* | 2275444 | 0.69% | 0.85% | -0.55 |
| Brown-W | CMAA2 | CMAA5 | 2275444 | 0.71% | 0.66% | -0.42 |
| Brown-W | CMAA2 | CMAA6 | 2275444 | 0.70% | 0.84% | -0.55 |
| Brown-W | CMAA2 | CMAA7* | 2275444 | 0.52% | 1.18% | -0.77 |
| Brown-W | CMAA2 | CMAA8 | 2275444 | 0.60% | 0.72% | -0.49 |
| Brown-W | CMAA2 | CMAA9* | 2275444 | 0.61% | 0.82% | -0.53 |
| Brown-W | CMAA3 | CMAA4* | 2275444 | 1.19% | 0.33% | 0.06 |
| Brown-W | CMAA3 | CMAA5 | 2275444 | 1.40% | 0.45% | 0.06 |
| Brown-W | CMAA3 | CMAA6 | 2275444 | 1.20% | 0.32% | 0.07 |
| Brown-W | CMAA3 | CMAA7* | 2275444 | 1.19% | 0.61% | -0.05 |
| Brown-W | CMAA3 | CMAA8 | 2275444 | 1.60% | 0.46% | 0.08 |
| Brown-W | CMAA3 | CMAA9* | 2275444 | 1.24% | 0.35% | 0.05 |
| Brown-W | CMAA4* | CMAA5 | 2275444 | 1.40% | 0.47% | 0.07 |
| Brown-W | CMAA4* | CMAA6 | 2275444 | 3.07% | 0.00% | 0.49 |
| Brown-W | CMAA4* | CMAA7* | 2275444 | 1.27% | 0.03% | 0.19 |
| Brown-W | CMAA4* | CMAA8 | 2275444 | 1.24% | 0.39% | 0.07 |
| Brown-W | CMAA4* | CMAA9* | 2275444 | 1.34% | 0.42% | 0.07 |
| Brown-W | CMAA5 | CMAA6 | 2275444 | 1.42% | 0.47% | 0.08 |
| Brown-W | CMAA5 | CMAA7* | 2275444 | 1.00% | 0.54% | -0.04 |

| | | | | | | |
|---|---|---|---|---|---|---|
| Brown-W | CMAA5 | CMAA8 | 2275444 | 1.18% | 0.52% | 0.02 |
| Brown-W | CMAA5 | CMAA9* | 2275444 | 1.29% | 0.49% | 0.04 |
| Brown-W | CMAA6 | CMAA7* | 2275444 | 1.28% | 0.02% | 0.19 |
| Brown-W | CMAA6 | CMAA8 | 2275444 | 1.25% | 0.38% | 0.07 |
| Brown-W | CMAA6 | CMAA9* | 2275444 | 1.35% | 0.41% | 0.07 |
| Brown-W | CMAA7* | CMAA8 | 2275444 | 1.18% | 0.65% | -0.04 |
| Brown-W | CMAA7* | CMAA9* | 2275444 | 1.22% | 0.54% | 0.01 |
| Brown-W | CMAA8 | CMAA9* | 2275444 | 1.58% | 0.20% | 0.19 |
| Brown-C | CMA10* | CMA11 | 2275444 | 2.08% | 1.31% | -0.06 |
| Brown-C | CMA10* | CMA12 | 2275444 | 5.28% | 0.00% | 0.49 |
| Brown-C | CMA10* | CMA13 | 2275444 | 2.18% | 1.19% | -0.04 |
| Brown-C | CMA10* | CMA14 | 2275444 | 1.86% | 1.03% | -0.02 |
| Brown-C | CMA11 | CMA12 | 2275444 | 2.10% | 1.30% | -0.06 |
| Brown-C | CMA11 | CMA13 | 2275444 | 2.40% | 0.92% | 0.04 |
| Brown-C | CMA11 | CMA14 | 2275444 | 2.37% | 1.12% | 0.00 |
| Brown-C | CMA12 | CMA13 | 2275444 | 2.19% | 1.19% | -0.03 |
| Brown-C | CMA12 | CMA14 | 2275444 | 1.86% | 1.02% | -0.02 |
| Brown-C | CMA13 | CMA14 | 2275444 | 2.69% | 0.55% | 0.13 |
| Brown-C | CMA10* | CMA15* | 2275444 | 2.10% | 1.08% | -0.04 |
| Brown-C | CMA10* | CMA16 | 2275444 | 1.98% | 1.14% | -0.03 |
| Brown-C | CMA10* | CMA18 | 2275444 | 1.71% | 1.37% | -0.12 |
| Brown-C | CMA10* | CMA4* | 2275444 | 1.73% | 1.35% | -0.11 |
| Brown-C | CMA10* | CMA8 | 2275444 | 1.76% | 1.64% | -0.24 |
| Brown-C | CMA10* | CMA9 | 2275444 | 1.98% | 1.11% | -0.02 |
| Brown-C | CMA11 | CMA15* | 2275444 | 2.71% | 0.02% | 0.22 |
| Brown-C | CMA11 | CMA16 | 2275444 | 2.12% | 1.29% | -0.05 |
| Brown-C | CMA11 | CMA18 | 2275444 | 1.90% | 1.53% | -0.14 |
| Brown-C | CMA11 | CMA4* | 2275444 | 1.92% | 1.50% | -0.13 |
| Brown-C | CMA11 | CMA8 | 2275444 | 1.62% | 1.58% | -0.26 |
| Brown-C | CMA11 | CMA9 | 2275444 | 1.95% | 1.45% | -0.10 |
| Brown-C | CMA12 | CMA15* | 2275444 | 2.11% | 1.07% | -0.03 |
| Brown-C | CMA12 | CMA16 | 2275444 | 1.99% | 1.13% | -0.02 |
| Brown-C | CMA12 | CMA18 | 2275444 | 1.72% | 1.36% | -0.12 |
| Brown-C | CMA12 | CMA4* | 2275444 | 1.74% | 1.35% | -0.11 |
| Brown-C | CMA12 | CMA8 | 2275444 | 1.76% | 1.64% | -0.24 |
| Brown-C | CMA12 | CMA9 | 2275444 | 1.99% | 1.11% | -0.02 |
| Brown-C | CMA13 | CMA15* | 2275444 | 2.46% | 1.24% | -0.01 |
| Brown-C | CMA13 | CMA16 | 2275444 | 2.25% | 1.22% | -0.04 |
| Brown-C | CMA13 | CMA18 | 2275444 | 2.17% | 1.65% | -0.15 |
| Brown-C | CMA13 | CMA4* | 2275444 | 2.20% | 1.63% | -0.14 |
| Brown-C | CMA13 | CMA8 | 2275444 | 1.57% | 1.58% | -0.27 |
| Brown-C | CMA13 | CMA9 | 2275444 | 2.26% | 0.85% | 0.03 |
| Brown-C | CMA14 | CMA15* | 2275444 | 2.39% | 0.88% | 0.03 |
| Brown-C | CMA14 | CMA16 | 2275444 | 2.18% | 1.09% | 0.00 |
| Brown-C | CMA14 | CMA18 | 2275444 | 2.06% | 1.13% | -0.04 |
| Brown-C | CMA14 | CMA4* | 2275444 | 2.08% | 1.12% | -0.03 |
| Brown-C | CMA14 | CMA8 | 2275444 | 1.58% | 1.59% | -0.25 |
| Brown-C | CMA14 | CMA9 | 2275444 | 2.25% | 1.02% | 0.02 |
| Brown-C | CMA15* | CMA16 | 2275444 | 2.18% | 1.22% | -0.05 |
| Brown-C | CMA15* | CMA18 | 2275444 | 2.82% | 0.04% | 0.22 |
| Brown-C | CMA15* | CMA4* | 2275444 | 2.86% | 0.03% | 0.22 |
| Brown-C | CMA15* | CMA8 | 2275444 | 1.73% | 1.56% | -0.27 |
| Brown-C | CMA15* | CMA9 | 2275444 | 2.37% | 1.44% | -0.08 |

| | | | | | | |
|---|---|---|---|---|---|---|
| Brown-C | CMA16 | CMA18 | 2275444 | 1.82% | 1.49% | -0.13 |
| Brown-C | CMA16 | CMA4* | 2275444 | 1.84% | 1.47% | -0.12 |
| Brown-C | CMA16 | CMA8 | 2275444 | 1.52% | 1.51% | -0.24 |
| Brown-C | CMA16 | CMA9 | 2275444 | 2.16% | 1.03% | 0.01 |
| Brown-C | CMA18 | CMA4* | 2275444 | 4.93% | 0.00% | 0.48 |
| Brown-C | CMA18 | CMA8 | 2275444 | 1.39% | 1.90% | -0.33 |
| Brown-C | CMA18 | CMA9 | 2275444 | 2.03% | 1.55% | -0.12 |
| Brown-C | CMA4* | CMA8 | 2275444 | 1.40% | 1.88% | -0.32 |
| Brown-C | CMA4* | CMA9 | 2275444 | 2.05% | 1.54% | -0.11 |
| Brown-C | CMA8 | CMA9 | 2275444 | 1.72% | 1.47% | -0.21 |
| Brown-E | CMH00 | CMH1 | 2275444 | 1.69% | 0.31% | 0.18 |
| Brown-E | CMH00 | CMH12* | 2275444 | 1.02% | 1.29% | -0.29 |
| Brown-E | CMH00 | CMH2 | 2275444 | 1.47% | 0.63% | -0.09 |
| Brown-E | CMH00 | CMH3 | 2275444 | 1.32% | 0.60% | -0.09 |
| Brown-E | CMH00 | CMH4* | 2275444 | 1.03% | 1.27% | -0.26 |
| Brown-E | CMH00 | CMH5 | 2275444 | 1.28% | 0.77% | -0.09 |
| Brown-E | CMH00 | CMH6 | 2275444 | 1.03% | 1.28% | -0.27 |
| Brown-E | CMH1 | CMH12* | 2275444 | 1.00% | 1.55% | -0.37 |
| Brown-E | CMH1 | CMH2 | 2275444 | 1.22% | 0.63% | -0.15 |
| Brown-E | CMH1 | CMH3 | 2275444 | 1.43% | 0.89% | -0.18 |
| Brown-E | CMH1 | CMH4* | 2275444 | 1.02% | 1.53% | -0.37 |
| Brown-E | CMH1 | CMH5 | 2275444 | 1.25% | 0.90% | -0.15 |
| Brown-E | CMH1 | CMH6 | 2275444 | 1.01% | 1.54% | -0.37 |
| Brown-E | CMH12* | CMH2 | 2275444 | 1.25% | 0.63% | -0.15 |
| Brown-E | CMH12* | CMH3 | 2275444 | 1.04% | 1.09% | -0.32 |
| Brown-E | CMH12* | CMH4* | 2275444 | 2.76% | 0.00% | 0.48 |
| Brown-E | CMH12* | CMH5 | 2275444 | 1.06% | 1.14% | -0.27 |
| Brown-E | CMH12* | CMH6 | 2275444 | 2.77% | 0.00% | 0.49 |
| Brown-E | CMH2 | CMH3 | 2275444 | 2.26% | 0.36% | 0.17 |
| Brown-E | CMH2 | CMH4* | 2275444 | 1.27% | 0.62% | -0.12 |
| Brown-E | CMH2 | CMH5 | 2275444 | 1.72% | 0.59% | 0.00 |
| Brown-E | CMH2 | CMH6 | 2275444 | 1.27% | 0.62% | -0.14 |
| Brown-E | CMH3 | CMH4* | 2275444 | 1.07% | 1.08% | -0.29 |
| Brown-E | CMH3 | CMH5 | 2275444 | 1.69% | 0.71% | -0.01 |
| Brown-E | CMH3 | CMH6 | 2275444 | 1.06% | 1.09% | -0.31 |
| Brown-E | CMH4* | CMH5 | 2275444 | 1.08% | 1.12% | -0.24 |
| Brown-E | CMH4* | CMH6 | 2275444 | 2.80% | 0.00% | 0.48 |
| Brown-E | CMH5 | CMH6 | 2275444 | 1.07% | 1.13% | -0.26 |
| Brown-E | CMH00 | CMH7* | 2275444 | 1.28% | 0.81% | -0.09 |
| Brown-E | CMH00 | CMH8 | 2275444 | 1.04% | 1.01% | -0.19 |
| Brown-E | CMH00 | CMH9 | 2275444 | 1.25% | 1.37% | -0.25 |
| Brown-E | CMH1 | CMH7* | 2275444 | 1.03% | 0.93% | -0.19 |
| Brown-E | CMH1 | CMH8 | 2275444 | 1.07% | 1.08% | -0.23 |
| Brown-E | CMH1 | CMH9 | 2275444 | 1.01% | 1.43% | -0.34 |
| Brown-E | CMH12* | CMH7* | 2275444 | 0.88% | 1.21% | -0.32 |
| Brown-E | CMH12* | CMH8 | 2275444 | 1.13% | 1.46% | -0.36 |
| Brown-E | CMH12* | CMH9 | 2275444 | 0.83% | 1.45% | -0.38 |
| Brown-E | CMH2 | CMH7* | 2275444 | 1.85% | 0.68% | -0.01 |
| Brown-E | CMH2 | CMH8 | 2275444 | 1.45% | 0.79% | -0.11 |
| Brown-E | CMH2 | CMH9 | 2275444 | 1.52% | 0.70% | -0.11 |
| Brown-E | CMH3 | CMH7* | 2275444 | 1.67% | 0.73% | -0.04 |
| Brown-E | CMH3 | CMH8 | 2275444 | 1.23% | 1.17% | -0.24 |
| Brown-E | CMH3 | CMH9 | 2275444 | 1.34% | 0.90% | -0.18 |

| | | | | | | |
|---|---|---|---|---|---|---|
| Brown-E | CMH4* | CMH7* | 2275444 | 0.89% | 1.20% | -0.28 |
| Brown-E | CMH4* | CMH8 | 2275444 | 1.16% | 1.45% | -0.32 |
| Brown-E | CMH4* | CMH9 | 2275444 | 0.85% | 1.44% | -0.35 |
| Brown-E | CMH5 | CMH7* | 2275444 | 1.41% | 1.02% | -0.11 |
| Brown-E | CMH5 | CMH8 | 2275444 | 0.90% | 0.92% | -0.16 |
| Brown-E | CMH5 | CMH9 | 2275444 | 1.10% | 0.90% | -0.16 |
| Brown-E | CMH6 | CMH7* | 2275444 | 0.89% | 1.20% | -0.30 |
| Brown-E | CMH6 | CMH8 | 2275444 | 1.15% | 1.45% | -0.34 |
| Brown-E | CMH6 | CMH9 | 2275444 | 0.84% | 1.44% | -0.36 |
| Brown-E | CMH7* | CMH8 | 2275444 | 1.20% | 0.46% | 0.04 |
| Brown-E | CMH7* | CMH9 | 2275444 | 1.95% | 0.13% | 0.25 |
| Brown-E | CMH8 | CMH9 | 2275444 | 0.96% | 0.73% | -0.11 |

Dataset S11: Summary metrics of the SNP of each sample. The high-quality SNPs indicate the bases with a call quality of Q20 or higher. The high-coverage sites are at least covered by five reads. Heterozygosity was defined as the number of heterozygous SNPs divided by the total callable sites. Blue indicates *Crossoptilon auritum* , and Brown indicates *Crossoptilon mantchuricum* . A represents autosomes, Z represents the Z chromosome, and M represents the mitogenome.

| | | | The percent of high quality SNPs | | | The percent of high coverage sites | | | The percent of missing SNPs | | | The number of heteozygous / substitutions | | Heterozygosity | |
|---|---|---|---|---|---|---|---|---|---|---|---|---|---|---|---|
| Species | Sample ID | Sample index | A | Z | M | A | Z | M | A | Z | M | A | Z | A | Z |
| Blue | CA00 | 1 | 94.78% | 93.66% | 95.25% | 98.50% | 98.16% | 100.00% | 0.04% | 0.28% | 0.00% | 760421 | 17881 | 0.00083 | 0.00025 |
| Blue | CA01 | 2 | 93.13% | 92.48% | 95.25% | 97.72% | 77.31% | 100.00% | 0.10% | 1.34% | 0.00% | 902604 | 16246 | 0.00099 | 0.00024 |
| Blue | CA02 | 3 | 93.78% | 94.36% | 95.26% | 97.79% | 97.68% | 100.00% | 0.12% | 0.12% | 0.00% | 756677 | 28595 | 0.00083 | 0.00040 |
| Blue | CA03 | 4 | 93.19% | 92.59% | 95.26% | 97.76% | 80.35% | 100.00% | 0.10% | 0.93% | 0.00% | 779739 | 15933 | 0.00086 | 0.00023 |
| Blue | CA04 | 5 | 93.69% | 92.91% | 95.26% | 98.15% | 90.75% | 100.00% | 0.09% | 0.62% | 0.00% | 722721 | 15973 | 0.00079 | 0.00023 |
| Blue | CA05 | 6 | 93.39% | 92.87% | 95.26% | 97.99% | 86.72% | 100.00% | 0.09% | 0.63% | 0.00% | 728717 | 15723 | 0.00080 | 0.00022 |
| Blue | CA06 | 7 | 93.77% | 94.35% | 95.26% | 97.93% | 97.88% | 100.00% | 0.11% | 0.14% | 0.00% | 728200 | 24951 | 0.00080 | 0.00035 |
| Blue | CA07 | 8 | 94.50% | 94.99% | 95.26% | 96.70% | 97.11% | 100.00% | 0.22% | 0.13% | 0.00% | 728940 | 26981 | 0.00080 | 0.00037 |
| Blue | CA08 | 9 | 95.00% | 95.27% | 95.26% | 97.04% | 96.82% | 100.00% | 0.16% | 0.22% | 0.00% | 721363 | 24411 | 0.00079 | 0.00034 |
| Blue | CA09 | 10 | 94.22% | 94.58% | 95.26% | 97.72% | 97.57% | 100.00% | 0.12% | 0.08% | 0.00% | 732472 | 25416 | 0.00080 | 0.00035 |
| Blue | CA10 | 11 | 93.63% | 92.70% | 95.26% | 98.05% | 85.95% | 100.00% | 0.09% | 0.63% | 0.00% | 740524 | 14987 | 0.00081 | 0.00021 |
| Brown | CMAA00 | 12 | 94.68% | 93.71% | 95.54% | 98.56% | 98.30% | 100.00% | 0.01% | 0.12% | 0.00% | 68230 | 13903 | 0.00007 | 0.00019 |
| Brown | CMAA01 | 13 | 94.92% | 93.99% | 95.54% | 97.34% | 77.13% | 100.00% | 0.02% | 0.53% | 0.00% | 63205 | 10840 | 0.00007 | 0.00016 |
| Brown | CMAA02 | 14 | 94.39% | 94.87% | 95.54% | 97.68% | 97.67% | 100.00% | 0.01% | 0.02% | 0.00% | 38525 | 1403 | 0.00004 | 0.00002 |
| Brown | CMAA03 | 15 | 92.27% | 92.00% | 95.54% | 97.69% | 74.81% | 100.00% | 0.02% | 0.59% | 0.00% | 80829 | 12038 | 0.00009 | 0.00018 |
| Brown | CMAA04 | 16 | 94.16% | 94.80% | 95.54% | 97.73% | 97.68% | 100.00% | 0.02% | 0.02% | 0.00% | 73818 | 1840 | 0.00008 | 0.00003 |
| Brown | CMAA05 | 17 | 92.22% | 91.39% | 95.54% | 98.10% | 84.59% | 100.00% | 0.01% | 0.41% | 0.00% | 74476 | 12417 | 0.00008 | 0.00018 |
| Brown | CMAA06 | 18 | 93.07% | 94.25% | 95.54% | 98.24% | 98.08% | 100.00% | 0.01% | 0.02% | 0.00% | 75001 | 1898 | 0.00008 | 0.00003 |

| | | | | | | | | | | | | | | |
|---|---|---|---|---|---|---|---|---|---|---|---|---|---|---|
| Brown | CMAA07 | 19 | 92.24% | 91.79% | 95.54% | 97.86% | 77.04% | 100.00% | 0.01% | 0.57% | 0.00% | 68547 | 11875 | 0.00008 | 0.00018 |
| Brown | CMAA08 | 20 | 94.48% | 93.87% | 95.54% | 98.09% | 87.52% | 100.00% | 0.01% | 0.34% | 0.00% | 73400 | 12521 | 0.00008 | 0.00018 |
| Brown | CMAA09 | 21 | 94.84% | 94.33% | 95.54% | 97.00% | 77.02% | 100.00% | 0.03% | 0.53% | 0.00% | 70336 | 11406 | 0.00008 | 0.00017 |
| Brown | CMAA10 | 22 | 91.75% | 89.07% | 95.54% | 83.37% | 45.00% | 100.00% | 0.37% | 4.14% | 0.00% | 49204 | 10382 | 0.00006 | 0.00021 |
| Brown | CMAA11 | 23 | 93.03% | 94.07% | 95.55% | 98.39% | 98.21% | 100.00% | 0.01% | 0.00% | 0.00% | 65444 | 2150 | 0.00007 | 0.00003 |
| Brown | CMAA12 | 24 | 93.93% | 93.48% | 95.55% | 98.21% | 88.87% | 100.00% | 0.01% | 0.36% | 0.00% | 63348 | 13922 | 0.00007 | 0.00020 |
| Brown | CMAA13 | 25 | 92.83% | 92.46% | 95.55% | 98.08% | 83.94% | 100.00% | 0.01% | 0.32% | 0.00% | 58156 | 12005 | 0.00006 | 0.00017 |
| Brown | CMAA14 | 26 | 94.50% | 94.15% | 95.55% | 98.19% | 85.63% | 100.00% | 0.01% | 0.30% | 0.00% | 74402 | 13709 | 0.00008 | 0.00020 |
| Brown | CMAA15 | 27 | 92.62% | 92.41% | 95.55% | 97.76% | 76.50% | 100.00% | 0.01% | 0.59% | 0.00% | 75143 | 12700 | 0.00008 | 0.00019 |
| Brown | CMAA16 | 28 | 91.92% | 92.82% | 95.55% | 97.98% | 97.82% | 100.00% | 0.01% | 0.01% | 0.00% | 77779 | 2145 | 0.00009 | 0.00003 |
| Brown | CMAA17 | 29 | 92.29% | 93.54% | 95.55% | 96.23% | 95.82% | 100.00% | 0.02% | 0.02% | 0.00% | 64647 | 2054 | 0.00007 | 0.00003 |
| Brown | CMA04 | 30 | 93.13% | 94.36% | 95.69% | 97.34% | 97.45% | 100.00% | 0.03% | 0.04% | 0.00% | 120600 | 1294 | 0.00013 | 0.00002 |
| Brown | CMA08 | 31 | 93.96% | 93.37% | 95.71% | 95.55% | 72.05% | 100.00% | 0.05% | 0.97% | 0.00% | 101425 | 13094 | 0.00011 | 0.00020 |
| Brown | CMA09 | 32 | 92.85% | 92.53% | 95.75% | 98.28% | 88.71% | 100.00% | 0.01% | 0.34% | 0.00% | 128238 | 12343 | 0.00014 | 0.00017 |
| Brown | CMA10 | 33 | 92.40% | 92.02% | 95.73% | 98.00% | 81.37% | 100.00% | 0.01% | 0.53% | 0.00% | 127557 | 12243 | 0.00014 | 0.00018 |
| Brown | CMA11 | 34 | 92.69% | 92.46% | 95.30% | 98.15% | 90.29% | 100.00% | 0.01% | 0.39% | 0.00% | 133880 | 12653 | 0.00015 | 0.00018 |
| Brown | CMA12 | 35 | 92.66% | 92.29% | 95.32% | 98.21% | 86.08% | 100.00% | 0.01% | 0.39% | 0.00% | 128242 | 12283 | 0.00014 | 0.00018 |
| Brown | CMA13 | 36 | 92.93% | 94.01% | 95.36% | 98.41% | 98.24% | 100.00% | 0.01% | 0.02% | 0.00% | 136818 | 2837 | 0.00015 | 0.00004 |
| Brown | CMA14 | 37 | 93.14% | 94.20% | 95.36% | 98.16% | 98.08% | 100.00% | 0.02% | 0.02% | 0.00% | 126997 | 2454 | 0.00014 | 0.00003 |
| Brown | CMA15 | 38 | 93.47% | 93.18% | 95.48% | 98.18% | 84.49% | 100.00% | 0.01% | 0.27% | 0.00% | 144027 | 12458 | 0.00016 | 0.00018 |
| Brown | CMA16 | 39 | 92.50% | 92.09% | 95.49% | 97.86% | 79.01% | 100.00% | 0.02% | 0.52% | 0.00% | 127677 | 12222 | 0.00014 | 0.00018 |
| Brown | CMA18 | 40 | 92.79% | 93.93% | 95.53% | 97.38% | 97.07% | 100.00% | 0.02% | 0.03% | 0.00% | 119486 | 1346 | 0.00013 | 0.00002 |
| Brown | CMH00 | 41 | 92.46% | 93.40% | 95.55% | 98.49% | 98.31% | 100.00% | 0.02% | 0.08% | 0.00% | 70061 | 808 | 0.00008 | 0.00001 |
| Brown | CMH01 | 42 | 94.17% | 93.06% | 95.55% | 97.84% | 83.94% | 100.00% | 0.04% | 0.37% | 0.00% | 66657 | 10978 | 0.00007 | 0.00016 |
| Brown | CMH02 | 43 | 94.00% | 94.66% | 95.55% | 98.18% | 98.44% | 100.00% | 0.03% | 0.03% | 0.00% | 105279 | 1392 | 0.00012 | 0.00002 |
| Brown | CMH03 | 44 | 93.44% | 92.77% | 95.55% | 98.19% | 87.08% | 100.00% | 0.02% | 0.35% | 0.00% | 99277 | 13337 | 0.00011 | 0.00019 |
| Brown | CMH04 | 45 | 91.98% | 93.04% | 95.41% | 98.23% | 98.09% | 100.00% | 0.03% | 0.02% | 0.00% | 70004 | 912 | 0.00008 | 0.00001 |
| Brown | CMH05 | 46 | 93.03% | 93.95% | 95.41% | 98.03% | 98.01% | 100.00% | 0.03% | 0.03% | 0.00% | 81476 | 2178 | 0.00009 | 0.00003 |

| | | | | | | | | | | | | | | | |
|---|---|---|---|---|---|---|---|---|---|---|---|---|---|---|---|
| Brown | CMH06 | 47 | 93.08% | 94.18% | 95.44% | 98.30% | 98.16% | 100.00% | 0.02% | 0.03% | 0.00% | 67604 | 953 | 0.00007 | 0.00001 |
| Brown | CMH07 | 48 | 93.94% | 93.23% | 95.44% | 97.97% | 84.65% | 100.00% | 0.03% | 0.31% | 0.00% | 78353 | 12207 | 0.00009 | 0.00018 |
| Brown | CMH08 | 49 | 92.99% | 92.63% | 95.44% | 97.64% | 77.13% | 100.00% | 0.03% | 0.53% | 0.00% | 77740 | 11520 | 0.00009 | 0.00017 |
| Brown | CMH09 | 50 | 93.38% | 92.78% | 95.45% | 98.13% | 87.84% | 100.00% | 0.02% | 0.32% | 0.00% | 69882 | 12318 | 0.00008 | 0.00018 |
| Brown | CMH12 | 51 | 90.21% | 91.22% | 95.24% | 98.09% | 97.95% | 100.00% | 0.03% | 0.04% | 0.00% | 66594 | 812 | 0.00007 | 0.00001 |

Dataset S12: Scaffolds on the sex chromosomes and mitochondrial genome.

| Z chromosome linked scaffolds | | Mitochondria linked scaffolds | |
|---|---|---|---|
| Scaffolds | The percent of homologous gene (%) | Scaffolds | The percent of homologous gene (%) |
| scaffold_74 | 25 | scaffold_1343 | 100 |
| scaffold_142 | 41.38 | scaffold_1701 | 100 |
| scaffold_34 | 46.24 | scaffold_1847 | 100 |
| scaffold_394 | 50 | | |
| scaffold_397 | 50 | | |
| scaffold_399 | 57.14 | | |
| scaffold_215 | 68.75 | | |
| scaffold_247 | 70.59 | | |
| scaffold_157 | 73.33 | | |
| scaffold_79 | 73.68 | | |
| scaffold_241 | 75 | | |
| scaffold_380 | 75 | | |
| scaffold_401 | 75 | | |
| scaffold_254 | 76.47 | | |
| scaffold_187 | 77.08 | | |
| scaffold_62 | 77.5 | | |
| scaffold_212 | 80 | | |
| scaffold_333 | 80 | | |
| scaffold_403 | 80 | | |
| scaffold_122 | 80.36 | | |
| scaffold_196 | 81.48 | | |
| scaffold_291 | 81.48 | | |
| scaffold_192 | 82.93 | | |
| scaffold_336 | 85.71 | | |
| scaffold_349 | 85.71 | | |
| scaffold_160 | 86.36 | | |
| scaffold_236 | 86.36 | | |
| scaffold_113 | 86.67 | | |
| scaffold_156 | 86.67 | | |
| scaffold_57 | 87.04 | | |
| scaffold_93 | 87.23 | | |
| scaffold_37 | 88.46 | | |
| scaffold_259 | 88.89 | | |
| scaffold_136 | 89.66 | | |

| | |
|---|---|
| scaffold_252 | 90 |
| scaffold_1249 | 100 |
| scaffold_1272 | 100 |
| scaffold_194 | 100 |
| scaffold_285 | 100 |
| scaffold_351 | 100 |
| scaffold_357 | 100 |
| scaffold_367 | 100 |
| scaffold_393 | 100 |
| scaffold_427 | 100 |
| scaffold_438 | 100 |
| scaffold_453 | 100 |
| scaffold_582 | 100 |
| scaffold_777 | 100 |
| scaffold_913 | 100 |